A MULTINUCLEAR NMR STUDY OF ORGANOSILANES

BY

PAUL JOHN KANYHA

A DISSERTATION PRESENTED TO THE GRADUATE SCHOOL OF THE UNIVERSITY OF FLORIDA IN PARTIAL FULFILLMENT OF THE REQUIREMENTS FOR THE DEGREE OF DOCTOR OF PHILOSOPHY

UNIVERSITY OF FLORIDA

1984

ACKNOWLEDGMENTS

The author wishes to thank the member of his supervisory committee and to express his sincere appreciation to Dr. W.S. Brey, Jr., chairman of the author's supervisory committee, for his constant guidance and help during the course of this work. The author gratefully thanks Dr. R.W. King for his assistance in mass spectral interpretation, Mr. D. Plant for his assistance in the synthesis of the chloroaminosilanes, glassblowers Mr. R. Strohschein and Mr. R. Moshier, and typist Ms. P. Victor.

The author wishes to acknowledge PCR, Inc., of Gainesville, Florida, who kindly donated some of the organosilanes to the Department of Chemistry and the Graduate School of the University of Florida for a graduate assistantship and to the Instrument Program, Chemistry Division, National Science Foundation, for aid in the purchase of the Nicolet NT-300 NMR spectrometer.

TABLE OF CONTENTS

		Page
ACKNOWLEDGMENTS		ii
ABSTRACT		iv
CHAPTER		
I	INTRODUCTION	1
	Evidence of (d-p)π Bonding	1
	Summary of the Literature Findings	40
	Aim of the Investigation	41
II	EXPERIMENTAL	43
	Materials	43
	Spectrometer	47
	Computer Calculations	49
III	NOVEL NMR METHODS	50
	Modified Selective Population Transfer Experiments	50
	^{13}C Spin-Echo J-Modulation Experiments	64
IV	RESULTS AND DISCUSSION	75
	Trimethylsilyl Compounds	75
	Methylsilanes	100
	Silylamines	110
V	CONCLUSIONS	130
REFERENCES		131
BIOGRAPHICAL SKETCH		144

Abstract of Dissertation Presented to the Graduate School of the University of Florida in Partial Fulfillment of the Requirements for the Degree of Doctor of Philosophy

A MULTINUCLEAR NMR STUDY OF ORGANOSILANCES

By

Paul John Kanyha

April 1984

Chairman: Dr. W.S. Brey, Jr.
Major Department: Chemistry

The ^{1}H, ^{13}C, ^{15}N and ^{29}Si chemical shifts and coupling constants including $^{1}J(^{29}Si^{13}C)$ and $^{1}J(^{29}Si^{15}N)$ are reported for 26 trimethylsilanes, 48 methylsilanes, and 33 silylamines. The chemical shift data are best interpreted in terms of competing (d-p)π and inductive effects. The $^{1}J(^{29}Si^{13}C)$ and $^{1}J(^{29}Si^{15}N)$ are strongly dominated by the Fermi contact interaction. For ^{29}Si nuclei in silylamines, T_2 scalar coupling relaxation is dominant. From the chemical shift and coupling constant data, it is concluded that there is significant (d-p)π bonding for Si-N and Si-O bonds, moderate to negligible (d-p)π bonding for Si-C (unsaturated carbon) and negligible (d-p)π bonding for Si-S and Si-Cl bonds.

In addition, novel NMR pulse sequences are described. One of these is a method to decouple selectively a group of magnetically equivalent protons which are also used for polarization transfer. The others are techniques to suppress strong unwanted signals and to differentiate between ^{13}C multiplicities.

CHAPTER I
INTRODUCTION

The question of (d-p)π bonding in organosilanes has long been an area of controversy, partly because (d-p)π bonding has often been invoked to explain the "unexplainable" (1-4). Most cases where the participation of silicon d orbitals in bonding has been cited have been concerned with physical and spectroscopic properties rather than chemical properties. Although the (d-p)π bonding model has been employed most often in the interpretation of Si-N and Si-O bonds, there is also some evidence of (d-p)π bonding in Si-F bonds and to a lesser extent in Si-Cl, Si-S, and Si-C (unsaturated carbon) bonds. Therefore, it is of considerable interest to determine the extent of double-bond formation in these bonds.

Evidence of (d-p)π Bonding

Because of the limited commercial availability, high volatility, and arduous synthesis of the fluorosilanes, only compounds containing Si-C, Si-N, Si-O, Si-S, and Si-Cl bonds were included in this investigation. In the next few pages, the literature will be briefly reviewed for evidence of (d-p)π bonding in these bonds.

Bond Lengths and Angles

Participation of (d-p)π bonds is usually claimed when bond lengths are shorter than predicted by the Schomaker-Stevenson equation (5) in which the bond length is taken to be the sum of atomic radii, less a correction for electronegativity. Judging by bond lengths, an increase in bond orders due to (d-p)π bonding occurs for Si-N and Si-O bonds. A quantitative estimation of the extent of π bonding from the bond shortening, however, is difficult for several reasons. Firstly the single bond reference length is only an estimate, and secondly it is well known that, as in carbon compounds, inductive effects (-I) and increased s character both result in bond shortening. Therefore, the shortening of the Si-O bond length with increasing electronegativity of X in the series $X_3SiOSiX_3$ can be attributed to increased bond-order due either to better (d-p)π overlap or to inductive effects. Table 1-1 presents typical bond lengths for simple compounds.

With the exception of the Si-N bond length for $Me_3SiN = NSiMe_3$, the bond lengths of Si-N and Si-O are 0.05 to 0.18 Å shorter than that predicted for a "single" bond by the Schomaker-Stevenson equation. The Si-N bond length of 1.81 Å for $Me_3SiN = NSiMe_3$ (6) seems to indicate an absence of (d-p)π bonding. The lengths of Si-C, Si-S, and Si-Cl bonds are within 0.04 Å of the Schomaker-Stevenson bond length, indicating that (d-p)π bonding is weak or absent. For example, from an electron-diffraction study (7) of $(Me_2N)_3SiCl$ a Si-N bond length of 1.715 Å was observed which is 0.08 Å shorter than

Table 1-1. Typical Si-X Bond Length (Å).[a]

Si-C 1.88[b]

$Me_3SiC{\equiv}CH$	1.825 SiC≡C (8)[c] 1.865 SiMe	$Me_2(Cl)SiCH{=}CH_2$	1.838 SiC=C (9) 1.876 SiMe
$H_3SiCH{=}CH_2$	1.853 (10)	Ph_4Si	1.872 (11)
$(Ph_3Si)_2O$	1.864 (12)	$(Ph_3Si)_2NH$	1.878 (13)
$(Me_3Si)_2NH$	1.876 (14)	$(Me_2SiNH)_3$	1.871 (15)
$(Me_2Si)_4$	1.889 (16)	$Cl_3SiCH_2SiCl_3$	1.866 (17)

Si-N 1.80[b]

H_3SiNMe_2	1.715 (18)	H_3SiNCO	1.703 (19)
Cl_3SiNMe_2	1.657 (20)	Cl_3SiNCO	1.646 (21)
F_3SiNMe_2	1.654 (20)	H_3SiNCS	1.714 (22)
$(H_3Si)_2NH$	1.724 (23)	$(H_3Si)_2NMe$	1.726 (24)
$(Me_3Si)_2NH$	1.735 (14)	$(Me_2SiNH)_3$	1.728 (15)
$(Ph_3Si)_2NH$	1.718 (13)	$(Me_2SiNPh)_2$	1.744 (25)
$(H_3Si)_3N$	1.734 (26)	$(Me_2N)_3SiCl$	1.715 (7)
$(H_3Si)_2N\text{-}N(SiH_3)_2$	1.713 (27)	$Me_3SiN{=}NSiMe_3$	1.81 (6)
$(H_3Si)_2NCN$	1.696 (28)	H_3SiN_3	1.719 (28)

Si-O 1.76[b]

$H_3SiOSiH_3$	1.631 (29,30)	H_3SiOCH_3	1.640 (30,31)
$Me_3SiOSiMe_3$	1.626 (29)	F_3SiOCH_3	1.580 (32)
$Ph_3SiOSiPh_3$	1.616 (12)	$(Bu_2SiO)_3$	1.654 (33)
$Cl_3SiOSiCl_3$	1.592 (32)	$F_3SiOSiF_3$	1.580 (34)

Si-S 2.16[b]

$H_3SiSSiH_3$ 2.136 (35)

Table 1-1 continued.

Si-Cl 2.05[b]					
$Cl_3SiCH_2SiCl_3$	2.027	(17)	$Cl_3SiOSiCl_3$	2.011	(32)
Cl_3SiNCO	2.014	(21)	Cl_3SiNMe_2	2.023	(20)
$(Me_2N)_3SiCl$	2.082	(7)	$Cl(Me_2)SiCH{=}CH_2$	2.078	(9)

[a] Me = CH_3, Bu = $(CH_3)_3C$, and Ph = C_6H_5.

[b] Schomaker-Stevenson (5) "single" bond length.

[c] Numbers in parentheses are references.

the "single" bond length predicted by the Schomaker-Stevenson equation. The observed Si-Cl bond length (7) is considerably longer than that in $Cl_3SiCH_2SiCl_3$ (17) and would seem to indicate a lack of (d-p)π bonding to chlorine.

Structural data indicate that unusual bond angles occur only for Si-N and Si-O compounds as compared to the bond angles for the carbon analogs. In contrast, the bond angles for Si-C and Si-S compounds are within 2° of the bond angles for the corresponding alkyl derivatives; therefore, these bond angles seem to indicate an absence of (d-p)π bonding. Typical bond angles for simple compounds and the analogous carbon derivatives are shown in Table 1-2.

Nitrogen is invariably planar when linked to two or three Si atoms, as in $(H_3Si)_3N$ (26), $(H_3Si)_2NH$ (23), $(H_3Si)_2NMe$ (24), $(H_3Si)_2NN(SiH_3)_2$ (7), and $(Me_3Si)_2NH$ (14). If, however, a single silyl group is bonded to nitrogen, nitrogen will not always be planar and can in fact be an approximately trigonal pyramid, similar to that of the alkylamines. This is demonstrated by H_3SiNMe_2 in which the Si-N bond is tilted out of the CNC plane by 27.8° (18). In contrast, planar nitrogen has been observed for F_3SiNMe_2 (20), Cl_3SiNMe_2 (20), and $(Me_2N)_3SiCl$ (7). An electron diffraction study (28) showed H_3SiN_3 to have a nonlinear SiN_3 skeleton with a Si-N-N bond angle of 123.8° while the molecule $(H_3Si)_2NCN$ has a planar Si_2NCN skeleton. This, therefore, suggests (d-p)π bonding in the cyanamide and an absence of (d-p)π bonding in the azide. As another example, the X-ray structure of

Table 1-2. Si-X-Si and Si-X-C Bond Angles: Comparison with Carbon Compounds.[a]

Compound	∡ (°)	Compound	∡ (°)
$H_3Si-CH_2-SiH_3$	114.4 (36)[b]	$H_3C-CH_2-CH_3$	112.4 (36)
$H_3Si-O-SiH_3$	142.2 (29,30)	$H_3C-O-CH_3$	111.6 (30)
$H_3Si-O-CH_3$	120.6 (30,31)		
$Ph_3Si-O-SiPh_3$	180.0 (12)	$Ph_3C-O-CPh_3$	127.9 (37)
$H_3Si-NH-SiH_3$	127.7 (23)	$H_3C-NH-CH_3$	112.2 (38)
$(H_3Si)_3N$	119.7 (24)	$(H_3C)_3N$	110.6 (36)
H_3SiNCO	180 (19)	H_3CNCO	140.0 (39)
H_3SiNCS	180 (22)	H_3CNCS	147.5 (39)
$H_3Si-S-SiH_3$	97.4 (35)	$H_3C-S-CH_3$	98.9 (40)

[a] Ph = C_6H_5.

[b] Numbers in parenthesis are references.

Table 1-3. Geometry of Some $X_3SiOSiX_3$ Molecules.

X[a]	Si-O Length (Å)	Si-O-Si Angle (°)	Ref.
H	1.631	142.2	(29)
Me	1.626	148.8	(29)
Cl	1.592	146	(32)
F	1.580	155.7	(34)
Ph	1.616	180.0	(12)
$PhCH_2$	--	180.0	(41)

[a]Me = CH_3 and Ph = C_6H_5.

bis(trimethylsilyl) diimide has shown the Si-N=N bond angle to be 120° with a Si-N bond length of 1.81 Å, suggesting an absence of (d-p)π bonding (6).

The Si-O-Si bond angle in disiloxanes is always larger than the angle predicted by the valence shell electron pair repulsion theory for single bonds. This increase in bond angle at oxygen must result from (d-p)π bonding, since as the σ bond assumes increasing sp hybrid character, there will be better pπ (or pπ') overlap with the $3d_{x^2-y^2}$ (or d_{z^2}) orbital. Therefore, in the series $X_3SiOSiX_3$ (X=H, Cl, F), the Si-O bond length decreases and the Si-O-Si bond angle increases with increasing electronegativity of X, as shown in Table 1-3. X-ray crystallographic studies have shown the Si-O-Si bond angle for $Ph_3SiOSiPh_3$ (12) and $(PhCH_2)_3SiOSi(CH_2Ph)_3$ (41) to be 180.0°. These large bond angles can be interpreted in terms of strong (d-p)π bonding, since the carbon analog, Ph_3COCPh_3 has a C-O-C bond angle of 127.9° (37). Table 1-3 presents Si-O-Si bond angles and Si-O bond lengths for some $X_3SiOSiX_3$ molecules.

Vibrational Spectroscopy

In theory, force constants calculated from infrared, Raman, or microwave spectra through normal coordinate analysis should be excellent indicators of the extent of (d-p)π bonding since force constants can be used to calculate bond orders by means of the Siebert formula (42). The Siebert formula is a linear correlation between the total bond order

and the ratio of the actual force constant to that for an ideal single bond AB, this being defined as $7.2 \times (Z_A Z_B / n_A^3 n_B^3)$ where Z is the atomic number and n the principal quantum number. In practice, however, the calculation of force constants is difficult especially for complex molecules and often is uncertain because of the numerous assumptions made. Therefore, even when force constants are available, the wide variations observed in published values, e.g., 5.56 and 5.05 mdyne/Å for the Si-O bond in $H_3SiOSiH_3$ (43,44) render any conclusions deduced from them exceedingly questionable.

Vibrational studies (45) have shown $X_{4-n}Si(NMe_2)_n$ (where X = H, Cl, Me and n = 0 to 4) compounds to have Si-N and Si-Cl bond orders greater than one. The calculated Si-Cl Siebert bond order of 1.3 from the reported force constant (45) of $(Me_2N)_3SiCl$ seems to indicate moderate (d-p)π bonding resulting in a corresponding shortening of the Si-Cl bond, when in fact, the observed bond length (7) is 0.03 Å longer than the Schomaker-Stevenson "single" bond length. Therefore, this further demonstrates the unreliability of force constant data in determining bond orders.

Höfler calculated force constants for the Si-C bond for $Ph_{4-n}SiX_n$ (where X = H, Cl, F, OH for n = 0 to 4) and found the force constants ranged from 3.06 to 3.44 mdyne/Å (46); these force constants correspond to Siebert bond orders of 1.1 to 1.2. Although the reported force constant of 3.44 mdyne/Å for the Si-C bond in $PhSiF_3$ (46) seems to indicate a moderate amount of (d-p)π bonding in the related compound

$MeSiF_3$ where no (d-p)π bonding is possible, the calculated force constant for the Si-C bond is 3.47 mdyne/Å (47). Consequently, the increased force constant must result from inductive effects (-I) rather than (d-p)π bonding. Comparison of the force constants for the Si-C bond for Ph_3SiH (46), 3.30 mdyne/Å with Me_3SiH (48), 2.97 mdyne/Å indicates increased bond order due to (d-p)π bonding. Therefore, the large force constants Höffler (46) observed can be interpreted as arising from both inductive effects and (d-p)π bonding.

A recent study of the molecular geometry of the series $Me_nSi(NCX)_{4-n}$ (where n = 0 to 3, X = S, O) by both infrared spectra and dipole moments indicates a linear structure for Si-N-C-X chains (49). A C_{3v} symmetry for monofunctional silicon compounds is unambiguously revealed by comparison of the IR spectra with that of the carbon analogs (39), which have structures that are bent at the N. The structural differences between the silicon and carbon compounds can be attributed to (d-p)π bonding in the former.

The extent of delocalization of nonbonding electron pairs can be determined by infrared measurements of acidity and basicity. In the absence of (d-p)π bonding, since silicon is more electropositive than carbon, silicon will attract bonding electrons less than carbon; consequently SiNH, SiOH, and SiSH compounds should be weaker acids than the corresponding carbon derivatives, while N, O, and S when linked to silicon should exhibit stronger Lewis base properties.

However, if the nonbonding pairs on N, O, or S are delocalized by (d-p)π bonding, the opposite behavior would result.

Ulbricht and coworkers (50) measured the oxygen basicity of the series $Me_{4-n}M(OEt)_n$ (where M = C, Si) by observing changes in the O-H stretching frequency of phenol. The results were that the oxygen basicity of Me_3SiOEt is lower and that of $MeSiOEt_3$ and $SiOEt_4$ is higher than the oxygen basicity of the corresponding carbon derivatives. The oxygen basicity in both species declines with the increasing number of ethoxy groups which is consistent with the inductive effect (-I) of the ethoxy group. The smaller decrease in the ethoxysilane series was ascribed to the lower transmission of the ethoxy electronic effect through the silicon and was argued (50) to be a result of both inductive (+I) and (d-p)π effects.

The basicity of silyamines and the corresponding carbon analogs was measured from the observed shifts in the C-D stretching frequencies of base and $CDCl_3$ (51). The results showed that the silylamines have a lower basicity and in fact $(Me_3Si)_3N$ had no effect on the C-D stretching frequencies at all; these results suggest that the nonbonding electron pair on nitrogen is engaged in (d-p)π bonding with silicon. Another study found the basicities of the compounds $R_3Si(CH_2)_nNH_3$ to be anomalously low when n is zero (52). An explanation for this observation is delocalization of the nitrogen lone pair by (d-p)π bonding. Lastly, West and coworkers (53) determined the thermodynamic constants

for hydrogen bonding of phenol to several siloxanes and alkoxysilanes, as well as to alkythiosilanes, by variable temperature infrared spectroscopy. The results indicated that the siloxanes are weaker bases than the corresponding ethers and the alkylthiosilanes are also significantly less basic than the corresponding dialkyl sulfides. These results are consistent with (d-p)π bonding between the Si-N and Si-S bonds.

Quantum Chemical Calculations

Quantum chemical calculations can possibly be useful in the determination of relative amounts of (d-p)π bonding. Parkanyi and coworkers (25) employing the Pariser-Parr-Pople (PPP) SCF method calculated π-bond orders of 0.325 and 0.346 for the C-N and Si-N bond, respectively, for tetramethyl N,N'-diphenylcyclodisilazane. Using the PPP SCF method, Perkins (54) calculated a (d-p)π bond energy of 67 kJ per Si-N bond in trisilylamine.

PPP and Del Re calculations were carried out on $PhNMe_2$, $(Me_3Si)_2NPh$, and $(Me_2HSi)_2NPh$ (55) and the reliability of the results was evaluated by comparing calculated ultraviolet spectra and dipole moments with experimental values. The results of these calculations (55) indicated that (d-p)π bonding between silicon and nitrogen reduces the Ph-N π-bond order from 0.346 in $PhNMe_2$ to 0.275 in $(Me_3Si)_2NPh$ and $(Me_2HSi)_2NPh$.

Quantum calculations were reported on the effects of silyl substituents on ethylene and benzene. Horn and

Murrell (56) employing ab initio SCFM calculations on ethylene, vinylsilane, and allylsilane found that inclusion of d orbitals in the basis set gave a better interpretation of the photoelectron spectra than their exclusion. Similar results were found by McLean (57) for the CNDO/2 calculation of the photoelectron spectra of phenylsilane and trimethylphenylsilane. Zeeck (58) showed that the inclusion of silicon d functions in ab initio SCFM calculations gives a quantitatively more accurate description of the bathochromic shift in the U.V. spectra produced by silicon substitution for vinylsilane and propene than does the exclusion of d orbitals. All three groups agree that (d-p)π interactions are significant.

A CNDO/2 calculation of the photoelectron spectrum of $Me_2Si(SMe)_2$ showed that (d-p)π bonding is significant (59). This result is consistent with a recent ultraviolet spectroscopic study (60) of ring and open chain compounds containing S-Si and S-Si-S bonds in which the n-σ^* transition showed a blue shift as compared with that in the analogous carbon compounds. The blue shift was ascribed to a (d-p)π interaction between the lone electron pair of sulfur and the d orbitals of silicon (60).

NMR Spectroscopy

It has been shown both experimentally and theoretically that chemical shifts of ^{13}C (61-64), ^{14}N or ^{15}N (65-68), ^{17}O (69-72), and ^{29}Si (73-75) can be strongly influenced both by inductive effects and by the π-electron density at the

observed nucleus. Although the theory of nuclear shielding is well established, it is not always possible to quantitatively relate observed chemical shifts, especially those of ^{29}Si, to theoretical concepts because of the complexity of the factors involved. The shielding constant of a nucleus can be presented as a sum of local and long range effects (76):

$$\sigma = \sigma^{d}_{loc} + \sigma^{p}_{loc} + \sigma' \qquad [1]$$

where the local contribution is further divided into a diamagnetic term, σ^{d}_{loc} and a paramagnetic term, σ^{p}_{loc}. The long range effects (σ') are contributions from other atoms in the molecule and include such factors as electric field, magnetic anisotropy and dispersion effects. The local diamagnetic term depends on the electron density at the nucleus and is given by Lamb's formula (77):

$$\sigma^{d}_{loc} = (\mu_0 e^2/12m\pi) \sum_i P_{ii} \langle r_i^{-1} \rangle \qquad [2]$$

where μ_0 is the permeability constant, e and m are the magnitudes of the electronic charge and the electronic mass, respectively, and P_{ii} is the charge density in the atomic orbital i which is at an average distance of r_i from the nucleus. Therefore, σ^{d}_{loc} is influenced by substituent electronegativity; substitution by an electronegative atom or group causes a reduction in the electron density at the nucleus in question, resulting in a downfield shift of the resonance. The local paramagnetic term may be written (78):

$$\sigma^{p}_{loc} = (-\mu_0 e^2 \hbar^2/6\pi m^2 \Delta E)[\langle r^{-3} \rangle_p P_u + \langle r^{-3} \rangle_d D_u] \qquad [3]$$

where ΔE is an average excitation energy (AEE), $\langle r^{-3} \rangle_p$ and $\langle r^{-3} \rangle_d$ are the mean inverse cubes of the distance of the valence shell p and d electrons, respectively from the nucleus, and P_u and D_u represent the unbalance of the p and d electron populations, respectively. The last terms, P_u and D_u include elements of the charge density and bond order matrix.

Problems in theoretical calculation of chemical shifts arise because of the need to employ a number of simplifying assumptions. Firstly, it is usually assumed that local effects dominate in nuclear shielding. This assumption is not always valid; for example, in nitrogen shielding, although $\sigma^d_{non\text{-}loc}$ is negligible, $\sigma^p_{non\text{-}loc}$ can be appreciable, particularly in cases of multiple bonding (79,80). Secondly, although it is generally assumed that changes in σ^p_{loc} are dominant for heavier nuclei as compared to σ^d_{loc}, this assumption has been strongly challenged (81-83). For nitrogen shieldings, σ^d_{loc} is approximately constant for nitrogen nuclei in a variety of molecular environments (84,85). Thirdly, although most calculations of nuclear shielding have employed the AEE approximation, this method is only successful in accounting for gross chemical shift trends in series of closely related molecules. Furthermore, a CNDO/2 calculation of ^{29}Si shielding in $Me_{4-n}SiX_n$ compounds has shown the assumption of a constant ΔE in σ^p_{loc} to be invalid (86). Fourthly, for ^{29}Si chemical shifts, there is the additional problem as to whether the d-orbital term can be neglected since the d-orbital term becomes important if

there is (d-p)π bonding. Consequently, it is apparent from the preceding discussion that a quantitative theoretical treatment of nuclear shielding is often impossible because of oversimplification of theory. Therefore, in most cases chemical shifts can only provide a qualitative interpretation of bonding.

Only two theoretical interpretations of ^{29}Si shielding have appeared in the literature. Both approaches neglected all the other terms in Eq. [1] except σ^{p}_{loc} which was used as given in Eq. [3] with the AEE approximation; neither considered the d orbitals of silicon.

The theory developed by Engelhardt and coworkers (87) was able to qualitatively predict ^{29}Si chemical shifts in compounds of the type $Me_{4-n}SiX_n$ by calculating relative paramagnetic screening constants, σ^*. In this model, only the $\langle r^{-3}\rangle_p P_u$ term in σ^{p}_{loc} with ΔE held constant is considered. In addition, the σ bonding structure was described by four localized orbitals with tetrahedral bond angles on silicon. In order to be able to predict experimental ^{29}Si chemical shifts, an empirical correction factor, f, must be included in the determination of σ^*. A mean deviation of $\pm$22.7 ppm was obtained between calculated and observed values of ^{29}Si chemical shift. Although Engelhardt and coworkers concluded that (d-p)π interactions are negligible, it is interesting to note that the X substituents most likely to π bond show the largest deviation between calculated and experimental results. In addition, a comparison of the ^{29}Si shielding

data of trimethylsilyl derivatives with the ^{13}C shielding data of the analogous t-butyl derivatives shows that the trend with electronegativity predicted by Engelhardt's theory is followed in the ^{13}C series but not in the ^{29}Si series. An angular correction factor was later introduced to account for rehybridization of the silicon atom for silanes with substituents of electronegatives significantly different from that of carbon (88). Wolff and Radeglia (89) qualitatively confirmed this model by CNDO/2 calculations for which the best results were found by neglecting d orbitals.

Ernst and coworkers (90) adopted the approached used by Letcher and Van Wazer (91,92) for ^{31}P chemical shifts to explain the different signs of the slopes observed in plots of $\delta^{29}Si$ vs. Hammett σ constants of X for a series of arylsilanes $XC_6H_4SiY_3$; the signs of the slope depended upon the nature of Y. This theory considers only changes in σ^p_{loc}, assumes the ratio $\langle r^{-3}\rangle_p/\Delta E$ is constant, neglects (d-p)π interactions, and derives chemical shift contributions from p electrons as a function of substituent electronegativities. Ernst successfully predicted the observed sign of the slope of these plots but could not predict the electronegativity of Y at which the sign changes; therefore, these results must be considered qualitative. In addition, Ernst was able to use a polynomial electronegativity summation over all the substituents in $R^IR^{II}R^{III}R^{IV}Si$ compounds to generate the observed U-shaped relationship between silicon-29 shielding and the sum of substituent electronegativity. The calculations

generally reproduced the observed ^{29}Si shielding to within ±10 ppm. Unfortunately, Ernst and coworkers did not show how this theory can account for differences between the trends in ^{29}Si and ^{13}C shieldings of the analogous carbon derivatives.

One of the earliest qualitative models of ^{29}Si shielding was proposed by Lauterbur (93) to account for the observed ^{13}C and ^{29}Si shieldings in the series $Me_{4-n}M(OEt)_n$ (where M = C, Si). Lauterbur observed that as n increased the ^{13}C resonance was shifted downfield progressively while the ^{29}Si resonance exhibited a "sagging" pattern with the opposite behavior (Fig. 1-1). Lauterbur's model views ^{29}Si shielding as a result of inductive effects which should be similar for both nuclei and (d-p)π interactions in the silanes. Therefore, the significant differences in substituent effects between the two nuclei were attributed to (d-p)π bonding which increases the shielding of silicon by increasing the electron density on the silicon atom.

Hunter and Reeves (94) further elaborated on Lauterbur's model by demonstrating graphically a linear dependence of the ^{29}Si chemical shifts of Me_3SiX compounds upon the electronegativity of the X substituent, χ_X. The results showed that the most shielded silicon nuclei appear in compounds with the least electronegative substituents and that an additional shielding effect is operative for X = N, O, and F. Since these substituents have the highest capabilities to form π bonds, this additional shielding effect was ascribed to (d-p)π bonding. Harris and coworkers (95,96) in a more extensive study of trimethylsilyl

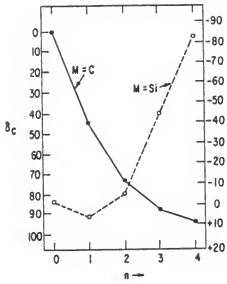

Figure 1-1. ^{13}C and ^{29}Si chemical shifts in the series $Me_{4-n}M(OEt)_n$ (where M = ^{13}C, ^{29}Si) (93). Shifts are in ppm relative to Me_4Si.

compounds found that ^{29}Si chemical shifts correlate poorly with substituent electronegativity (Fig. 1-2). Since $\delta^{29}Si$ does not vary smoothly with χ_X as Engelhardt's theory (87) predicts, Harris and coworkers (95,96) suggested that his theory is oversimplified. In addition, Harris found no correlation between ^{29}Si shielding and ^{13}C shielding of the trimethylsilyl group. Rakita and Worsham (97) reported ^{13}C chemical shift data of $Me_{4-n}SiX_n$ compounds and found that a replacement of a methyl by a first-row donor atom (C, N, O) leads to an upfield shift of the remaining methyls, regardless of the presence or absence of unshared pairs or π-type orbitals on the atom in question. These results suggest ^{29}Si chemical shifts in trimethylsilyl compounds depend on other factors beside simple inductive effects including (d-p)π bonding.

Data showing the effects of multiple α substitution on ^{29}Si shieldings for $Me_{4-n}SiX_n$ compounds are presented in Fig. 1-3 and Fig. 1-4. Data are from ref. 74 and references therein; data for X = Cl, $CH_2CH = CH_2$, $CH = CH_2$, and H are from refs. 98, 99, 100, and 98, respectively. Figure 1-3 shows the "sagging" pattern observed for electronegative substituents. This "sagging" pattern has been attributed to opposing (d-p)π bonding and inductive effects for these derivatives (93,94,101-104). The deshielding of the ^{29}Si nuclei with increasing n in the series $Me_{4-n}Si(SMe)_n$ is ascribed to dispersion forces and diamagnetic anisotropy of the C-S bond (102). In contrast to Fig. 1-3, no "sagging" pattern is observed for the substituents shown in Fig. 1-4.

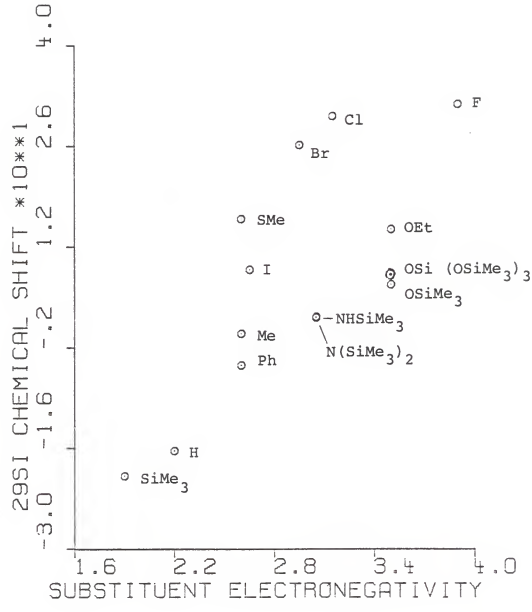

Figure 1-2. Plot of ^{29}Si chemical shifts vs. substituent electronegativity, χ_X, for trimethylsilyl compounds, Me_3SiX (95,96).

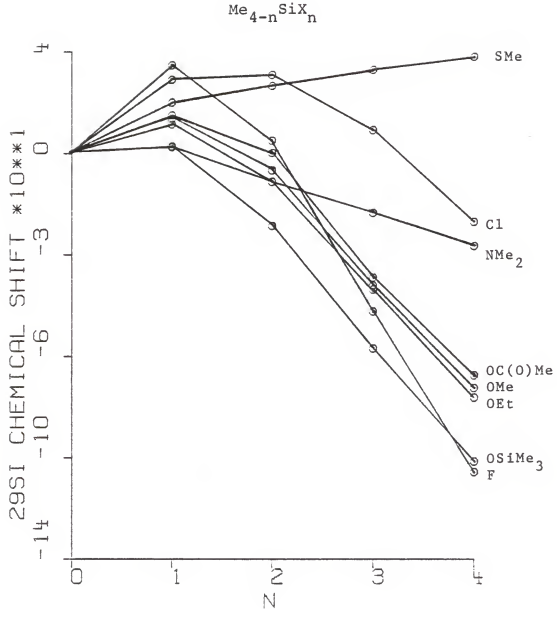

Figure 1-3. ^{29}Si chemical shifts (in ppm relative to Me_4Si) for methylsilanes $Me_{4-n}SiX_n$.

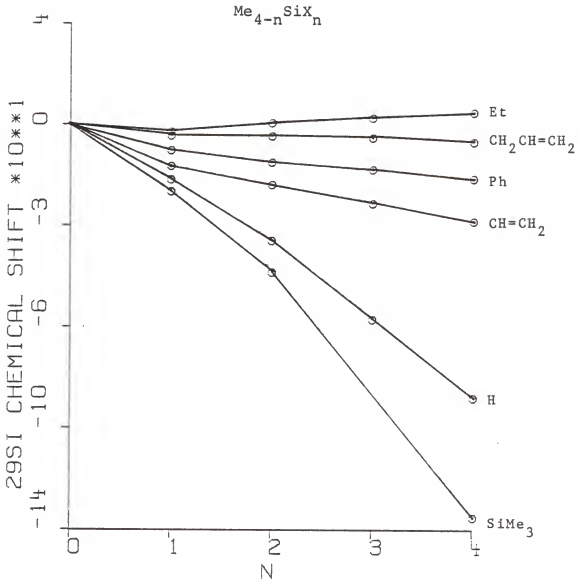

Figure 1-4. ^{29}Si chemical shifts (in ppm relative to Me_4Si) for methylsilanes $Me_{4-n}SiX_n$.

It has been suggested that this is caused by an absence of opposing (d-p)π bonding and inductive effects for these derivatives (74).

Several groups have reported NMR studies of alkenylsilanes. Schraml and coworkers (105) measured both ^{13}C and ^{29}Si chemical shifts of a series of $Me_{3-n}X_nSi(CH_2)_mCH=CH_2$ (where m = 0, 1). Their findings showed the ^{29}Si nuclei in vinylic compounds are shielded by several ppm more than in the corresponding ethyl or methyl silane. In the allyl compounds, silicon is less shielded and the olefinic carbons are more shielded than in the vinyl silanes. These results were attributed to delocalization of the π electrons of the vinyl group toward the silicon atom; for allyl compounds, this delocalization is decreased when compared to the vinylic compounds. Schraml also noted that this delocalization of π electron density could be assigned equally to (d-p)π bonding or to hyperconjugation (σ-π interaction). Pitt (106) from the results of CNDO/2 calculations of compounds containing Si, Ge, and Sn claimed hyperconjugation is dominant over (d-p)π bonding for delocalization of π electron density in bonds containing Si, Ge, and Sn. Since unfortunately, the NMR experiment cannot distinguish between the two effects and the prevailing theories support the (d-p)π bonding model over the hyperconjugation model, all delocalization phenomena involving silicon will be ascribed to (d-p)π bonding in this paper. In the series $Me_{4-n}Si(CH=CH_2)_n$ (where n = 0 to 4), the ^{29}Si nuclei are shielded about 6.5 ppm per vinyl group, the protons of the vinyl group in the

organosilane are deshielded with respect to the vinylic protons in the carbon analog, and the α-carbon is shielded and the β-carbon is deshielded as compared to the corresponding carbons in the carbon analog (100). These results were attributed both to a mesomeric (-M) effect from the vinyl group to the Si atom and to the electron-supplying inductive effect (+I) of the Me_nSi group. A similar interpretation of the observed ^{13}C shieldings of the vinylic carbon was offered in the series $CH_2 = CHMX_3$ (where M = C, Si) (107); the results showed that the α-carbon is shielded and the β-carbon is deshielded with respect to the hydrocarbon analog. Lastly, a ^{29}Si NMR study (108) indicated that the phenyl derivatives are shielded in comparison with the corresponding benzyl derivatives and that both phenyl and benzyl silanes are shielded with respect to the methyl derivatives. These results were discussed in terms of (d-p)π bonding with a minor contribution to shielding from ring current effects.

Scholl and coworkers (109) were one of the first groups to note the increased sensitivity of ^{29}Si chemical shifts to substituent effects in X_3SiOR as compared to X_3SiCH_2R compounds. In a later study of silicon shielding in compounds containing a Me_3SiOC fragment, Schraml and coworkers (110) found the large sensitivity of ^{29}Si shielding to substitution is comparable to substituent effects of multiply bonded carbon. Schraml and coworkers (111) in a recent study found the sensitivity of silicon shielding to substituent effects (change in R) in $Me_{4-n-m}Cl_nSi(OR)_m$ decreases with

increasing numbers of chlorines or oxygens bonded to silicon. This result was interpreted in terms of competing (d-p)π back-bonding to silicon from both chlorine and oxygen.

Harris and Kimber (103) reported the ^{17}O chemical shifts of methylethyoxysilanes which are shown in Table 1-4. The ^{17}O shielding in the series $Me_nSi(OEt)_{4-n}$ shows a U-shaped dependence of ^{17}O shielding upon n with a maximum for n = 2. These results were interpreted in terms of the scheme proposed by Jaffé (112) in which the effectiveness of π-bonding in reducing electron density at oxygen decreases as the number of alkoxy groups increases. However, comparison of the ^{17}O shielding of methylethoxysilanes with the corresponding carbon analogs (113) (see Table 1-4) shows the silicon derivatives to be more shielded. This implies the ^{17}O shielding of siloxanes is dominated by a strong inductive (+I) effect of silicon with only a small contribution from (d-p)π effects. A recent determination of the ^{17}O shielding of hexamethyldisiloxane (43 ppm) (114) and di-t-butyl ether (90 ppm) (114) also further supports this interpretation.

Table 1-4. Comparison of ^{17}O Chemical Shifts[a] of Siloxanes and the Corresponding Ether.[b]

Siloxane	$\delta^{17}O$/ppm	Ref.	Ether	$\delta^{17}O$/ppm	Ref.
Me_3SiOEt	10	(103)	Me_3COEt	--	--
$Me_2Si(OEt)_2$	25	(103)	$Me_2C(OEt)_2$	52.0	(113)
$MeSi(OEt)_3$	21	(103)	$MeC(OEt)_3$	58.5	(113)
$Si(OEt)_4$	9	(103)	$C(OEt)_4$	56.5	(113)
$Me_3SiOSiMe_3$	43	(114)	Me_3COCMe_3	90	(114)

[a] All shift references to external $H_2{}^{17}O$.

[b] Me = CH_3 and Et = CH_2CH_3.

Several groups have reported NMR studies of silylamines. Jancke and coworkers (115) measured the ^{29}Si shielding of 17 silylamines; their results showed that increasing the number of nitrogens bonded to silicon results in increased shielding. Although no explanation was offered for this observation, it is apparent that (d-p)π bonding is responsible for the higher shielding. In a recent ^{15}N and ^{29}Si NMR study of the Si-N bond in silylamines, Filleux-Blanchard and Nguyen Dinh An (116) observed that increasing the number of chlorines bonded to silicon in N,N-dimethylaminosilanes, N,N-diethylaminosilanes, and N,N-diisopropylaminosilanes results in higher shielding of the ^{29}Si nuclei while the ^{15}N nuclei become deshielded. These results were attributed to increased nitrogen pair delocalization which is enhanced through inductive effects (-I) of the chlorine bonded to silicon. The first nitrogen NMR

investigation of the Si-N bond determined ^{14}N chemical shifts of six silylamines (117). The results, which were interpreted in terms of the (d-p)π bonding model, showed that an increase in the number of alkoxy groups attached to silicon increases ^{14}N shielding; hence, the delocalization of the lone pair electrons of nitrogen is decreased. Nöth and coworkers (118) in a latter study by ^{14}N and ^{11}B NMR on 39 silylamines and 19 silylaminoboranes interpreted both the ^{14}N and ^{11}B shieldings in terms of the Si-N (d-p)π bonding model. Comparison of ^{14}N shieldings of $(Me_3Si)_nNR_{3-n}$ with H_nNR_{3-n} for n = 1, 2, 3 shows a deshielding of the ^{14}N resonance upon introduction of a trimethylsilyl group. This observation was accounted for by contributions from the well-known β effect and (d-p)π bonding. Increasing the number of chlorines bonded to silicon deshields the ^{14}N nuclei. Although Nöth and coworkers (118) attributed this result to the -I effect of the chlorine and to better (d-p)π overlap, it is apparent from a theoretical viewpoint that the inductive effect of chlorine will increase shielding of the nitrogen nucleus, and hence (d-p)π bonding alone is responsible for this deshielding. The high field shifts of the methoxysilylamines were interpreted by Nöth and coworkers (118) in terms of a weakening of the Si-N bond which raises the electron density of the nitrogen through the resonance of the methoxy groups. In addition, the

$$Me—\ddot{\underset{\cdot\cdot}{O}}\text{-}Si = N \rightleftarrows Me—\ddot{O} = Si\text{-}\ddot{N}$$

deshielding of the ^{14}N nucleus in the series Me_3SiNMe_2 (-374 ppm), $(Me_3Si)_2NMe$ (-370 ppm), and $(Me_3Si)_3N$

(-344 ppm) was ascribed to increased delocalization of the nitrogen lone pair of electrons. Lastly, the results of a more recent study of ^{14}N shieldings of trimethylsilylamines (119) showed the ^{14}N shieldings are influenced by the strong +I effect of the trimethylsilyl groups (shielding) with a small contribution from (d-p)π effects (deshielding).

Nuclear spin-spin coupling like nuclear shielding can provide information on bonding since the indirect coupling is transmitted via the electronic system of the molecule. The calculation and interpretation are usually based on Ramsey's formulation (120). Within this framework the spin-spin coupling constant, J(A-B), between nuclei A and B is expressed as a summation of contributions arising from the

$$J(A\text{-}B) = J(A\text{-}B)_C + J(A\text{-}B)_O + J(A\text{-}B)_D \qquad [4]$$

contact, orbital, and dipolar interactions, respectively. The contact interaction arises from electrons which are in orbitals having a finite density at the nucleus. The orbital term accounts for the interaction between the nuclear magnetic moments and the field produced by the orbital motions of the electrons. The dipole interaction arises from a dipole-dipole interaction between nuclear and electron spins.

Self-consistent perturbation theory (SCPT) calculations employing the INDO-MO method have been used most frequently and successfully in the calculations of indirect spin-spin coupling. The expressions of various contributions to J(A-B) using this method were developed by Blizzard and Santry (121).

Excluding d orbitals, the orbital term is given by

$$J(A\text{-}B)_O = \frac{\hbar}{3\pi^2}\,\mu_O\mu_B^2\gamma_A\gamma_B\langle r_A^{-3}\rangle_p\langle r_B^{-3}\rangle_p[P_{zBzB}+P_{yBzB}+P_{xBzB}] \quad [5]$$

where μ_B equals the Bohr magneton, γ_A and γ_B represent the magnetogyric ratios of nuclei A and B respectively, and the P's refer to the first order elements of the charge-density, σ and π bond-order matrix. The dipolar term excluding d orbitals appears as

$$J(A\text{-}B)_D = \frac{\hbar^3}{10\pi^2}\,\mu_O\mu_B^2\gamma_A\gamma_B$$

$$\langle r_A^{-3}\rangle_p\langle r_B^{-3}\rangle_p[2P^{\alpha\alpha}_{zBzB}-P^{\alpha\alpha}_{xBxB}-P^{\alpha\alpha}_{yByB}+3P^{\alpha\beta}_{xBzB}-3Q^{\alpha\beta}_{yBzB}] \quad [6]$$

where the superscripts α and β refer to the spin orbitals with α and β spins respectively and $Q^{\alpha\beta}$ is the imaginary part of the first order matrix. The contact term is given by

$$J(A\text{-}B)_C = \frac{16\hbar}{9}\,\mu_O\mu_B^2\gamma_A\gamma_B S_A^2(0)S_B^2(0)P^{\alpha}_{S_AS_B} \quad [7]$$

where $S_A^2(0)$ and $S_B^2(0)$ are the electron density in the s-valence orbitals at the nucleus of atoms A and B respectively and $P^{\alpha}_{S_AS_B}$ is a diagonal element of the first-order σ bond order matrix of orbitals S_A and S_B. The integrals $S_A^2(0)S_B^2(0)$ and $\langle r_A^{-3}\rangle_p\langle r_B^{-3}\rangle_p$ are usually treated as empirical parameters which are evaluated from the best least-squares agreement between the calculated and experimental coupling constants.

From Eqs. [5] and [6], it is apparent that the orbital and dipolar terms are only important for atoms having valence p electrons. Consequently, these contributions vanish if the

spin-spin coupling involves a proton. The contact contribution is also usually the dominant term for other nuclei which are singly bonded. Since both the orbital and dipolar terms depend upon the expectation value of the inverse cube of the radius of the orbitals on atoms A and B and elements of the π-bond order matrix, in cases of multiple bonding, these terms increase in magnitude and can dominate the spin-spin interaction. For example, INDO calculations have shown that $^{1}J(^{15}N{=}^{13}C)$ and $^{1}J(^{15}N{\equiv}^{13}C)$ are dominated by non-contact interactions (122-124) whereas $^{1}J(^{15}N{-}^{13}C)$ is dominated by the Fermi contact interaction (122-127). A similar situation holds for $^{1}J(^{13}C{-}^{13}C)$ which is dominated by the contact contribution where the bond is single, as compared to multiply bonded carbon in which there is a significant contribution from the orbital and dipolar terms (128,129). Thus, significant contributions from the non-contact terms to $^{1}J\ (^{29}Si^{13}C)$ and $^{1}J\ (^{29}Si^{15}N)$ may be taken as evidence of the (d-p)π bonding in those compounds.

Equation [7] indicates that when the contact term is dominant, the spin-spin coupling will depend upon the amount of s character in the single bond joining the nuclei. Thus, based on an INDO-MO calculation of hybridization parameters, the following relationship was derived for $^{1}J(^{13}C^{1}H)$ (130):

$$^{1}J(^{13}C^{1}H) = 5.7 \quad (\%\ s) - 18.4\ [Hz] \qquad [8]$$

An empirical expression was found for $^{1}J(^{13}C_X{}^{13}C_Y)$ (131):

$$^{1}J(^{13}C_X C_Y) - 7.3 \quad (\%\ s_X) \quad (\%\ s_Y) - 17\ [Hz] \qquad [9]$$

while an expression for $^{1}J(^{15}N^{13}C)$ based upon the finite perturbation technique employing the INDO-MO method was derived (124):

$$^{1}J(^{15}N\text{-}^{13}C) = -94 \quad (\%\ s_N) \quad (\%\ s_C) \qquad [10]$$

However, some deviations from the linearity implied by Eq. [10] are observed for singly bound $^{1}J(^{15}N\text{-}^{13}C)$ values even when the Fermi contact term dominates the coupling. These deviations are attributed to the effects of lone-pair electrons in orbitals with s character on the coupled nuclei (124). The presence of lone pairs in orbitals with p character does not interfere with the linear relationships given by Eq. [10]. Similar deviations have been revealed through finite perturbation (FP) (132) and sum-over-states perturbation (SOS) (133) calculations employing the INDO-MO method of some $^{15}N\text{-}^{15}N$ couplings. Since nitrogen is invariably planar (lone pair electrons are contained in a p orbital) when bonded to two or three Si atoms, these types of deviations between the $^{1}J(^{29}Si^{15}N)$ and s character of the Si and N atoms are not expected. However, these deviations may be observed for a single silyl group bonded to nitrogen, since available structural data indicates the nitrogen is not always planar in these types of molecules.

If the Fermi contact term is dominant, removal of electron density brought about by substitution by an electronegative substituent will increase the effective nuclear charge of the nucleus in question. This augments the probability of the valence s electrons for nuclear contact and hence, an increase of J(A-B) should result. Consequently, correlations of J(A-B)

with substituent inductive parameters, i.e., electronegativity, are often taken to indicate the dominance of the contact contribution. For example, a linear correlation was found between the $^1J(^{29}Si^{13}C)$ of Me_3SiX compounds and substituent electronegativity, χ_X, (95,96) which is shown in Fig. 1-5. The relationship is

$$|^1J(^{29}Si^{13}C)| = 8.00\ \chi_X + 31.6 \qquad [11]$$

In addition, Harris and coworkers (95,96) showed that there is a linear relationship between $^1J(^{29}Si^{13}C)$ in trimethylsilyl compounds and $^1J(^{13}C^{13}C)$ in the corresponding t-butyl derivatives (134) (see Fig. 1-6):

$$|^1J(^{29}Si^{13}C)| = 1.65\ (^1J(^{13}C^{13}C)) - 6.46 \qquad [12]$$

From these results, Harris concluded that the Fermi contact term is the dominant contribution to spin-spin coupling and that the silicon d orbitals do not participate to any great extent in the Si-C bondings, or, if they do, their participation varies smoothly with the same substituent parameters that determine the coupling. The variation in $^1J(^{29}Si^{13}C)$ for the series of methylethoxysilanes $Me_{4-n}Si(OEt)_n$ was investigated by the same authors (103). It was concluded that since these changes were too large to be attributed solely to s-character variations, another mechanism, possibly (d-p)π bonding, contributes to the coupling.

Other groups have investigated the dependence of $^1J(^{29}Si^{13}C)$ upon various theoretical and experimental parameters. Levy and coworkers (135) were the first group to note a rough

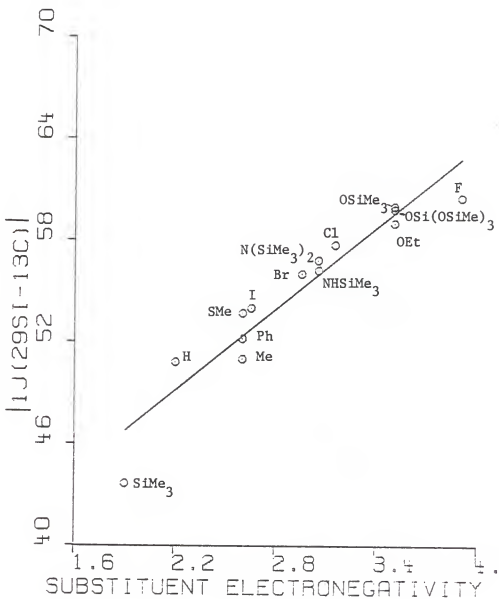

Figure 1-5. Plot of $|^{1}J(^{29}Si^{13}C)|$ vs. substituent electronegativity in Me_3SiX compounds (95,96).

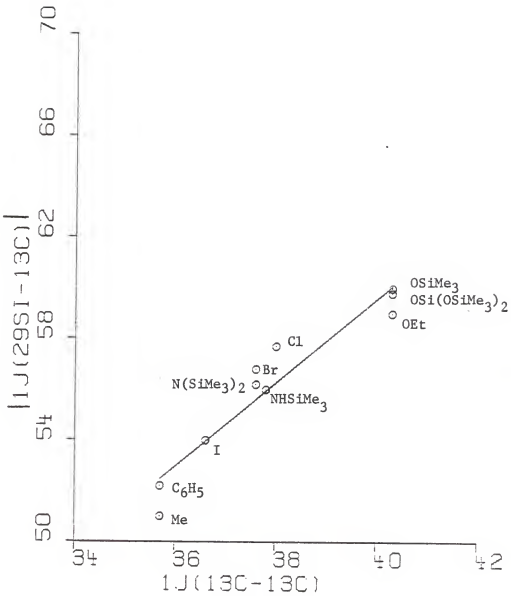

Figure 1-6. Plot of $|^{1}J(^{29}Si^{13}C)|$ in Me_3SiX vs. $^{1}J(^{13}C^{13}C)$ in Me_3CX compounds (95,96). The value of $^{1}J(^{13}C^{13}C)$ for NH_2 has been used with $^{1}J(^{29}Si^{13}C)$ for $N(SiMe_3)_2$ and $NHSiMe_3$ and the value of $^{1}J(^{13}C^{13}C)$ for OMe has been used with $^{1}J(^{29}Si^{13}C)$ for OEt, $OSiMe_3$, and $OSi(OSiMe_3)_3$.

proportionality between the magnitude of $^{1}J(^{29}Si^{13}C)$ and the s character of the carbon nucleus in several organosilanes containing only Si, C, and H. Kovacević and Maksić (136), through calculations based on the maximum overlap approximation method, reproduced this trend and derived a relationship between $^{1}J(^{29}Si^{13}C)$ of these compounds and the s character of the bonded carbon and silicon atoms:

$$^{1}J(^{29}Si^{13}C) = 5.554 \quad (\%\, s_C) \quad (\%\, s_{Si}) + 18.2 \text{ [Hz]} \text{ [13]}$$

These calculations neglected silicon d orbitals and assumed the Fermi contact term is dominant. The results showed that the hybridization of the Si atom remains approximately sp^3. Dreeskamp and Hildenbrand (137) investigated couplings to silicon in tetravinylsilane as well as in some vinyl- and chloro-silanes. They found $^{1}J(^{29}Si^{13}C)$ to be proportional to the s character of the orbitals forming this bond whereas $^{2}J(^{29}SiCH)$ depends on the hybridization of both the silicon atom and of the intervening carbon atom.

Summerhays and Deprez (138), employing the FP-INDO method, calculated $^{1}J(^{29}Si^{13}C)$ of trimethylsilyl compounds and compared their results with the experimental data of Harris and Kimber (95). These calculations assumed the contact term is dominant and the silicon d orbitals were neglected. Although the calculated results generally reproduce the experimental data, the largest deviations (ca. 10% lower than experimental values) are for substituents (N, O) most likely to (d-p)π bond. Consequently, it was concluded that the contact term alone is adequate to reproduce the trends of $^{1}J(^{29}Si^{13}C)$ and that inclusion of

silicon d orbitals in the basis set will improve the overall agreement between calculated and experimental constants. Beer and Grinter (139) using an sp basis set in FP-INDO calculations calculated 20 $^{1}J(^{29}Si^{13}C)$ values. Their results indicated that the orbital and dipolar terms are of opposite signs and that the combined non-contact contributions are less than 1% of the observed coupling, and that inclusion of silicon d orbitals is not required. However, since their data set excluded siloxanes and silylamines which are compounds most likely to have $(d\text{-}p)\pi$ bonds, the latter conclusion may not be necessarily valid. Lastly, in a recent calculation of 30 $^{1}J(^{29}Si^{13}C)$ by SCPT-INDO calculations, Duangthai and Webb (140) showed that $^{1}J(^{29}Si^{13}C)$ is dominated by the contact interaction. The orbital terms are larger and the dipolar terms are smaller than the previously reported values (139); the combined non-contact contributions are less than 4% of the observed coupling. The authors concluded that the $^{1}J(^{29}Si^{13}C)$ data are satisfactorily reproduced by calculations employing a sp basis set. Since, however, only three siloxanes and no silylamines were included in their data set, this conclusion is questionable.

Randall and Zuckerman (141), from observations of moderate variations of $^{1}J(^{15}N^{1}H)$ in $Me_3M\text{-}NH\text{-}Ar$ (with M = C, Si, Ge), concluded that there is no stereochemical evidence for $(d\text{-}p)\pi$ bonding in these compounds. Their conclusion was based upon the Randall equation (142):

$$\% \, s_N = 0.34 \, |^{1}J(^{15}N^{1}H)| \ [Hz] \qquad [14]$$

which was derived independently of the Binsch equation (143):

$$\% s_N = 0.43 \left| {}^1J(^{15}N^1H) \right| - 6 \text{ [Hz]} \qquad [15]$$

Equations [14] and [15] were established on the basis of tetrahedral and trigonal-planar nitrogen geometries. In a later study of $^1J(^{15}N^1H)$ in N-P, N-As, N-S, and N-Si compounds, Cowley and Schweiger (144) measured $^1J(^{15}N^1H)$ in $(Me_3Si)_2NH$ and $(H_3Si)_2NH$. On the basis of Eqs. [14] and [15], these compounds are predicted to possess sp^3 hybridized nitrogen bonding orbitals. However, electron diffraction studies (14,23) of these compounds indicate the nitrogens are planar (sp^2). Therefore, it was concluded that the Randall and Binsch equations are not applicable when the atoms bonded to nitrogen have very different electronegativities from that of carbon.

No investigations of the dependence of $^1J(^{29}Si^{15}N)$ upon theoretical or experimental parameters have been reported. To this author's knowledge, there are only six published values of $^1J(^{29}Si^{15}N)$; these are listed in Table 1-5. Nitrogen-15 enriched compounds were used for the determination of spin-spin couplings in these compounds.

Table 1-5. Published Values of $^1J(^{29}Si^{15}N)$.

Compound	$^1J(^{29}Si^{15}N)$/Hz	Ref.
$ClCH_2Si(OCH_2CH_2)_3N$	1.5	(145)
$(H_3Si)_3N$	+6	(146)
trans-$[PtI(PEt_3)_2\{H_2SiN(SiH_3)_2\}]$	+12	(147)
$H_3SiNCSe$	+15.1	(148)
H_3SiNCS	+16.8	(148)
H_3SiNCO	+18.6	(148)

Dynamic (variable-temperature) NMR spectroscopy can be useful in the determination of inversion and rotational barriers. Overlap of d-p orbitals may be involved in the lowering of the C-N rotational barrier between cisoid and transoid formation from 9.49 kJ/mol in $HC(O)NHCMe_3$ to 83.2 kJ/mol in $HC(O)NHSiMe_3$ (149). In this case the electron-donating inductive (+I) effect of silicon should favor the resonance shown below, thus increasing the rotational barrier.

A ^1H NMR study (150) of eight silylamines including bis-(Dimethylamino)methylphenylsilane and trimethylsilylaziridine showed equivalent N-methyl and methylene groups at temperatures as low as 145°K, corresponding to a free energy barrier of less than 33.6 kJ/mole. Many phosphinoamines, on the other hand, show much larger barriers ranging from 61.3 kJ/mole for $PhPClN(i\text{-}Bu)_2$ to less than 33.6 kJ/mole for F_2PNMe_2 (151). Even higher free energy barriers are found for sulfenamines ranging as high as 74.7 kJ/mole for $ArSN(Ph)CH_2Ph$ (152). These results suggest lone pair repulsion as the dominant factor affecting rotational barriers. This explains the low rotational barrier in silylamines, where there is only one lone pair, and the increase in the free energy barrier in going from phosphinaomines to sulfenamines, increasing the number of interacting lone pairs from two to three.

In another ^{1}H NMR study (153) of barriers to torsion around Si-N bonds in aminosilanes, the free energy barrier to rotation for N,N-diisopropylaminophenyldichlorosilane was shown to be 37 kJ/mole at the coalescence temperature of 176°K. Spectra of other N,N-diisopropylaminosilanes showed the isopropyl doublets broadened and apparently coalescing in the region of 173°K ± 5°K but upon further cooling, the spectra remained broad and did not split out into discrete frequencies. Spectra of N,N-diethyl- and N,N-dimethyl-silylamines showed no broadening at temperatures above 170°K. In a recent ^{13}C NMR study (116) of the barrier to rotation in N,N-dimethyl-, N,N-diethyl-, and N,N-diisopropyl-silylamines, no splitting of signals could be observed down to temperatures as low as 145°K for the N,N-dimethyl- and N,N-diethyl-silylamines. A free energy barrier to rotation of 32 kJ/mole and 37 kJ/mole was measured for N,N-diisopropylaminodiphenylchlorosilane, and N,N-diisopropylaminophenyldichlorosilane, respectively. These results suggest the barrier to rotation in silylamines is largely steric in nature with only a minimal contribution from (d-p)π bonding.

Summary of the Literature Findings

Although there is a considerable amount of evidence for (d-p)π bonding in Si-N and Si-O bonds and to a lesser extent in Si-C (unsaturated carbon), Si-S, and Si-Cl bonds, the (d-p)π bonding model is controversial. From available structural data, the bond lengths and angles of Si-N and Si-O bonds

seem to indicate (d-p)π bonding; for Si-C, Si-S and Si-Cl bonds, there appears to be little or no (d-p)π bonding. For silylamines, nitrogen is invariably planar when linked to two or more silicons but for a single silicon nitrogen may or may not be trigonal planar. Vibrational studies have revealed evidence of (d-p)π bonding in Si-C, Si-N, and Si-O bonds. Measurements of acidity and basicity by infrared spectroscopy showed that compounds containing Si-N, Si-O, and Si-S bonds are weaker bases than the corresponding carbon analog; this is attributed to (d-p)π bonding. Quantum calculations provide evidence of (d-p)π bonding in Si-C (unsaturated carbon), Si-N, and Si-S bonds through calculations of (d-p)π bond orders and calculated photoelectron spectra. Shieldings of ^{29}Si, ^{17}O, and ^{14}N or ^{15}N of organosilanes have been interpreted qualitatively in terms of inductive and (d-p)π bond effects. The one-bond ^{29}Si-^{13}C coupling constant has been shown to be dominated by the Fermi contact interaction and the results have been interpreted in terms of an absence of (d-p)π bonding. There are too few data for $^{1}J(^{29}Si^{15}N)$ to permit conclusions to be drawn. Dynamic NMR studies have attributed the barriers to rotation in silylamines to steric effects with a negligible contribution from (d-p)π bonding.

Aim of the Investigation

The present NMR investigation was undertaken to obtain more information about the nature of Si-C, Si-N, Si-O, and Si-S bonds in organosilanes. Two types of organosilanes, namely methylsilanes and silylamines, were studied to see

if nuclear shielding and spin-spin coupling could provide some insight into the extent of (d-p)π bonding in these compounds. Since numerous trimethylsilyl compounds are readily available commercially and these are the easiest compounds for which to interpret substituent effects, most of the methylsilanes that were studied were trimethylsilyl compounds. In the NMR study of methylsilanes particular emphasis was placed on $^{1}J(^{29}Si^{13}C)$ in providing information of (d-p)π bonding. In addition, since few values of spin-spin coupling to silicon-29 have been reported, it would be interesting to relate these couplings to substituent effects. Finally, through a ^{1}H, ^{13}C, ^{15}N, and ^{29}Si NMR study of silylamines, it was hoped that information on the nature of the Si-N bond could be obtained. Of particular interest was relating the $^{1}J(^{29}Si^{15}N)$ to theoretical concepts since there is a paucity of data for this coupling.

CHAPTER II
EXPERIMENTAL

Materials

The compounds $(Et_2N)_nSiCl_{4-n}$ (where n = 1 to 3), $(Et_2N)_nSiMeCl_{3-n}$ (where n = 1, 2), and $(Me_2N)_nSiCl_{4-n}$ (where n = 1, 2) were synthesized. The other organosilanes were kindly donated by PCR Research Chemicals, Inc., Gainesville, Florida, or were purchased from Petrarch Systems, Inc., Bristol, Pennsylvania. These materials were used without any further purification. The solvents, acetone-d_6, benzene-d_6, chloroform-d_1, and dimethyl-d_6 sulfoxide, were obtained from Merck Sharp & Dohme Isotopes, St. Louis, Missouri.

Synthesis

Since chloraminosilanes are extremely sensitive towards atmospheric moisture (154), all synthesis experiments involving these compounds were carried out under a blanket of dry nitrogen in dried glassware. Benzene was dried by azeotropic distillation and anhydrous ether was used without further purification. These solvents were obtained from Fisher Scientific Company, Fair Lawn, New Jersey. Methyltrichlorosilane and tetrachlorosilane, which were generously donated by PCR Research Chemicals, Inc., Gainesville, Florida, were distilled before use. Anhydrous dimethylamine and diethylamines obtained from Eastman Kodak Company, Rochester, New York,

were used as obtained. Proton NMR spectra were used for purity determination. Mass spectral data obtained on the AEI MS30 interfaced with a KRATOS DS-55 data system operating at an ionising potential of 70 eV were used for structural confirmation.

N,N-Dimethylaminotrichlorosilane. The procedure for synthesis of this material illustrates the general method for preparation of chloraminosilanes. In a three-necked, 1-liter flask equipped with condenser, pressure-equalizing addition funnel, and magnetic stirrer were placed 94.4 g (0.55 mole) of tetrachlorosilane and 300 ml of anhydrous ether. The solution was cooled to -50°C in a dry-ice/methyl alcohol bath and treated with a solution of 50.0 g (1.10 mole) of anhydrous dimethylamine in 50 ml of anhydrous ether over a one hour period, causing formation of a voluminous precipitate of dimethylamine hydrochloride. Filtration through a sintered glass filter gave a white cloudy filtrate which was concentrated to ca. 150 ml by distillation at atmospheric pressure and fractionated through a 20 cm column filled with glass helices. The product N,N-dimethylaminotrichlorosilane is a white cloudy oil-like liquid, b.p. 45-46°C (19 mm) which fumes violently on contact with air. The mass spectral data for this compound is listed in Table 2-1.

Compounds prepared in an analogous fashion are listed in Table 2-2. Two equivalents of Me_2NH or Et_2NH were used for each Si-Cl bond to be replaced.

Table 2-1. Mass Spectral Data of N,N-Dimethylaminotrichlorosilane.

m/e	Relative Abundance	Assigned Formula
181	9.0	$C_2H_6NSi^{35}Cl^{37}Cl_2$
180	34.9	$C_2H_5NSi^{35}Cl^{37}Cl_2$
179	27.5	$C_2H_6NSi^{35}Cl_2{}^{37}Cl$
178	98.9	$C_2H_5NSi^{35}Cl_2{}^{37}Cl$
177	28.4	$C_2H_6NSi^{35}Cl_3$
176	100.0	$C_2H_5NSi^{35}Cl_3$
144	21.4	$C_2H_6NSi^{35}Cl^{37}Cl$
142	32.1	$C_2H_6NSi^{35}Cl_2$
137	11.0	$Si^{35}Cl^{37}Cl_2$
135	32.2	$Si^{35}Cl_2{}^{37}Cl$
133	32.3	$Si^{35}Cl_3$
63	14.1	$Si^{35}Cl$
44	34.3	C_2H_6N
42	52.4	C_2H_4N

Table 2-2. Chloraminosilanes Prepared.

Chlorosilane	Product	B.p. [°C(mm)]	Solvent	Synthesis Procedure
$SiCl_4$	Me_2NSiCl_3	45-46 (19)	Et_2O	(155) (gas phase)
$SiCl_4$	$(Me_2N)_2SiCl_2$	73 (10)	Et_2O	(155) (gas phase)
$SiCl_4$	Et_2NSiCl_3	55-60 (17)	Et_2O	(156)
$SiCl_4$	$(Et_2N)_2SiCl_2$	50-60 (2-4)	C_6H_6	(156)
$(Et_2N)_2SiCl_2$	$(Et_2N)_3SiCl$	115 (5)	C_6H_6	(156)
$MeSiCl_3$	$Et_2NSiMeCl_2$	60-70 (20-25)	C_6H_6	(157)
$MeSiCl_3$	$(Et_2N)_2SiMeCl$	95-105 (22-25)	C_6H_6	(157)

Mass spectra data which were obtained on each of the synthesized chloraminosilanes confirmed the structure of the isolated product. Facile interpretation of the mass spectral data was achieved through the recognition of the relative isotopic abundance of ^{35}Cl and ^{37}Cl in the ions. The prominent fragmentation pathways for N,N-dimethylaminochlorosilanes are loss of H, Cl, and NMe_2; for N,N-diethylaminochlorosilanes, they are loss of Me, Cl, Et_2N, and loss of both Et and Me to form a rearranged ion.

Sample Preparation

Since aminosilanes (154-157) and thiosilanes (158) are extremely sensitive to atmospheric moisture, solutions of these samples were prepared in a homebuilt Plexiglas dry-box under a dry N_2 (g) environment. Only solvents thoroughly dried over molecular sieve were used. The 80% v/v solutions were degassed by the freeze-pump-thaw technique and sealed under vacuum into 12 mm o.d. NMR sample tubes. These sealed NMR sample tubes were stored on dry ice. For the other organosilanes, the solutions were prepared outside the dry-box and contained in unsealed NMR sample tubes.

Spectrometer

All experiments for aminosilanes and thiosilanes were performed on a Nicolet NT-300 spectrometer equipped with a 293-C pulse programmer and a Nicolet 1280 computer. Spectra of ^{1}H, ^{13}C, ^{15}N, and ^{29}Si NMR were obtained at 300.07, 75.45, 30.41, and 59.61 MHz, respectively. These spectra were

obtained at ambient temperature, 22°C. For ^{15}N and ^{29}Si NMR spectra, sensitivity enhancement was obtained through the INEPT (159), INEPTD (160), and SPT (161-164) pulsed experiments. In addition to these techniques, a method was developed to decouple selectively a group of magnetically equivalent protons which are also used for polarization transfer; this method is discussed in Chapter III. These techniques transfer spin polarization from protons to nuclei such as ^{15}N via the scalar couplings between the nuclear spins involved, e.g., $J(^{15}N^{1}H)$. Theoretically, one can expect an enhancement factor of $\gamma(^{1}H)/\gamma(^{15}N) = 9.9$ for ^{15}N spectra and an enhancement factor of 5.0 for ^{29}Si spectra. Further gains in sensitivity can be expected within these methods, since faster pulse repetition rates are possible due to the shorter relaxation times of protons. The amplitude, $\gamma H_2/2\pi$, of the ^{1}H decoupler output was calibrated by the standard off-resonance decoupling method (165) using a sample of chloroform for the 46 to 122 MHz broadband probe and formamide for the 21 to 46 MHz broadband probe. All samples were contained in 12-mm-o.d. sample tubes.

For the other organosilanes, the ^{13}C NMR spectra were obtained at 25.16 MHz on a Varian XL-100-15 spectrometer equipped with a NIC-80 32K computer system, a Varian Gyrocode decoupler, MONA multinuclear accessory, and 18-mm probe, at 25.00 MHz on a Jeol FX-100 spectrometer equipped with a switchable dual band $^{1}H/^{13}C$ 5-mm probe, or at 75.45 MHz on the Nicolet NT-300 spectrometer described above. The spectra were obtained at ambient temperature, 22°C for the FX-100 and NT-300 and 26°C

for the XL-100-15. The ^{29}Si NMR spectra were obtained at 59.61 MHz on the NT-300 and 19.88 MHz on the XL-100-15 spectrometer. Sensitivity enhancement techniques were employed for the ^{29}Si NMR spectra. The ^{1}H NMR spectra were obtained on the NT-300 or the FX-100 spectrometers at 300.07 and 99.55 MHz, respectively.

Computer Calculations

Analysis of the non-first order spectra was performed using the ITRCAL program provided by Nicolet for the Nicolet 1280 computer system. This program is adapted from the LAOCN3 program written by Bothner-By and Castellano (166). Least squares analysis of experimental data was accomplished employing a program written in Basic for the Nicolet 1280 computer system. The levels of significance reported in these calculations are those obtained from a two-sided t test and give the probability that a correlation exists between the two variables.

CHAPTER III
NOVEL NMR METHODS

During the multinuclear NMR investigation of organosilanes, it was desirable to develop a method to decouple selectively a group of magnetically equivalent protons which are also used for polarization transfer. In addition, techniques to suppress strong unwanted signals and to differentiate between ^{13}C multiplicities were developed. The discussion of these modified selective population transfer experiments and spin-echo J-modulation experiments are presented in this chapter. Portions of this material have already been published (167,168).

Modified Selective Population Transfer Experiments

Selective population transfer (SPT), induced by the application of one or more (161) selective π pulses to ^{1}H satellite spectra followed by a nonselective "read" pulse, has been widely utilized as a method of enhancing the sensitivity of spin-coupled NMR signals for less-receptive nuclei. Examples include magnetization transfer to ^{13}C (162), ^{15}N (163), and ^{29}Si (164) NMR spin multiplets. The assignment and relative signs of coupling constants may be obtained simultaneously from such experiments (169). The ordinary SPT method does not, however, lead to a net magnetization

transfer and the multiplet lines will appear with an antiphase relationship. Thus, the total integral of the multiplet is zero (provided the native magnetization is suppressed) and a spin decoupled spectrum can be recorded only following suitably delayed decoupling and acquisition (170). An alternative procedure for obtaining noise decoupled SPT spectra has been suggested by Harris and coworkers (171). In general, the drawback of the SPT method is the high selectivity required for irradiation in the hydrogen spectrum. However, this has been overcome with the advent of the INEPT (159), DEPT (172), and JCP (173) pulse sequences which apply hard, nonselective pulses but require a spectrometer with 90° proton phase shifting hardware. More recently methods have been devised which avoid this hardware requirement and thus allow magnetization transfer experiment using nonselective pulses to be performed on older spectrometers (174). Enhanced proton coupled as well as fully decoupled spectra with multiplicity spectra may be obtained using these methods (159,170,172-175) or variants of these experiments (176).

In many cases selective decoupling is desirable to simplify the frequently rather complex proton coupled spectra resulting from an SPT (or INEPT) experiment. Especially this is valid when the J coupling utilized for SPT is of similar magnitude to other coupling constants of the observed nucleus, thus resulting in overlap between positively and negatively enhanced lines in the coupled spectrum. In other experiments it is of interest to observe directly

weak resonances hidden by other intense NMR signals. For example, in the observation of satellite spectra of lines obscured by a solvent resonance, suppression of the main signal is often required. SPT combined with difference spectroscopy has earlier proven useful in such experiments (177) although at the expense of a loss in signal-to-noise ratio. In the next few pages, some new and improved techniques which extend the SPT method to cope with such experimental situations are described.

Selective Population Transfer with Selective Proton Decoupling

Two different situations must be considered when performing selective decoupling experiments in a spin system for which one of the spins is observed using the SPT method or other polarization transfer techniques. In the first case, the selective decoupling field is applied for the elimination of coupling to a proton (or group of protons) which is not involved in the polarization transfer process. Experiments associated with this case are readily performed using a second proton frequency source with selective irradiation applied continuously during the time of the experiment. Alternatively, the proton irradiation source used for polarization transfer may also be applied for the selective decoupling (on during acquisition only) provided computer control of power level/frequency changes is available for this channel. This has been applied in an INEPT experiment using a state-of-the-art spectrometer (178). Since these

experiments are in general straightforward, they will not be further discussed. In the second situation, the protons used for polarization transfer are also selectively decoupled; this type of experiment is more difficult than the first situation, as is evident from the following discussion.

The observation of NMR spectra of low-γ nuclei via polarization transfer is especially advantageous when a group of magnetically equivalent protons can be utilized for the transfer. The reason is that large improvements in S/N are obtained both for the multiplets in a coupled spectrum (162) and for a proton decoupled spectrum (160). Examples of commonly encountered spin systems with groups of magnetically equivalent protons and low-γ X nuclei include molecular fragments such as $-^{29}Si(CH_3)_3$, $\rangle^{15}N\text{-}CH_3$, and $-^{13}C(CH_3)_3$. However, in many such cases the J coupling between the observed X nucleus and the group of protons used for polarization transfer is similar to the magnitudes of the coupling constants between the X nucleus and other protons in the spin system. This gives rise to severe overlap between positive and negative enhanced lines in the coupled spectrum. Thus spectral analysis is rendered almost impossible not only because of the complexity of the spectrum, but also because the antiphase nature of the lines makes it difficult to obtain exact line positions. Obviously, selective decoupling of the magnetically equivalent protons, following their use for polarization transfer, would be very useful for such systems. However, application of the usual refocusing

technique (with two 180° pulses) (175) to the coupled antiphase spectrum followed by selective decoupling does not work because J modulation from other protons in the spin system leads to extensive phase errors. Although simplification of such polarization transfer enhanced spectra by selective decoupling has not previously been demonstrated experimentally, it has been suggested (179) that a selectively decoupled spectrum may be obtained by a mathematical processing of the coupled spectrum.

The pulse sequence shown in Fig. 3-1 was applied for selective decoupling of the group of protons used for polarization transfer in an SPT experiment (i.e., case (b)). The delay τ_1 following the polarization transfer is used for refocusing of the antiphased multiplet before the selective decoupling field is turned on. This delay is optimized according to the number of equivalent protons (N) used for the polarization transfer, i.e., to give a maximum for the term $\sin(\pi J\tau_1)\{\cos \pi J\tau_1)\}^{N-1}$ (160,175,176) and is shown in Table 3-1. J-coupling evolution arising from scalar coupling between the X nucleus and other spins (e.g., protons) within the system also occurs during the period τ_1. The resulting defocused multiplet lines, however, are focused after a delay τ_2 by means of the 180° X pulse and by allowing for an addition τ_2 delay before the acquisition. Obviously, the condition $\tau_2 \geq \tau_1$ must be fulfilled.

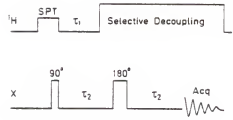

Figure 3-1. Pulse sequence for selective decoupling of a group of magnetically equivalent protons used for polarization transfer in an SPT experiment.

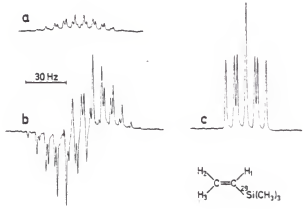

Figure 3-2. ^{29}Si NMR spectra (four scans each) of vinyltrimethylsilane (75% v/v in acetone-d_6). (a) Normal proton coupled spectrum without NOE. (b) SPT-enhanced coupled spectrum with polarization transfer from the trimethylsilyl protons using $\gamma H_2/2\pi$ = 2.5 Hz, τ = 0.2 sec ($\gamma H_2 \tau = \pi$), and applying the SPT π pulse to the high-frequency ^{29}Si satellite in the ^{1}H spectrum ($^2J(^{29}Si\text{-}CH_3)$ = 6.63 Hz). (c) SPT-enhanced coupled spectrum with selective decoupling of the trimethylsilyl protons obtained using the sequence shown in Fig. 3-1 (τ_1 = 16.3 msec, τ_2 = 25 msec, and a selective decoupling amplitude $\gamma H_2/2\pi$ = 62 Hz). The SPT conditions are similar to those in (b).

Table 3-1. Values of τ_1 to Give the Maximum Decoupled Enhancement as a Function of the Number of Scalar Coupled Protons.

N	1	2	3	4	6	8	9
τ_1[a]	0.50	0.25	0.196	0.167	0.134	0.115	0.108

[a] In units of J^{-1}.

A spectrum resulting from the sequence in Fig. 3-1 is enhanced with all the advantages of proton polarization transfer as well as being simplified to permit more facile interpretation. Furthermore, the selectively decoupled spectrum is easily phased to give a spectrum with all multiplet lines in positive absorption. This is easily demonstrated for the SPT-enhanced ^{29}Si NMR spectra of vinyltrimethylsilane shown in Fig. 3-2. The spectra were obtained without (Fig. 3-2b) and with (Fig. 3-2c) selective decoupling of the trimethylsilyl protons which were also used for SPT. Clearly, it would be very difficult, if not impossible, to extract values for the ^{29}Si-^{1}H couplings involving the vinyl protons from the polarization transfer enhanced spectrum recorded without selective decoupling (Fig. 3-2b). Of course a precise determination of coupling constants from spectra such as that recorded in Fig. 3-2c requires a complete analysis based on the double resonance Hamiltonian. Thus the strength of the selective decoupling field (γH_2) and its frequency offset from other resonances of other protons within the spin system must be known. The ^{29}Si-^{1}H coupling constants

determined from analysis of the spectrum in Fig. 3-2c are $^{2}J(^{29}Si\text{-}H1) = 6.42$ Hz, $^{3}J(^{29}Si\text{-}H2) = 15.26$ Hz, and $^{3}J(^{29}Si\text{-}H3) = 8.59$ Hz. The defocusing effect arising from the $^{29}Si\text{-}^{1}H$ (vinyl) J-coupling evolution is illustrated in the spectra of Fig. 3-3 where the 180° refocusing pulse of Fig. 3-1 has been omitted. From these experiments the length of the $2\tau_2$ delay has been varied; this results in a series of spectra with different phase properties which can be predicted from the $J(^{29}Si\text{-}H)$ couplings.

Selective Population Transfer with Suppression of Unwanted Signals

A number of experimental methods have been introduced for the direct observation of weak NMR resonances hidden below other strong signals, e.g., solvent peaks or "parent" signals in satellite spectra. These techniques include difference spectroscopy combined with various double resonance methods (177,180)(e.g., SPT difference spectroscopy (177, 181,182)), pulse sequences utilizing the creation of double quantum coherence (183-186), and other pulse sequences for the observation of X-nuclei satellite spectra in ^{13}C NMR and ^{1}H NMR such as double SPT and reverse INEPT (161,187,188). However, the methods based on "ordinary" difference spectroscopy suffer from the disadvantage that subtraction of an "unperturbed" spectrum in alternate scans will degrade the S/N ratio by a factor of 2 compared to the methods which utilize a "perturbed" spectrum in each scan. Furthermore, these subtraction techniques involve acquisition of the

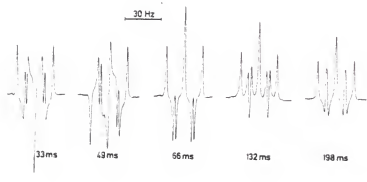

Figure 3-3. SPT-enhanced proton-coupled ^{29}Si spectra (four scans each) of vinyltrimethylsilane with selective decoupling recorded similar to that in Fig. 3-2c but without the 180° refocusing pulse of Fig. 3-1. The total $2\tau_2$ delay has been varied for each experiment and is given below the individual spectra. These have been phase corrected so as to display the low-frequency peak in positive absorption.

strong unwanted signals leading to incomplete cancellation of these unwanted signals and possible dynamic range problems.

As an improvement of the SPT difference spectroscopy technique a method was devised which proved useful for suppression of strong signals with the simultaneous observation of weak resonances hidden by the strong peaks. The basic pulse sequence, in which SPT π pulses are applied alternately to the low- and high-frequency satellites (e.g., ^{13}C satellites) in the ^{1}H spectrum with a concurrent 180° phase shift of the 90° ^{13}C "read" pulse, may be written

SPT, $180°(^{1}H,\nu)-90°_{+x}(^{13}C)$-Acq.-PD-SPT,

$$180°(^{1}H,\ \nu+J)-90°_{-x}(^{13}C)\text{-Acq.-PD-} \qquad [1]$$

where PD is a pulse delay. Thus, the SPT-enhanced signals add for each data acquisition. Although the strong signals are acquired in each FID using sequence [1], all resonances arising from native ^{13}C equilibrium magnetization including the unwanted strong signals will be canceled or greatly attenuated in the final spectrum. Figure 3-4 demonstrates the frequency-alternating SPT π pulses of sequence [1] to a mixture of CH_3CN (10% v/v) and CD_3CN (90% v/v; 99% deuterium enriched). For this sample the proton decoupled ^{13}C spectrum for the methyl region without NOE (Fig. 3-4a) and the proton coupled SPT enhanced -1:-1:1:1 quartet spectrum of CH_3CN obtained using sequence [1](Fig. 3-4b) illustrate the degree of suppression achieved for the

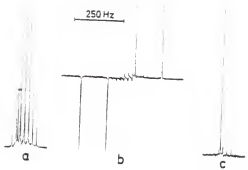

Figure 3-4. ^{13}C NMR spectra for the methyl region of a mixture of CH_3CN (10% v/v) and CD_3CN (90% v/v); 99% deuterium enriched). (a) Normal proton-decoupled spectra (32 scans); the resonance for the protio compound is marked with an asterisk. (b) SPT-enhanced proton-coupled spectrum (32 scans) with suppression of the CD_3CN solvent signal obtained using the pulse sequence [1]. (c) Proton-decoupled version (four scans) of the spectrum in (b) obtained by introduction of refocusing delays before the data acquisitions in sequence [1].

Figure 3-5. SPT-enhanced proton-coupled ^{13}C NMR spectrum (32 scans) for the mixture of CH_3CN (10% v/v) and CD_3CN (90% v/v; 99% deuterium enriched) obtained using the pulse sequence [2]. The SPT frequency has been shifted slightly to lower frequency compared to the experiment in Fig. 3-4b in order to optimize the enhancement of the six observed resonance peaks (marked with asterisks) for the CHD_2CN isotopomer present in the CD_3CN solvent (see text for further discussion).

CD_3CN solvent resonances by this simple method. The proton decoupled version of the spectrum in Fig. 3-4b is shown in Fig. 3-4c. This spectrum was obtained by extending the sequence [1] with refocusing delays following the $90°_{\pm x}$ ^{13}C "read" pulses and applying broadband proton decoupling during data acquisition.

A significant improvement in the suppression of the CD_3CN solvent peaks, as compared, for example, to the residual signals observed in Fig. 3-4b, may be achieved by preceding the SPT π pulses in sequence [1] by $90°$ ^{13}C pulses for which the phase is alternated between positive and negative x axes. Thus, this improved sequence, which may be written

$$90°_{\pm x}(^{13}C)\text{-SPT},\ 180°(^{1}H,\nu)\text{-}90°_{+x}(^{13}C)\text{-AT-PD-}90°_{\pm x}(^{13}C)\text{-SPT},$$
$$180°(^{1}H,\ \nu+J)\text{-}90°_{-x}(^{13}C)\text{-AT-PD-} \qquad [2]$$

avoids the acquisition of strong unwanted signals. Furthermore, the $\pm x$ axis phase cycling of the $90°(^{13}C)$ pulses preceding the SPT π pulses ensures almost complete elimination of any residual unsuppressed resonances arising from non-ideal $90°(^{13}C)$ pulses. The improvements of sequence [2] over [1] are illustrated in Fig. 3-5 employing the same sample as used for the spectra in Fig. 3-4, i.e., a mixture of 10% v/v CH_3CN and 90% v/v CD_3CN. In addition to the observation of the proton coupled -1:-1:1:1 quartet ^{13}C spectrum for the methyl carbon in CH_3CN and almost perfect

suppression of the CD_3CN solvent peaks, the spectrum in Fig. 3-5 also demonstrates that the proton coupled ^{13}C spectrum for the CHD_2CN isotopomer (six peaks marked with asterisks), originating from the 99%-deuterium-enriched CD_3CN solvent, may also be uncovered. The different intensities (pairwise negative/positive) for the six peaks for this isotopomer are related to the relative sign for the $^1J(^{13}C\text{-}D)$ and $^2J(^1H\text{-}D)$ coupling constants and to the frequency of the SPT π pulse (169). In the actual experiment of Fig. 3-5 the SPT frequency was positioned at the second highest frequency line in the ten line ^1H spectrum for the $^{13}CHD_2CN$ isotopomer (a doublet of pentets; $^1J(^{13}C\text{-}H) = 136.2$ Hz and $^2J(^1H\text{-}D) \simeq 2.6$ Hz) as is shown in Fig. 3-6. Thus the spectrum (Fig. 3-5) shows that $^1J(^{13}C\text{-}D) \times {}^2J(^1H\text{-}D) < 0$ in accordance with the well-known absolute signs for these types of coupling constants. It should be mentioned that the deuterium isotope effect for the two deuterium atoms on the ^1H chemical shift for CH_3CN (ca. 6.8 Hz to lower frequency at 300 MHz) must be taken into account when optimizing SPT frequencies for the CHD_2CN isotopomer.

Experimental

Materials. Vinyltrimethylsilane was generously donated by PCR Research Chemicals, Inc., Gainesville, Florida. Acetonitrile was obtained from Mallinckrodt, Inc., Paris, Kentucky, and acetonitrile-d_3, 99%-deuterium-enriched ("gold label"), was obtained from Aldrich Chemical Co., Milwaukee,

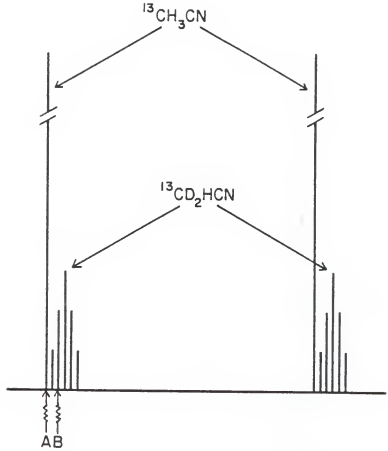

Figure 3-6. ^{1}H NMR spectrum showing the irradiation positions of the SPT π pulses employed for the generation of spectra in Fig. 3-4b(A) and Fig. 3-5(B).

Wisconsin. Acetone-d_6 was obtained from Merck Sharp & Dohme Isotopes, St. Louis, Missouri. These materials were used without any further purification.

Spectrometer. All experiments were performed on a Nicolet NT-300 spectrometer equipped with a 293-C pulse programmer and a Nicolet 1280 computer. ^{1}H, ^{13}C, and ^{29}Si NMR spectra were obtained at 300.07, 75.45, and 59.61 MHz, respectively. These spectra were obtained at ambient temperature, 22°C. The amplitude, $\gamma H_2/2\pi$, of the ^{1}H decoupler was calibrated using the standard off-resonance decoupling method (165) or by optimization of a $^{13}C-\{^{1}H\}$ SPT experiment using a sample of $CHCl_3$ in both cases. The switching of the decoupler frequency and amplitude required for the pulse sequences described in this work was performed by means of the 293-C pulse programmer. All samples were contained in 12-mm-o.d. sample tubes.

^{13}C Spin-Echo J-Modulation Experiments

Spin-echo J modulations, a well-known and established technique in ^{2}H homonuclear pulse NMR (189), has been shown to be an elegant method for the determination of CH_3, CH_2, CH, and quaternary C multiplicities in proton-decoupled ^{13}C NMR (190-199). Thus, this technique represents a welcome replacement for the off-resonance decoupling experiment (200). Burum and Ernst (190) have demonstrated the applicability of the INEPT (159) pulse sequence with refocusing pulses. However, the INEPT experiment cannot readily be

performed on many older and routine FT NMR spectrometers. This has led to the design of alternative methods (192-199) for the retrieval of this important multiplicity information from decoupled ^{13}C NMR spectra. These techniques employ heteronuclear spin-echo J modulation, decoupling only during the acquisition time (197,198), or various other gated broadband proton decoupling patterns (192-196,199). Furthermore, several variations using subtraction or addition of spectra resulting from such experiments also have been reported (194-196,198).

With these simple spin-echo J-modulation experiments (i.e., without the use of the INEPT sequence) the signals for CH and CH_3 groups, on the one hand, are easily distinguished from those of CH_2 and quaternary carbons, on the other. The resonances of CH_2 and quaternary carbons may also be readily differentiated from one another by performing a second experiment in which use is made of the much slower time evolution of the quaternary carbon signals ($^1J(^{13}C^1H) > {}^nJ(^{13}C^1H)$). However, the CH and CH_3 carbon signals are not as easily differentiated (difference spectroscopy has been used (195,196)) as in the INEPT sequence, a fact that may lead to ambiguities.

Two of the pulse sequences which may be used for the observation of proton-decoupled spin-echo J-modulated ^{13}C spectra are shown in Fig. 3-7. Figure 3-7 represents the heteronuclear J-modulation experiment with broadband proton decoupling during the acquisition period. Figure 3-7b

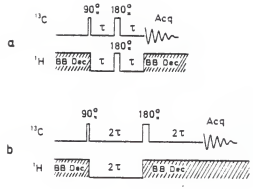

Figure 3-7. Pulse sequences for the observation of proton broadband-decoupled spin echo J-modulated ^{13}C NMR spectra. (a) Heteronuclear J-modulation experiment with proton decoupling during acquisition. (b) Delayed decoupling sequence with 180° ^{13}C spin-echo pulse.

illustrates the simple delayed decoupling sequence with a 180° ^{13}C spin-echo pulse to prevent phase errors. For both sequences the time evolution of the J modulation occurs during a total period of 2τ sec, i.e., during the time in which the broadband decoupler is turned off.

Analytical expressions for the intensity modulation of the proton-decoupled singlets from CH, CH_2, and CH_3 carbons observed using either of the sequences in Fig. 3-7 may be calculated from simple vector pictures (Fig. 3-8). Neglecting transverse relaxation and using normalized intensities (i.e., taking the intensities of the normal fully relaxed decoupled ^{13}C spectrum as unity), the intensity modulation for the CH, CH_2, and CH_3 carbon singlets is described by

$$I(CH) = -\cos(2\pi J\tau), \qquad [1]$$

$$I(CH_2) = -\{\tfrac{1}{2} + \tfrac{1}{2}\cos(4\pi J\tau)\}, \qquad [2]$$

$$I(CH_3) = -\{\tfrac{1}{4}\cos(6\pi J\tau) + \tfrac{3}{4}\cos(2\pi J\tau)\}, \qquad [3]$$

where τ refers to the evolution periods indicated in Fig. 3-7 and the minus signs result from the 180° ^{13}C refocusing pulse. Figure 3-9 shows how the amplitudes of the detected singlets depend on 2τ (the minus signs of Eqs. [1] to [3] have been omitted). It is clear from the figure that the CH and CH_3 lines are easily separated from the CH_2 and quaternary carbon signals for $2\tau = 1/J$. Further, it is also evident that all types of protonated carbon signals with equal values for the one-bond ^{13}C-^{1}H coupling constants can

Figure 3-8. Spin vector representation of the ^{13}C spins for a ^{13}C coupled to a ^{1}H using the pulse sequence in Fig. 3-7a. (a) At equilibrium, the spin vectors α and β are aligned along the z-axis. (b) Applying a $90^{\circ}_{+x}(^{13}C)$ pulse causes the spin vectors to become aligned along the Y axis. (c) After a τ period, the spin vectors begin to fan out in the X-Y plane. Here the spin vector α represents the higher frequency transition of the doublet. (d) The 180°_{+x} (^{13}C) pulse reverses the sign of the Y-component of the vectors. The 180°_{+x} (^{1}H) pulse reverses the labels of the spins since each carbon spin is associated with a particular proton spin. (e) After another τ period the spin vectors are symmetrically aligned about the y-axis with an angle of $4\pi J\tau$ between them. At this point, the proton decoupler is turned on causing the spin vectors to collapse into the Y-axis and the receiver is turned on. Since the intensity of the observed signal is proportional to the magnitude of the y-component of the vectors, for a CH, the detected intensity is proportional to $\cos(2\pi J\tau)$.

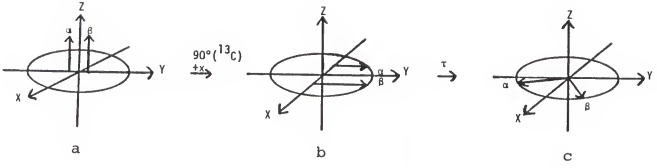
Z
α
β
Y
X
a
90°(13C)
+x
b
τ
c
180°(13C)
180°(1H)
+x
d
4πJτ
e

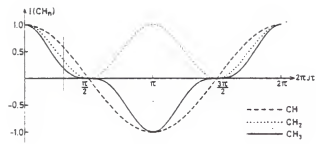

Figure 3-9. Dependence of the detected intensities on the evolution period 2τ for CH, CH_2, and CH_3 spin systems in proton-decoupled spin-echo J-modulated ^{13}C spectra; i.e., Eqs. [1] to [3], where the minus signs have been omitted. The "magic angle" of 54.74° is indicated by the vertical bar.

be suppressed for $2\tau = 1/2J$ thereby allowing quaternary carbons (or protonated carbons of appreciably different carbon constants) to be selectively observed. In this way CH_2 and quaternary carbon signals may be distinguished from one another. Thus, the remaining assignment problem is differentiating the CH and CH_3 carbon lines.

The most straightforward solution to the differentiation between CH and CH_3 singlets appears to be a determination of the angle $2\pi J\tau$ for which the maximum difference between the intensities of these resonances is observed (197). The difference between the normalized intensity expressions [1] and [3] is given by

$$\Delta I = I(CH) - I(CH_3) = \tfrac{1}{4}\{\cos\ (6\pi J\tau) - \cos\ (2\pi J\tau)\}$$

or

$$\Delta I = \cos^3\ (2\pi J\tau) - \cos\ (2\pi J\tau), \qquad [4]$$

from which

$$\frac{d(\Delta I)}{d(2\pi J\tau)} = \sin\ (2\pi J\tau)\{1 - 3\cos^2\ (2\pi J\tau)\} \qquad [5]$$

is obtained. The extrema for ΔI, determined from $d(\Delta I)/d(2\pi J\tau) = 0$, show that for $2\pi J\tau < \pi/2$ the maximum difference between the intensities for CH and CH_3 of equal coupling constants occurs at an angle of 54.74° (in solid-state NMR known as the "magic angle" for the magic-angle spinning experiment). This angle corresponds to an evolution time $2\tau = 0.304/J$ and to normalized absolute intensity values for $I(CH) = 0.58$ and $I(CH_3) = 0.19$. Thus, neglecting

relaxation effects, the CH and CH_3 singlet intensities at the "magic angle" are reduced by 42 and 81%, respectively, as compared to those of the "normal" decoupled spectrum (or of the spectrum observed for $2\tau = 1/J$). The magnitude of this intensity difference is large enough to allow CH and CH_3 singlets to be distinguished from one another and thereby make a complete multiplicity assignment of the decoupled ^{13}C spectrum.

This spin-echo J-modulation multiplicity assignment method is illustrated for the proton-decoupled ^{13}C NMR spectra of β-pinene at 75.46 MHz (Fig. 3-10). In Fig. 3-10c, the CH and CH_3 lines are separated from the CH_2 and quaternary carbon signals using the simple pulse sequence in Fig. 3-7b with $2\tau = 1/J$. Examination of the signal at 41.1 ppm in the spectrum presented in Fig. 3-10c shows the signal is composed of a positive shoulder (carbon 6) on a large negative peak (carbon 5). Quaternary and CH_2 carbon signals are distinguished from one another in the spectrum of Fig. 3-10d in which the quaternary carbon resonances are selectively observed employing $2\tau = 1/2J$. The spectrum shown in Fig. 3-10b which was observed at the "magic angle" of 54.74° (i.e., using $2\tau = 0.304/J$) clearly shows the expected pronounced reduction of the CH line intensities relative to the CH singlets by comparing it with the intensities of Fig. 3-10a or Fig. 3-10c.

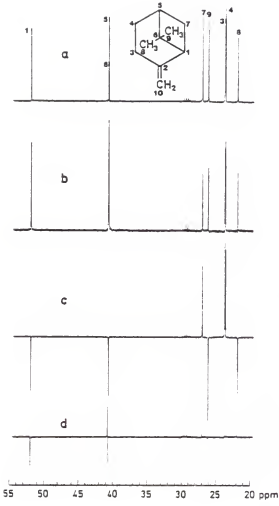

Figure 3-10. Proton-decoupled 75.46-MHz ^{13}C NMR spectra of β-pinene in $(CD_3)_2CO$. (a) "Normal" spectrum shown with the assignment given by Stothers (201). (b)-(d) Spin-echo J-modulated ^{13}C spectra obtained using (b) $2\tau = 0.304/J$ = 2.4 msec (J = 125 Hz) (i.e., at the "magic angle" of 54.74°), (c) $2\tau = 1/J = 8.0$ msec (J = 125 Hz), and (d) $2\tau = 1/2J = 4.0$ msec (J = 125 Hz). Phase corrections have been made so quaternary and CH_2 carbon resonances appear as positive signals in all spectra.

In conclusion, the method proposed in this communication for the differentiation between CH and CH_3 multiplicities shows that assignment of ^{13}C resonances to CH_3, CH_2, and CH, and quaternary carbon sites in large molecules may be performed routinely without the need of subtraction or addition of spectra. Finally, the spin-echo J-modulation pulse sequences in Fig. 3-7 not only preserve the NOE intensity gain which in ^{13}C NMR is virtually as great as the INEPT polarization transfer enhancement but can also be performed on older and FT NMR spectrometers without phase-shifting capability.

Experimental

Materials. ß-pinene was obtained from a shelf bottle and the solvent acetone-d_6 was obtained from Merck Sharp & Dohme Isotopes, St. Louis, Missouri. These materials were used without any further purification. The sample was contained in a 12 mm-o.d. tube.

Spectrometer. The ^{13}C NMR spectra were obtained at 75.46 MHz on a Nicolet NT-300 spectrometer equipped with a 293-C pulse programmer. Spin-echo J-modulation pulse sequences were generated through microprogramming of the 293-C pulse programmer for the NT-300 spectrometer. A spectral width of 14085 Hz and 64K data points at 75.46 MHz was used.

CHAPTER 4
RESULTS AND DISCUSSION

For the purposes of discussion, the carbons and hydrogens of vinyl, phenyl, and ethyl groups will be denoted as follows:

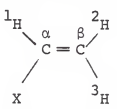

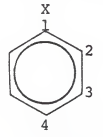

$$X\text{-}\overset{\alpha}{C}H_2\overset{\beta}{C}H_3$$

The chemical shifts are reproducible to ±0.05 ppm and the coupling constants are reproducible to ±0.05 Hz. The ^{1}H, ^{13}C, and ^{29}Si chemical shifts are all reported with reference to internal TMS; a positive value indicates deshielding. The ^{15}N shifts are reported with reference to external 80% v/v nitromethane in the same solvent as the sample.

Trimethylsilyl Compounds

Chemical Shifts

The ^{1}H, ^{13}C, and ^{29}Si compound shifts of the trimethylsilyl group for compounds of the type Me_3SiX are presented in Table 4-1. The ^{1}H and ^{13}C chemical shift data of the X group are listed for completeness in Table 4-2.

Table 4-1. Chemical Shifts[a] of the Trimethylsilyl Group for Compounds of the Type Me_3SiX.

X	^1H/ppm	^{13}C/ppm	^{29}Si/ppm
Me	0.00	0.00	0.00
$CH_2CH=CH_2$	0.20	-1.75	0.30
$CH_2C_6H_5$	-0.05	-1.95	1.16
$CH=CH_2$	0.05	-1.59	-6.96
C_6H_5	0.21	-0.63	-4.08
CH_2Br	0.13	-2.53	3.14
CH_2Cl	0.11	-3.12	3.08
$CHClCH_3$	0.09	-3.97	5.41
$C{\equiv}CSiMe_3$	0.13	0.05	19.42
$SSiMe_3$	0.06	4.16	14.01
SEt	0.27	0.97	14.74
SC_6H_5	0.21	0.80	16.98
$N(SiMe_3)_2$	0.20	5.49	2.46
$NHSiMe_3$	0.04	2.57	2.14
$NMeSiMe_3$	0.07	1.28	6.05
NHC_6H_5	0.18	0.08	1.71
NMe_2	0.08	1.30	6.48
NEt_2	0.03	0.16	3.67
$N=C=NSiMe_3$	0.14	1.09	-1.03
N=C=S	0.32	0.00	5.84
N=C=O	0.23	0.65	4.16
N=N=N	0.24	-1.05	15.81
$OSiMe_2H$	0.07	1.64	8.99
$OSiMe_3$	0.07	1.96	6.86
OMe	0.06	-0.97	17.35
OEt	0.06	-0.41	15.14

[a]Chemical shifts are relative to TMS.

Table 4-2. ^{1}H and ^{13}C Chemical Shifts[a] of the X Substituent for Compounds of the Type Me_3SiX.

X	^{1}H/ppm[b]	^{13}C/ppm[b]
$CH_2CH=CH_2$	1.69 (CH_2) 4.98 (H_2) 5.93 (H_1) 5.00 (H_3)	25.21 (CH_2) 135.30 (α) 113.19 (β)
$CH_2C_6H_5$	2.01 (CH_2) 6.90-7.00 (3H) 7.07-7.14 (2H)	26.98 (CH_2) 128.25 (C_3) 140.24 (C_1) 124.11 (C_4) 128.11 (C_2)
$CH=CH_2$	6.13 (H_1) 5.64 (H_3) 5.87 (H_2)	140.22 (α) 130.99 (β)
C_6H_5	7.16-7.23 (3H) 7.41-7.47 (2H)	140.56 (C_1) 128.40 (C_3) 133.86 (C_2) 129.40 (C_4)
CH_2Br	2.47	17.89
CH_2Cl	2.73	30.90
$CHClCH_3$	3.34 (CHCl) 1.47 (CH_3)	45.33 (CHCl) 20.01 (CH_3)
$C{\equiv}CSiMe_3$		113.43
SEt	2.49 (α) 1.24 (β)	20.50 (α) 18.75 (β)
SC_6H_5	7.04-7.20 (3H) 7.32-7.42 (2H)	131.65 (C_1) 128.72 (C_3) 135.13 (C_2) 126.80 (C_4)
$NHSiMe_3$	--[c] (NH)	

Table 4-2 continued.

X	^{1}H/ppm[b]	^{13}C/ppm[b]
$NMeSiMe_3$	2.47	30.93
NHC_6H_5	4.10 (NH) 6.56-6.64 (3H) 6.96-7.05 (2H)	147.88 (C_1) 117.12 (C_4) 116.30 (C_2) 129.06 (C_3)
NMe_2	2.49	37.89
NEt_2	2.79 (α) 0.96 (β)	40.57 (α) 16.27 (β)
$N{=}C{=}NSiMe_3$		123.85
$N{=}C{=}S$		142.50
$N{=}C{=}O$		124.97
$OSiMe_2H$	0.13 ($SiMe_2$) 4.73 (SiH)	0.90
OMe	3.36	49.81
OEt	3.62 (α) 1.12 (β)	58.15 (α) 18.83 (β)

[a] Chemical shifts are relative to TMS.

[b] For the α, β, H_1, H_2, H_3, C_1, C_2, C_3, C_4 notation see the text.

[c] The NH resonance could not be detected, presumably because of excessive line broadening caused by nitrogen quadrupolar effects.

An extremely crude correlation (80% level of significance) is obtained between ^{29}Si chemical shifts and Swain-Lupton field effect parameters, F (202), which are measures for the inductive effect exerted by the substituent, X (see Fig. 4-1). The relationship is

$$\delta^{29}Si = 27F + 2.6 \text{ [ppm]} \qquad [1]$$

$$(r = 0.29, \sigma = 6.1, N = 26)$$

This correlation implies ^{29}Si shieldings in trimethylsilyl compounds are influenced by inductive effects. Although no correlation can be found between ^{29}Si chemical shifts for compounds containing nitrogen and oxygen substituents (substituents most likely to (d-p)π bond) and the F values, a correlation is obtained at the 90% level of significance for the carbon and sulfur substituents (substituents least likely to (d-p)π bond). The relationship is

$$\delta^{29}Si = 56F + 0.3 \text{ [ppm]} \qquad [2]$$

$$(r = 0.56, \sigma = 6.0, N = 12)$$

The higher shielding of vinyl (-6.96 ppm) and phenyl (-4.08 ppm) in comparison to methyl (0.00 ppm) substituted trimethylsilane seems to indicate (d-p)π bonding. The unusually large deshielding of silicon for $C{\equiv}CSiMe_3$, SC_6H_5, SEt, and $SSiMe_3$ substituents may be explained by bond polarization which

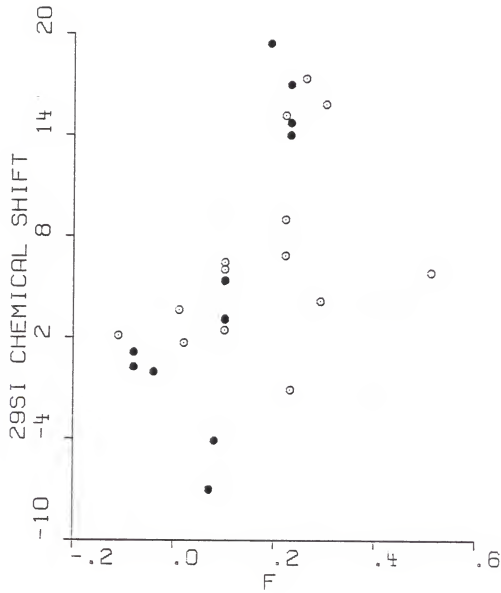

Figure 4-1. Plot of $\delta^{29}Si$ vs. Swain-Lupton field effect parameters, F, for Me_3SiX compounds. Open circles are for molecules with N and O substituents; closed circles are for those with C and S substituents.

increases the apparent electron-withdrawing power of these substituents. The ^{29}Si chemical shifts of CH_2Cl (3.08 ppm), CH_2Br (3.14 ppm), and CH_3 (0.00 ppm) substituted trimethylsilane are not in the predicted order for inductive effects alone. Therefore, these results suggest ^{29}Si chemical shifts in trimethylsilyl compounds depend on other factors beside simple inductive effects, including (d-p)π bonding.

No correlation can be found between $\delta^{13}C$ of the trimethylsilyl group and the substituent F value. The largest deviations (deshielding) from this relationship are for substituents having a number of δ methyls. Examples and the observed shifts include $N(SiMe_3)_2$ (5.49 ppm), $NHSiMe_3$ (2.57 ppm), $NMeSiMe_3$ (1.28 ppm), and $OSiMe_3$ (1.96 ppm). Comparison of ^{13}C shifts of the trimethylsilyl group in Me_3SiX compounds for X = CH_3, CH_2Br, and CH_2Cl shows the ^{13}C shifts are in the opposite direction from that predicted from inductive effects. These results suggest that other factors including steric effects are operating in ^{13}C shielding.

Although no overall correlation can be found between $\delta^{29}Si$ and $\delta^{13}C$ of the trimethylsilyl group for Me_3SiX compounds, the data in Fig. 4-2 can be divided into three groups. The first contains the four data points corresponding to the three sulfur substituents and $C{\equiv}CSiMe_3$; it appears there is an additional deshielding mechanism operational in these compounds in comparison to that for ^{29}Si shieldings of the remaining carbon substituted compounds. The second group contains all the nitrogen and oxygen substituents; there

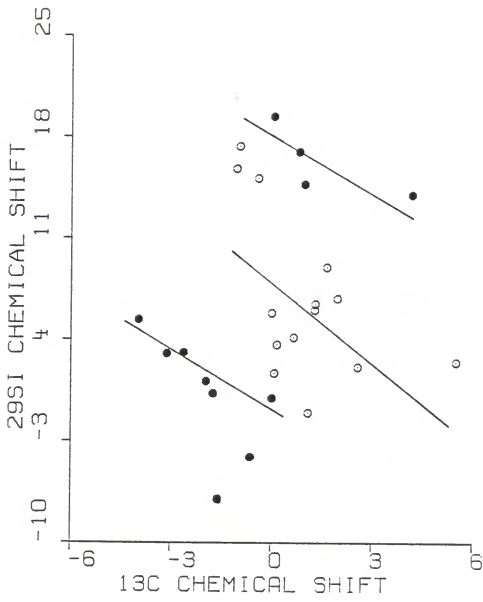

Figure 4-2. Plot of δ^{29}Si vs. δ^{13}C of the trimethylsilyl group for Me_3SiX compounds. Open circles are for molecules with N and O substituents; closed circles are for those with C and S substituents.

is no significant correlation between $\delta^{29}Si$ and $\delta^{13}C$ for this group. The third group contains the remaining carbon substituents. If the two substituents most likely to $(d-p)\pi$ bond ($CH=CH_2$ and C_6H_5) are eliminated from this group, then a correlation at the 95% level of significance is obtained with the following relationship:

$$\delta^{29}Si = -1.4\ \delta^{13}C - 0.9\ [ppm] \qquad [3]$$

$$(r = 0.82,\ \sigma = 1.0,\ N = 6)$$

The negative sign of the slope is correctly predicted from inductive effects. In addition, the two other groups of data also have negative slopes. Thus, although ^{29}Si and ^{13}C shifts are significantly influenced by inductive effects, other contributions to shielding such as $(d-p)\pi$ bonding are important.

An extremely crude correlation (80% level of significance) is obtained between $\delta^{1}H$ of the trimethylsilyl group and the corresponding F value (see Fig. 4-3). The relationship is:

$$\delta^{1}H = 0.36F + 0.06\ [ppm] \qquad [4]$$

$$(r = 0.30,\ \sigma = 0.08,\ N = 26)$$

The positive sign of the slope is correctly predicted by assuming inductive effects dominate ^{1}H shielding. The deviations of ^{1}H chemical shifts from this relationship may be due to anisotropic effects since the largest deviations are for groups with the largest anisotropy (e.g., $CH_2CH=CH_2$, $CH_2C_6H_5$, C_6H_5, and $NH(C_6H_5)$). In addition, there may be differences in the transmission of inductive effects through the silicon atom.

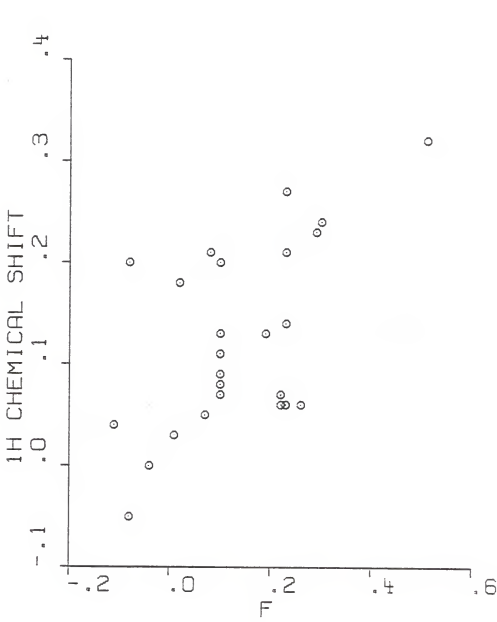

Figure 4-3. Plot of δ^1H of the trimethylsilyl group for Me_3SiX compounds vs. substituent F values.

Data comparing ^{13}C and ^{29}Si chemical shifts in analogous trimethylsilyl and tertiary butyl compounds are presented in Table 4-3. For the t-butyl derivatives the ^{13}C chemical shifts increase with increasing electron-withdrawing power of the substituents as would be expected on the basis of inductive effects alone. On the other hand $\delta^{29}Si$ values vary irregularly with increasing inductive withdrawing power of the substituents. Comparison of the ^{13}C shifts referenced to $Me_4{}^{13}C$ with ^{29}Si shifts clearly shows increased shielding for C_6H_5, nitrogen, and oxygen substituents. Since the inductive effects of the substituents are the same in both ^{13}C and ^{29}Si compounds, the increased shielding of these substituents indicates contributions from (d-p)π bonding.

In Table 4-4 are presented data comparing ^{13}C shifts of the methyl group of trimethylsilyl and tertiary butyl compounds. These data show the ^{13}C shifts of the trimethylsilyl compounds are dominated by the strong inductive effect (+I) of the silicon since the silicon derivatives are shielded by about 30 ppm in comparison to the carbon derivatives.

Coupling Constants

The values of coupling constants involving nuclei of the trimethylsilyl group for Me_3SiX compounds are given in Table 4-5. ^{29}Si-^{1}H and ^{29}Si-^{13}C coupling constants of the X substituent for Me_3SiX compounds are listed in Table 4-6.

The $^{1}J(^{29}Si^{13}C)$ were measured from the ^{29}Si satellites in the ^{13}C-^{1}H decoupled spectra with NOE. Figure 4-4 shows

Table 4-3. Comparison of ^{13}C and ^{29}Si Chemical Shifts for M in Me_3MX Compounds, where M = ^{13}C and ^{29}Si.[a]

X[b]	^{13}C/ppm[c]	Ref.	^{29}Si/ppm[d]
Me	26.7 (0.0)	203	0.00
$CH_2CH=CH_2$	30.74 (4.0)	204	0.30
$CH_2C_6H_5$	29.5 (2.8)	205	1.16
C_6H_5	33.0 (6.3)	87	-4.08
SC_6H_5	44.9 (18.2)	206	16.98
NMe_2	53.15 (26.5)	207	6.48
$N=C=NSiMe_3$	54.3[e] (27.6)	208	-1.03
N=C=S	58.4 (31.7)	209	5.84
OMe	72.1 (45.4)	203	17.35
OEt	72.2 (45.5)	203	15.14

[a] Chemical shifts are referenced to Me_4Si.

[b] Me = CH_3 and Et = CH_2CH_3.

[c] Values in parentheses are referenced to $Me_4{}^{13}C$.

[d] Data from this study.

[e] For comparison purposes, the value of $\delta^{13}C$ for $N=C=NCHMe_2$ has been used with $\delta^{29}Si$ for $N=C=NSiMe_3$.

Table 4-4. Comparison of ^{13}C chemical Shifts in $(^{13}CH_3)_3MX$ (where M = C, Si).

X	M=C	Ref.	M=Si[a]
$CH_2CH=CH_2$	29.38	204	-1.75
$CH_2C_6H_5$	28.9	205	-1.95
SC_6H_5	30.8	206	0.80
NMe_2	25.62	207	1.30
$N=C=NSiMe_3$	31.1[b]	208	1.09
N=C=S	30.9	209	0.00
OMe	26.7	203	-0.97
OEt	27.7	203	-0.41

[a]Data from this study.

[b]For comparison purposes, the value of $\delta^{13}C$ for $Me_3CN=C=NCHMe_2$ has been used with $\delta^{13}C$ for $Me_3SiN=C=NSiMe_3$.

Table 4-5. Coupling Constants Involving Nuclei of the Trimethylsilyl Group for Compounds of the Type Me_3SiX.

X	$^1J^{13}CH$/Hz	$\lvert^3J^{13}CSiCH\rvert$/Hz	$\lvert^1J^{29}Si^{13}C\rvert$/Hz	$\lvert^2J^{29}SiCH\rvert$/Hz
Me	118.14	2.11	50.96	6.62
$CH_2CH=CH_2$	118.66	1.91	51.49	6.77
$CH_2C_6H_5$	118.81	1.88	51.27	6.79
$CH=CH_2$	118.84	2.03	52.37	6.73
C_6H_5	119.02	2.10	52.11	6.62
CH_2Br	119.50	1.79	52.88	6.69
CH_2Cl	119.47	1.73	53.06	6.68
$CHClCH_3$	119.44	1.96	53.10	6.66
$C{\equiv}CSiMe_3$	119.86	2.00	56.15	7.06
$SSiMe_3$	120.06	1.89	54.10	6.86
SEt	120.02	1.87	53.72	6.84
SC_6H_5	120.56	1.81	54.29	6.81
$N(SiMe_3)_2$	118.15	1.93	56.43	6.48
$NHSiMe_3$	117.69	1.66	56.12	6.61
$NMeSiMe_3$	117.87	1.85	56.57	6.67
NHC_6H_5	118.60	1.72	57.19	6.68
NMe_2	117.80	1.76	56.73	6.52
NEt_2	117.70	1.67	56.55	6.52
$N{=}C{=}NSiMe_3$	118.96	1.66	59.35	6.92

Table 4-5 continued.

X	$^{1}J^{13}CH$/Hz	$\lvert^{3}J^{13}CSiCH\rvert$/Hz	$\lvert^{1}J^{29}Si^{13}C\rvert$/Hz	$\lvert^{2}J^{29}SiCH\rvert$/Hz
N=C=S	120.55	1.47	60.14	7.23
N=C=O	119.72	1.62	60.23	7.15
N=N=N	119.93	1.68	58.59	6.90
$OSiMe_2H$	117.85	1.60	59.66	6.74
$OSiMe_3$	117.73	1.57	59.63	6.73
OMe	117.96	1.55	58.83	6.61
OEt	117.96	1.60	59.08	6.61

Table 4-6. ^{29}Si-^{1}H and ^{29}Si-^{13}C Coupling Constants[a] of the X Substituent for Compounds of the Type Me_3SiX.

X[b]	$\lvert {}^1J^{29}Si^{13}C\rvert$/Hz	$\lvert {}^2J^{29}SiCH\rvert$/Hz	$\lvert {}^3J^{29}SiH\rvert$/Hz
$CH_2CH{=}CH_2$[c]	47.13	8.79	2.15
$CH_2C_6H_5$[d]	46.34	8.49	--
$CH{=}CH_2$	64.72	6.42	15.26 (H_2)[e] 8.59 (H_3)
C_6H_5[f]	65.89	--	5.09
CH_2Br	50.54	3.35	--
CH_2Cl	51.08	3.63	--
$CHClCH_3$	54.31	3.48	5.47
$C{\equiv}CSiMe_3$[g]	78.47	--	--
SEt	--	--	3.72
$NMeSiMe_3$	--	--	4.63
NMe_2	--	--	3.44
NEt_2	--	--	3.74
$OSiMe_2H$[h]	59.07	7.09	1.08
OMe	--	--	4.17
OEt	--	--	3.28

[a] Coupling Constants are reproducible to ±0.05 Hz.

[b] $Me{=}CH_3$ and $Et{=}CH_2CH_3$.

[c] $\lvert {}^4J^{29}SiCCCH\rvert$ = 2.15 Hz.

[d] $\lvert {}^4J^{29}SiCCCH\rvert = \lvert {}^5J^{29}SiCCCCH\rvert = \lvert {}^6J^{29}SiCCCCCH\rvert$ = 0.63 Hz.

[e] For H_2, H_3 notation see the text.

[f] $\lvert {}^4J^{29}SiCCCH\rvert = \lvert {}^5J^{29}SiCCCCH\rvert$ = 0.80 Hz.

[g] $\lvert {}^2J^{29}SiC{\equiv}{}^{13}C\rvert$ = 12.74 Hz.

[h] $\lvert {}^1J^{29}SiH\rvert$ = 203.55 Hz.

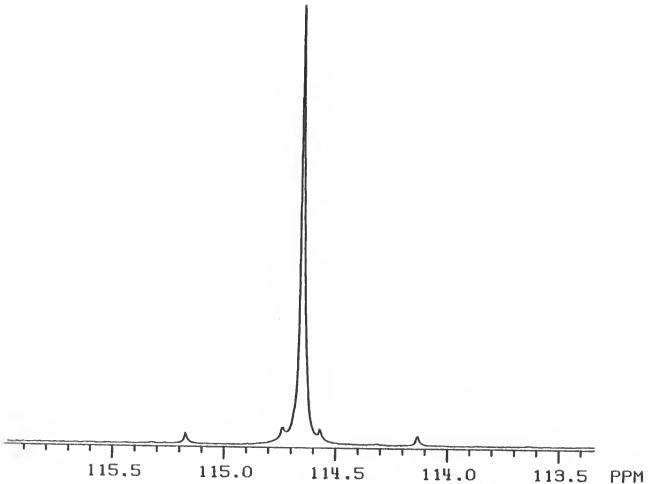

Figure 4-4. ^{1}H-decoupled ^{13}C spectrum with NOE of the acetylene carbon of bis-(trimethylsily) acetylene.

satellites for both the $^{1}J(^{29}Si^{13}C)$ and the $^{2}J(^{29}Si^{13}C)$ to the acetylene carbon of bis-(trimethylsilyl) acetylene.

The $^{1}J(^{29}Si^{13}C)$ is strongly correlated (99.9% level of significance) with the Huggins' electronegativity (210) χ_X, of the X-group atom directly bonded to silicon (see Fig. 4-5). The relationship is:

$$|^{1}J(^{29}Si^{13}C)| = 7.9\ \chi_X + 32.8\ [Hz] \qquad [5]$$

$$(r = 0.73,\ \sigma = 1.6,\ N = 26)$$

Even for a data set containing a large number of substituents capable of (d-p)π bonding, this correlation further supports Harris' conclusion (95,96) (see Fig. 1-5) that the Fermi contact term dominates $^{1}J(^{29}Si^{13}C)$ in trimethylsilyl compounds. As a better measure of the inductive effect of a substituent, Swain-Lupton field effect parameters, F, were used. Figure 4-6 shows a plot of $|^{1}J(^{29}Si^{13}C)|$ vs. F parameters. The interesting feature of this plot is that, with the exception of the substituent $C{\equiv}CSiMe_3$, all the points fall on one of two lines. The upper line contains data for nitrogen and oxygen substituents which are the substituents most likely to (d-p)π bond. The relationship is:

$$|^{1}J(^{29}Si^{13}C)| = 8.3F + 56.8\ [Hz] \qquad [6]$$

$$(r = 0.71,\ \sigma = 0.9,\ N = 14)$$

The lower line contains carbon and sulfur substituents which are the least likely to (d-p)π bond. The relationship is:

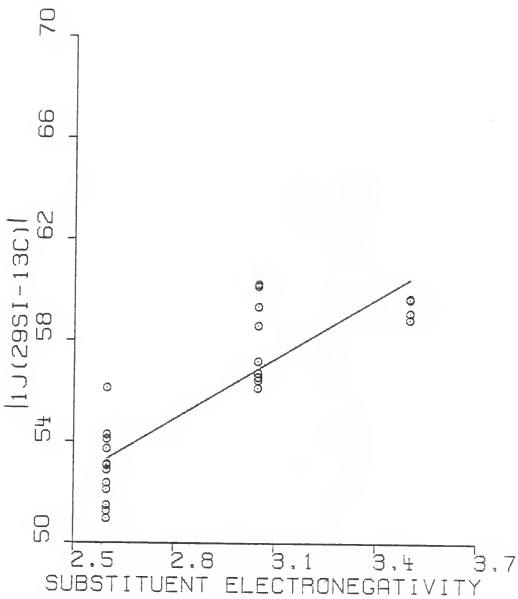

Figure 4-5. Plot of $|^{1}J(^{29}Si^{13}C)|$ in trimethylsilyl compounds vs. substituent electronegativity.

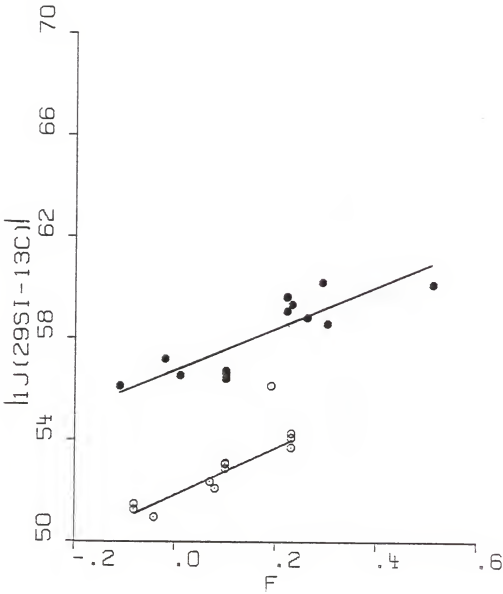

Figure 4-6. Plot of $|^{1}J(^{29}Si^{13}C)|$ in trimethylsilyl compounds vs. field effect parameters, F. Open circles are for molecules with N and O substituents; closed circles are for those with C and S substituents.

$$|{}^{1}J({}^{29}Si{}^{13}C)| = 11F + 51.9 \text{ [Hz]} \qquad [7]$$

$$(r = 0.73, \sigma = 0.8, N = 12)$$

Both of these correlations are at the 99% level of significance. These results suggest that there is an additional contribution to the spin-spin coupling from the non-contact terms for substituents most likely to (d-p)π bond. Thus, this appears to be evidence of (d-p)π bonding in Si-N and Si-O bonds. The unusual position of C≡CSiMe$_3$ which is intermediate between the two lines may indicate moderate (d-p)π bonding; however, since this F value was approximated from the value of C≡CH, this conclusion cannot be drawn with any degree of certainty.

Two separate correlations are also obtained in a plot of $^{2}J(^{29}SiCH)$ vs. $^{1}J(^{29}Si^{13}C)$ (see Fig. 4-7). For carbon and sulfur substituents, the relationship is:

$$|{}^{2}J({}^{29}SiCH)| = 0.064\ |{}^{1}J({}^{29}Si{}^{13}C)| + 3.4 \text{ [Hz]} \qquad [8]$$

$$(r = 0.57, \sigma = 0.09, N = 12)$$

The relationship for nitrogen and oxygen substituents is:

$$|{}^{2}J({}^{29}SiCH)| = 0.11\ |{}^{1}J({}^{29}Si{}^{13}C)| + 0.2 \text{ [Hz]} \qquad [9]$$

$$(r = 0.56, \sigma = 0.16, N = 14)$$

Both of these correlations are at the 95% level of significance. Since both $^{2}J(^{29}SiCH)$ and $^{1}J(^{29}Si^{13}C)$ are expected to be dependent upon the hybridization of the silicon and carbon atoms (137) (Fermi contact term is dominant), it appears the silicon hydribidization differs significantly for the two types of substituents. Therefore, these results suggest that there

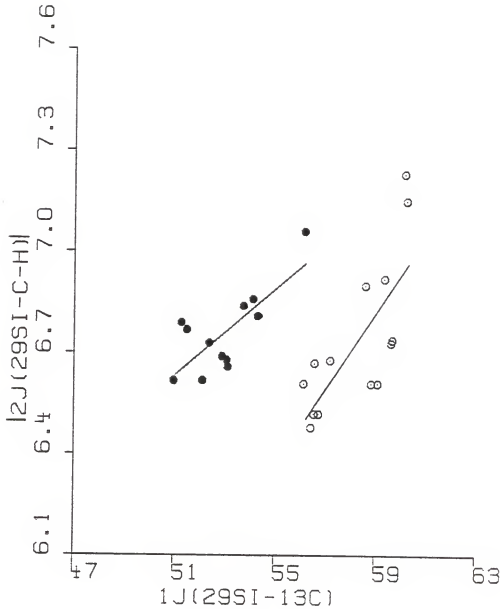

Figure 4-7. Plot of $|^{2}J(^{29}SiCH)|$ vs. $|^{1}J(^{29}Si^{13}C)|$ in trimethylsilyl compounds. Open circles are for molecules with N and O substituents; closed circles are for those with C and S substituents.

is (d-p)π bonding with the nitrogen and oxygen substituents and an absence of (d-p)π bonding for the carbon and sulfur substituents.

Two separate correlations are also obtained between $^{1}J(^{13}CH)$ in the methyl group and the field effect parameter, F (see Fig. 4-8). For carbon and sulfur substituents, the correlation is at the 99.9% level of significance and the relationship is:

$$^{1}J(^{13}CH) = 5.5F + 118.8 \text{ [Hz]} \qquad [10]$$

$$(r = 0.83, \sigma = 0.30, N = 12)$$

The correlation is at the 90% level of significance for nitrogen and oxygen substituents. The relationship is:

$$^{1}J(^{13}CH) = 4.5F + 117.7 \text{ [Hz]} \qquad [11]$$

$$(r = 0.52, \sigma = 0.69, N = 14)$$

Since two separate correlations are obtained, it is apparent that there is a difference in the transmission of inductive effects through the silicon for the two types of substituents. This may be caused by (d-p)π bonding with the nitrogen and oxygen and an absence of (d-p)π bonding for the carbon and sulfur substituents.

The $^{3}J(^{13}CSiCH)$ within the trimethylsilyl group is strongly correlated (99.9% level of significance) with $^{1}J(^{29}Si^{13}C)$ (see Fig. 4-9). The relationship is:

$$|^{3}J(^{13}CSiCH)| = -0.047\ |^{1}J(^{29}Si^{13}C)| + 4.4 \text{ [Hz]} \qquad [12]$$

$$(r = 0.67, \sigma = 0.1, N = 26)$$

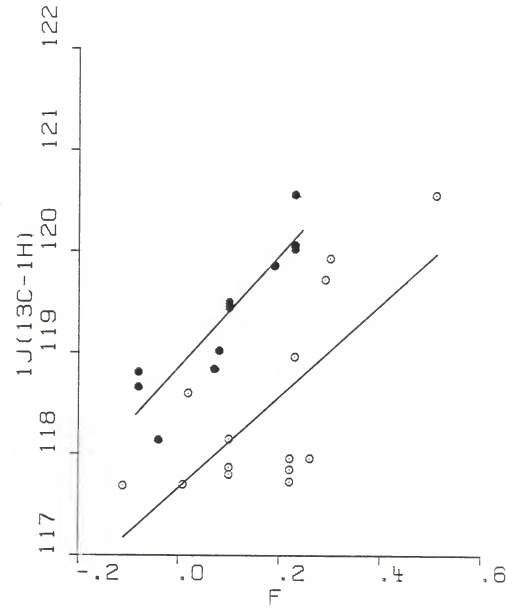

Figure 4-8. Plot of $^{1}J(^{13}CH)$ of the trimethylsilyl group in Me_3SiX compounds vs. the field effect parameter, F, of the X group. Open circles are for molecules with N and O substituents; closed circles are for those with C and S substituents.

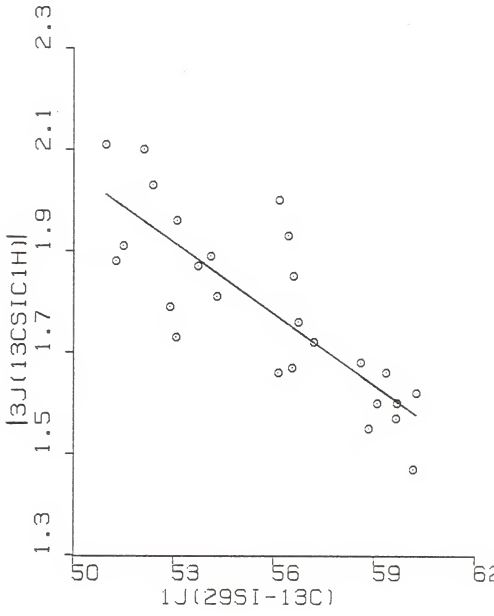

Figure 4-9. Plot of $|^{3}J(^{13}CSiCH)|$ vs. $|^{1}J(^{29}Si^{13}C)|$ of the trimethylsilyl group in Me_3SiX compounds.

The magnitude of this coupling constant is expected to be dependent upon the hybridization of the ^{13}C and the intervening Si and C atoms. In addition, this coupling is expected to be dependent upon the dihedral angle between the ^{13}C-Si and C-H bonds. Therefore, the deviations from this relationship may be attributed to changes in the dihedral angle and to variable transmission of inductive effects through the silicon.

Methylsilanes

Chemical Shifts

The ^{1}H, ^{13}C, and ^{29}Si chemical shifts of the methylsilyl group in $MeSiR^{I}R^{II}R^{III}$ compounds are listed in Tables 4-1 and 4-7. The ^{1}H and ^{13}C shifts of the R group are presented in Tables 4-2 and 4-8.

Of the 44 methylsilanes investigated in this study, the most shielded ^{29}Si nuclei are in compounds containing two or more nitrogens or oxygens directly bonded to silicon. Examples and observed shifts include $MeSi(NMe_2)_3$ (-16.24 ppm), $MeSi(OC(O)Me)_3$ (-42.27 ppm), and $MeSi(OEt)_3$ (-43.85 ppm). The results also show that replacing an amino group with a chlorine is always deshielding as in comparison of $Me_2Si(NMe_2)_2$ (-1.92 ppm) with $Me_2Si(Cl)NMe_2$ (13.69 ppm) and in comparison of $Me(Cl)Si(NEt_2)_2$ (-10.44 ppm) with $Me(Cl)_2SiNEt_2$ (-2.13 ppm). These results suggest that there is significant (d-p)π bonding in Si-N and Si-O bonds while there is negligible (d-p)π bonding in Si-Cl bonds.

Table 4-7. Chemical Shifts[a] of the Methylsilyl Group for Compounds of the Type $MeSiR^{I}R^{II}R^{III}$.[b]

R^{I}	R^{II}	R^{III}	^{1}H/ppm	^{13}C/ppm	^{29}Si/ppm
$CH_2CH=CH_2$	$CH_2CH=CH_2$	Me	0.00	-4.14	0.22
CH_2Cl	$CH=CH_2$	Me	0.18	-4.85	-5.45
$N(SiMe_2H)_2$	Me	H	0.19	0.65	-10.94
$NHSiMe_2H$	Me	H	0.12	0.55	-12.14
NEt_2	Me	H	0.09	-1.24	-8.00
$NHSiMe_2(CH_2Cl)$	CH_2Cl	Me	0.17	-1.12	1.11
NMe_2	NMe_2	H	0.05	-3.98	-10.41
$OSiMe_3$	Me	H	0.13	0.90	-7.48
OEt	$CH=CH_2$	Me	0.12	-1.95	3.76
$OSiMe_2C_6H_5$	C_6H_5	Me	0.32	0.86	-1.25
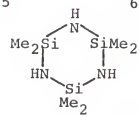			0.50	4.27	-5.10
NMe_2	NMe_2	Me	0.08	-3.48	-1.92
NEt_2	NEt_2	Me	0.03	-0.99	-5.50

Table 4-7 continued.

R^I	R^{II}	R^{III}	^1H/ppm	^{13}C/ppm	^{29}Si/ppm
NMe_2	NMe_2	$CH=CH_2$	0.05	-4.83	-11.51
Cl	NMe_2	Me	0.44	1.42	13.69
NMe_2	NMe_2	NMe_2	0.02	-6.18	-16.24
Cl	NEt_2	NEt_2	0.37	1.51	-10.44
Cl	Cl	NEt_2	0.76	4.36	-2.13
Cl	Cl	NMe_2	0.81	3.68	-0.10
OEt	OEt	Me	0.03	-3.10	-5.79
OEt	OEt	OEt	0.01	-6.90	-43.85
OC(O)Me	OC(O)Me	OC(O)Me	0.62	-3.66	-42.27

[a] Chemical shifts are relative to TMS.

[b] For chemical shifts of trimethylsilyl compounds, see Table 4-1.

Table 4-8. ^{1}H and ^{13}C Chemical Shifts[a] of the R Group for Compounds of the Type $MeSiR^{I}R^{II}R^{III}$.[b,c]

R^{I}	R^{II}	R^{III}	^{1}H/ppm[d]	^{13}C/ppm[d]
$CH_2CH=CH_2$	$CH_2CH=CH_2$	Me	1.53 (CH_2) 4.74 (H_2) 5.75 (H_1) 4.87 (H_3)	22.93 (CH_2) 134.64 (α) 113.27 (β)
CH_2Cl	$CH=CH_2$	Me	2.77 (CH_2Cl) 5.98 (H_2) 6.10 (H_1) 5.74 (H_3)	29.85 (CH_2Cl) 136.03 (α) 133.66 (β)
OEt	$CH=CH_2$	Me	3.63 (α) 6.10 (H_1) 1.12 (β) 5.95 (H_2) 5.75 (H_3)	58.40 (α-Et) 138.34 (α) 18.73 (β-Et) 132.72 (β)
$OSiMe_2C_6H_5$	C_6H_5	Me	7.21-7.25 (3H) 7.52-7.56 (2H)	139.63 (C_1) 127.89 (C_3) 133.10 (C_2) 129.42 (C_4)
OEt	OEt	Me	3.71 (α) 1.16 (β)	58.10 (α) 18.68 (β)
OEt	OEt	OEt	3.76 (α) 1.17 (β)	58.45 (α) 18.56 (β)
OC(O)Me	OC(O)Me	OC(O)Me	2.08	22.15 (Me) 169.68 (C=O)

[a]Chemical shifts are relative to TMS.

[b]For ^{1}H and ^{13}C chemical shifts of trimethylsilyl compounds, see tables 4-1 and 4-2.

[c]For chemical shifts of silylamines and related structures, see table 4-11.

[d]For the α, β, H_1, H_2, H_3, C_1, C_2, C_3, C_4 notation, see the text.

The ^{13}C shifts of the methylsilyl group range from 5.49 ppm to -6.90 ppm. The most shielded methyl carbons are those in compounds with the most electronegative substituents bonded to silicon. Examples and observed shifts include $MeSi(OEt)_3$ (-6.90 ppm), $MeSi(NMe_2)_3$ (-6.18 ppm), and $MeSi(NMe_2)_2CH{=}CH_2$ (-4.83 ppm). However, there are a number of notable exceptions to this generalization, for example, $MeSi(Cl)_2NEt_2$ (4.36 ppm), $MeSi(Cl)_2NMe_2$ (3.68 ppm), $Me_2Si(Cl)NMe_2$ (1.42 ppm), $MeSi(Cl)(NEt_2)_2$ (1.51 ppm), and $N(SiMe_3)_3$ (5.49 ppm). This deshielding of the methyl carbons contradicts the earlier findings of Rakita and Worsham (97) who reported that the replacement of a methyl by a first-row donor atom (C, N, O) leads to an upfield shift of the remaining methyls, regardless of the presence of absence of unshared pairs or π-type orbitals on the atom in question in $Me_{4-n}SiX_n$ compounds. The results from this current investigation suggest that other factors besides inductive effects influence the ^{13}C shielding of the methylsilyl group.

Coupling Constants

Coupling constants involving nuclei of the methylsilyl group for compounds of the type $MeSiR^IR^{II}R^{III}$ are listed in Tables 4-5 and 4-9. Values of $^{29}Si-^{1}H$ and $^{29}Si-^{13}C$ coupling constants of the R groups for methylsilanes are presented in Tables 4-6 and 4-10.

The $^{1}J(^{29}Si^{13}C)$ for methylsilyl compounds is strongly correlated (99.9% level of significance) with the sum of

Table 4-9. Coupling Constants Involving Nuclei of the Methylsilyl Group for Compounds of the Type $MeSiR^{I}R^{II}R^{III}$.[a]

R^{I}	R^{II}	R^{III}	$^{1}J^{13}CH$/Hz	$\lvert^{3}J^{13}CSiCH\rvert$/Hz	$\lvert^{1}J^{29}Si^{13}C\rvert$/Hz	$\lvert^{2}J^{29}SiCH\rvert$/Hz
$CH_2CH{=}CH_2$	$CH_2CH{=}CH_2$	Me	120.09	1.72	51.67	6.48
CH_2Cl	$CH{=}CH_2$	Me	120.05	1.00	54.93	6.80
$N(SiMe_2H)_2$	Me	H	119.21	1.85	56.27	7.00
$NHSiMe_2H$	Me	H	119.38	1.99	55.68	7.05
NEt_2	Me	H	118.67	1.97	55.64	6.95
$NHSiMe_2(CH_2Cl)$	CH_2Cl	Me	119.21	1.42	59.34	6.85
NMe_2	NMe_2	H	118.52	--	64.81	6.85
$OSiMe_2H$	Me	H	118.64	1.86	59.07	7.09
OEt	$CH{=}CH_2$	Me	118.52	1.12	61.47	6.73
$OSiMe_2C_6H_5$	C_6H_5	Me	118.62	1.51	61.23	6.68
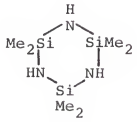			117.33	1.20	62.61	6.84
NMe_2	NMe_2	Me	117.59	1.34	65.75	6.64

Table 4-9 continued.

R^I	R^{II}	R^{III}	$^1J^{13}CH$/Hz	$\lvert^3J^{13}CSiCH\rvert$/Hz	$\lvert^1J^{29}Si^{13}C\rvert$/Hz	$\lvert^2J^{29}SiCH\rvert$/Hz
NEt_2	NEt_2	Me	117.45	1.43	65.24	6.77
NMe_2	NMe_2	$CH{=}CH_2$	118.13	0.00	67.98	6.57
Cl	NMe_2	Me	120.71	1.26	70.76	7.41
NMe_2	NMe_2	NMe_2	117.39	--	79.40	7.01
Cl	NEt_2	NEt_2	120.14	--	82.21	7.74
Cl	Cl	NEt_2	123.14	--	85.85	8.57
Cl	Cl	NMe_2	123.30	--	86.35	8.49
OEt	OEt	Me	118.15	0.74	73.73	7.11
OEt	OEt	OEt	118.86	--	96.68	8.29
OC(O)Me	OC(O)Me	OC(O)Me	123.11	--	97.36	9.48

[a]For coupling constants of trimethylsilyl compounds, see table 4-5.

Table 4-10. ^{29}Si-^{1}H and ^{29}Si-^{13}C Coupling Constants of the R Groups for Compounds of the Type $MeSiR^{I}R^{II}R^{III}$.[a,b]

R^{I}	R^{II}	R^{III}	$\lvert {}^{1}J^{29}Si^{13}C\rvert$/Hz[c]	$\lvert {}^{2}J^{29}SiCH\rvert$/Hz	$\lvert {}^{3}J^{29}SiH\rvert$/Hz
$CH_2CH=CH_2$	$CH_2CH=CH_2$	Me	47.41	--[d]	--[d]
CH_2Cl	$CH=CH_2$	Me	54.94 (CH_2Cl) 67.91 (α)	3.73 (CH_2Cl)	--[d]
OEt	$CH=CH_2$	Me	73.59	--[d]	--[d]
$OSiMe_2C_6H_5$	C_6H_5	Me[e]	77.46	--	5.53
OEt	OEt	Me	--	--	3.01
OEt	OEt	OEt	--	--	2.91

[a] For ^{29}Si coupling constants of trimethylsilyl compounds, see tables 4-5 and 4-6.

[b] For ^{29}Si coupling constants of silylamines and related structures, see table 4-13.

[c] For the α notation see the text.

[d] The ^{29}Si-^{1}H coupled spectrum is too complex to be analyzed since every ^{1}H in the molecule is coupled to the ^{29}Si nucleus.

[e] $\lvert {}^{4}J^{29}SiCCCH\rvert = \lvert {}^{5}J^{29}SiCCCCH\rvert = 0.89$ Hz.

Huggins' electronegativities (210), $\Sigma\chi_R$, of the R-group atoms directly bonded to silicon (see Fig. 4-10). The relationship is:

$$|^1J(^{29}Si^{13}C)| = 16.2\ \Sigma\chi_R - 74.3\ [Hz] \qquad [13]$$
$$(r = 0.88,\ \sigma = 4.0,\ N = 48)$$

This correlation indicates that the Fermi contact term is dominant even for compounds with multiple nitrogen and oxygen substituents. However, it is interesting to note that the largest deviations from this relationship are for compounds containing Si-N and Si-O bonds. Although these deviations suggest (d-p)π bonding in compounds containing Si-N and Si-O bonds, the deviations are smaller than those of the $^1J(^{13}C^{13}C)$ in cases of multiple bonding where there is a significant contribution from the orbital and dipolar terms (128,129). A possible explanation for this observation is that the orbital and dipolar terms may be large and opposite in sign, thereby producing only a small non-contact contribution to spin-spin coupling.

The dominance of the Fermi contact term in $^1J(^{29}Si^{13}C)$ is further supported by comparison of $^1J(^{29}Si^{13}C)$ in compounds containing both an sp^3 and sp^2 hybridized carbon bonded to silicon since the value of $^1J(^{29}Si^{13}C)$ should increase with increasing s character of the carbon. Examples and the observed $^1J(^{29}Si^{13}C)$ include $Me_3SiCH{=}CH_2$ (51.49 Hz sp^3, 64.72 (d-p)π Hz sp^2), $Me_3SiC_6H_5$ (52.11 Hz sp^3, 65.89 Hz sp^2), $Me_2Si(CH_2Cl)CH{=}CH_2$ (54.93 Hz sp^3, 67.91 Hz sp^2),

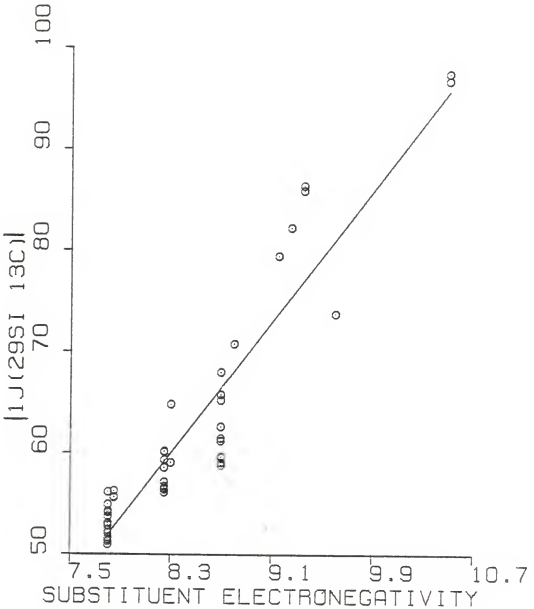

Figure 4-10. Plot of $|^{1}J(^{29}Si^{13}C)|$ vs. the sum of substituent electronegativity for methylsilyl compounds.

$Me_2Si(OEt)CH=CH_2$ (61.47 Hz sp^3, 73.59 Hz sp^2), and $(Me_2(C_6H_5)Si)_2O$ (61.23 Hz sp^3, 77.46 Hz sp^2). An even larger increase in the value of $^1J(^{29}Si^{13}C)$ is observed in bis-(trimethylsilyl) acetylene where for the sp^3 carbon, $^1J(^{29}Si^{13}C)$ = 56.15 Hz and for the sp carbon, $^1J(^{29}Si^{13}C)$ = 78.47 Hz.

The trends previously discussed for $^2J(^{29}SiCH)$, $^3J(^{13}CSiCH)$, and $^1J(^{13}CH)$ in trimethylsilyl compounds are also found for methylsilanes.

Silylamines

For the purposes of discussion, the carbon hydrogens of N,N-dimethylamino and N,N-diethylamino groups are denoted as follows:

$$X\text{-}N(\overset{\alpha}{C}H_3)_2 \qquad\qquad X\text{-}N(\overset{\alpha}{C}H_2\overset{\beta}{C}H_3)_2$$

Chemical Shifts

The ^1H, ^{13}C, and ^{29}Si chemical shifts for silylamines and related structures are presented in Table 4-11.

No correlation can be found between ^{15}N and ^{29}Si chemical shifts of N,N-dimethylamino or N,N-diethylamino silanes. This may be explained by competing inductive and (d-p)π effects. On the basis of solely inductive effects, substitution of an electronegative substituent at silicon will deshield the ^{29}Si nucleus and shield the ^{15}N nucleus. On the other hand, (d-p)π effects will produce the opposite behavior since delocalization of the nitrogen's lone pair electrons will be enhanced by substitution of an electronegative substituent at silicon.

Table 4-11. Chemical Shifts[a] for Silylamines and Related Structures.[b,c,d]

$R^IR^{II}R^{III}SiNMe_2$:

R^I	R^{II}	R^{III}	$^1H(\alpha)$/ppm	$^{13}C(\alpha)$/ppm	^{15}N/ppm	^{29}Si/ppm
Me	Me	Me	2.49	37.89	-379.94	6.48
NMe_2	Me	H[e]	2.46	37.63	-372.60	-10.41
NMe_2	Me	Me	2.52	37.60	-374.50	-1.92
NMe_2	$CH=CH_2$	Me[f]	2.46	37.73	-375.78	-11.51
NMe_2	NMe_2	H[g]	2.45	36.83	-373.09	-24.87
Cl	Me	Me	2.49	37.23	-365.85	13.69
NMe_2	NMe_2	Me	2.43	37.54	-374.04	-16.24
NMe_2	NMe_2	C_6H_5[h]	2.51	38.19	-374.25	-25.14
Cl	Cl	Me	2.59	36.65	-360.09	-0.10
NMe_2	NMe_2	NMe_2	2.48	37.18	-370.33	-28.15
Cl	NMe_2	NMe_2	2.48	37.16	-370.32	-28.57
Cl	Cl	NMe_2	2.58	36.87	-364.13	-28.54
Cl	Cl	Cl	2.69	36.81	-355.37	-25.79

$R^IR^{II}R^{III}SiNEt_2$:

R^I	R^{II}	R^{III}	$^1H(\alpha)$/ppm	$^1H(\beta)$/ppm	$^{13}C(\alpha)$/ppm	$^{13}C(\beta)$/ppm	^{15}N/ppm	^{29}Si/ppm
Me	Me	H[i]	2.82	0.98	41.50	16.03	-351.11	-8.00
Me	Me	Me	2.79	0.96	40.57	16.27	-348.19	3.67
NEt_2	Me	Me	2.81	0.96	39.73	15.87	-343.47	-5.50

Table 4-11 continued.

$R^{I}R^{II}R^{III}SiNEt_2$:

R^{I}	R^{II}	R^{III}	$^{1}H(\alpha)$/ppm	$^{1}H(\beta)$/ppm	$^{13}C(\alpha)$/ppm	$^{13}C(\beta)$/ppm	^{15}N/ppm	^{29}Si/ppm
Cl	NEt_2	Me	2.90	1.02	39.29	15.15	-338.60	-10.44
Cl	Cl	Me	2.99	1.07	39.77	15.10	-329.76	-2.13
NEt_2	NEt_2	NEt_2	2.85	1.00	38.92	15.20	-341.84	-28.20
Cl	NEt_2	NEt_2	2.92	1.03	38.71	14.46	-341.81	-29.94
Cl	Cl	NEt_2	3.03	1.08	39.61	14.72	-334.47	-30.75
Cl	Cl	Cl	3.12	1.11	40.30	14.91	-325.37	-27.44

$R^{I}Me_2SiNR^{II}R^{III}$:

R^{I}	R^{II}	R^{III}	^{15}N/ppm	^{29}Si/ppm
H	$SiMe_2H$	$SiMe_2H$[j]	-358.03	-10.94
H	H	$SiMe_2H$[k]	-363.96	-12.14
Me	$SiMe_3$	$SiMe_3$	-345.91	2.46
Me	H	$SiMe_3$	-353.70	2.14
CH_2Cl	H	$SiMe_2(CH_2Cl)$[ℓ]	-359.74	1.11
Me	Me	$SiMe_3$	-371.94	6.05

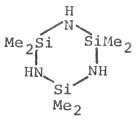

-346.40 -5.10

Table 4-11 continued.

$R^{I}Me_2SiNR^{II}R^{III}$:

R^{I}	R^{II}	R^{III}	^{15}N/ppm	^{29}Si/ppm
Me	C_6H_5	H	-313.78	1.71
Me		=C=S	-246.06	5.84
Me		$=C=N-SiMe_3$	-329.71	-1.03
Me		=C=O	-346.34	4.16

[a] ^{1}H, ^{13}C and ^{29}Si chemical shifts are relative to TMS; ^{15}N chemical shifts are relative to external 80% v/v nitromethane in the same solvent as the sample.

[b] For ^{1}H and ^{13}C chemical shifts of trimethylsilyl compounds, see tables 4-1 and 4-2.

[c] For ^{1}H and ^{13}C chemical shifts of the methylsilyl group, see table 4-7.

[d] For the α and β notation see the text.

[e] $\delta^{1}H$ (SiH) = 4.34 ppm.

[f] $\delta^{1}H$ (H_1) = 6.05 ppm, $\delta^{1}H$ (H_2) = 5.91 ppm, $\delta^{1}H$ (H_3) = 5.65 ppm, $\delta^{13}C(\alpha)$ = 137.29 ppm, and $\delta^{13}C(\beta)$ = 132.52 ppm.

[g] $\delta^{1}H$(SiH) = 4.12 ppm

[h] $\delta^{1}H$ = 7.53 - 7.56 ppm (2H), $\delta^{1}H$ = 7.31 - 7.36 ppm (3H), $\delta^{13}C$ (C_1) = 136.44 ppm, $\delta^{13}C$ (C_2) = 135.46 ppm, $\delta^{13}C$ (C_3) = 127.70 ppm, and $\delta^{13}C$ (C_4) = 129.09 ppm.

[i] $\delta^{1}H$ (SiH) = 4.44 ppm.

Table 4-11 continued.

j δ^1H (SiH) = 4.57 ppm.

k δ^1H (NH) = 1.17 ppm, δ^1H (SiH) = 4.48 ppm.

ℓ δ^1H (NH) = 1.51 ppm, δ^1H (CH_2Cl) = 2.71 ppm, and δ^{13}C (CH_2Cl) = 31.96 ppm.

The results show that the most shielded ^{29}Si nuclei are those in compounds which have multiple Si-N bonds or Si-Cl bonds for the N,N-diethylamino and N,N-diethylamino silanes. In contrast, the most deshielded ^{15}N nuclei are those in compounds containing one or two amino groups and at least one electronegative substituent bonded to silicon. Examples and observed shifts include $Cl_2MeSiNMe_2$ (-360.09 ppm), $Cl_2Si(NMe_2)_2$ (-364.13 ppm), Cl_3SiNMe_2 (-355.37 ppm), $Cl_2MeSiNEt_2$ (-329.76 ppm), and Cl_3SiNEt_2 (-325.37 ppm). These results suggest that delocalization of the nitrogen's lone pair electrons is enhanced by substitution of an electronegative substituent at the silicon and that the extent of the (d-p)π bonding per bond decreases with increasing numbers of Si-N bonds.

Comparison of ^{15}N chemical shifts of N,N-dimethylamino with N,N-diethylamino silanes show that the N,N-diethylamino silanes are deshielded by about 30 ppm. Examples and observed shifts include comparison of Me_3SiNMe_2 (-379.94 ppm) with Me_3SiNEt_2 (3-48.19 ppm) and comparison of $Cl_2MeSiNMe_2$ (-360.09 ppm) with $Cl_2MeSiNEt_2$ (-329.76 ppm). This deshielding is attributed to the well-known β effect. The deshielding of the ^{15}N nucleus by 15 ppm per β carbon in silylamines compares favorably with the reported value of 12 ppm per β carbon in alkylamines (211).

Data comparing ^{15}N chemical shifts of silanes with the corresponding hydrocarbons are presented in Table 4-12. These data indicate that ^{15}N shielding in organosilanes is dominated by the strong +I effect of the silicon since the nitrogens in the organosilanes are shielded by about 30 ppm in comparison to the corresponding hydrocarbon.

Table 4-12. Comparison of ^{15}N Chemical Shifts in Silanes with the Corresponding Hydrocarbon.

Silane	^{15}N/ppm[a]	Hydrocarbon	^{15}N/ppm	Ref.
Me_3SiNMe_2	-379.94	Me_3CNMe_2	-348.8	211
$Me_3SiN{=}C{=}O$	-346.34	$Me_3CN{=}C{=}O$	-324.2	212
$Me_3SiN{=}C{=}NSiMe_3$	-329.71	$Me_3C^{15}N{=}C{=}NCHMe_2$	-267.6	213
$(Me_3Si)_2NH$	-353.70	$Me_3SiNHCMe_3$	-325	119
$(Me_3Si)_3N$	-345.91	$(Me_3Si)_2NCMe_3$	-320	119

[a]Data from this study.

The ^{13}C chemical shifts of the N,N-dimethylamino group range from 36.65 ppm to 38.19 ppm while the ^{1}H chemical shifts range from 2.43 to 2.69 ppm. The ^{13}C chemical shifts of the α carbon in the N,N-diethylamino group range from 38.92 ppm to 41.50 ppm while the ^{1}H chemical shifts range from 2.82 to 3.12 ppm. There are no correlations between these shifts and inductive parameters. Therefore, other factors besides inductive effects influence these shieldings.

The ^{13}C chemical shifts of the β carbon in the N,N-diethylamino group decrease with increasing electronegativity of the substituents bonded to silicon. The ^{1}H chemical shifts of the protons attached to the β carbon increase with increasing electronegativity of the substituents bonded to silicon. These results suggest that inductive effects strongly influence the shieldings of the β carbon and protons in the N,N-diethylamino group.

Coupling Constants

Values of coupling constants and corrected ^{29}Si linewidths for silylamines and related structures are presented in Table 4-13. The corrected ^{29}Si linewidth is defined as sample linewidth at half-height minus TMS linewidth at half-height.

The value of $^{1}J(^{29}Si^{15}N)$ were measured from the ^{29}Si satellites in the ^{15}N INEPT or INEPTD spectrum. Figure 4-11 shows satellites in the INEPTD spectrum of the nitrogen of N,N-diethylaminomethyldichlorosilane not only for $^{1}J(^{29}Si^{15}N)$ but also for $^{1}J(^{15}N^{13}C)$ and $^{2}J(^{15}N^{13}C)$. Figure 4-12 shows

Table 4-13. Coupling Constants and ^{29}Si Corrected Linewidths[a] for Silylamines and Related Structures.[b,c,d]

$R^IR^{II}R^{III}SiNMe_2$:

R^I	R^{II}	R^{III}	$\lvert^1J^{13}C_\alpha H\rvert$/Hz	$\lvert^3J^{13}C_\alpha NCH\rvert$/Hz	$\lvert^3J^{29}SiNCH\rvert$/Hz	$\lvert^1J^{29}Si^{15}N\rvert$/Hz	$\nu_{1/2(corr.)}$/Hz
Me	Me	Me	132.35	5.33	3.44	18.34	3.06
NMe_2	Me	H[e]	132.74	5.09	--[f]	21.01	9.99
NMe_2	Me	Me	132.38	5.23	3.40	22.42	6.25
NMe_2	$CH=CH_2$	Me	132.66	5.18	3.21	24.03	7.45
NMe_2	NMe_2	H[g]	132.80	5.08	3.62	28.15	13.8
Cl	Me	Me	134.14	5.11	4.60	20.33	4.45
NMe_2	NMe_2	Me	132.39	5.17	3.30	27.74	12.7
NMe_2	NMe_2	C_6H_5[h]	132.80	5.13	3.37	29.44	5.34
Cl	Cl	Me[i]	135.57	4.90	4.85	28.39	6.81
NMe_2	NMe_2	NMe_2	133.92	4.94	--[f]	39.25	13.0
Cl	NMe_2	NMe_2	133.94	4.95	3.89	39.37	13.0
Cl	Cl	NMe_2	135.46	4.79	4.94	40.99	18.5
Cl	Cl	Cl	136.85	4.66	5.66	41.28	16.5

$R^IR^{II}R^{III}SiNEt_2$:

R^I	R^{II}	R^{III}	$^3J_{HCCH}$/Hz	$\lvert^1J^{13}C_\alpha H\rvert$/Hz	$\lvert^2J^{13}C_\alpha CH\rvert$/Hz	$\lvert^3J^{13}CNCH\rvert$/Hz	$\lvert^1J^{13}C_\beta H\rvert$/Hz	$\lvert^2J^{13}C_\beta CH\rvert$/Hz	$\lvert^3J^{15}NCCH\rvert$/Hz	$\lvert^3J^{29}SiNCH\rvert$/Hz	$\lvert^1J^{29}Si^{15}N\rvert$/Hz	$\nu_{1/2(corr.)}$/Hz
Me	Me	H[j]	7.10	132.22	4.48	5.68	124.85	2.28	2.41	4.01	20.26	3.10
Me	Me	Me	7.06	131.82	5.82	4.43	124.70	2.19	--[k]	3.74	19.57	1.59
NEt_2	Me	Me	7.10	131.95	4.40	5.68	124.59	2.25	--[k]	3.92	24.81	3.24
Cl	NEt_2	Me	7.08	133.49	4.44	5.34	125.11	2.43	--[f]	--[f]	29.80	4.04
Cl	Cl	Me[l]	7.13	134.79	4.35	5.38	125.74	2.50	--[f]	5.54	29.71	4.08
NEt_2	NEt_2	NEt_2	7.07	132.41	5.41	4.34	124.68	2.37	2.48	4.02	38.76	5.62
Cl	NEt_2	NEt_2	7.03	133.51	4.34	5.19	125.03	2.48	2.48	4.49	38.78	3.39
Cl	Cl	NEt_2	7.06	134.85	4.42	5.21	125.56	2.57	2.60	5.59	40.27	7.08
Cl	Cl	Cl	7.05	136.05	4.33	5.26	126.12	2.55	2.78	--[f]	40.71	8.94

Table 4-13 continued.

$R^{I}Me_2SiNR^{II}R^{III}$,

R^{I}	R^{II}	R^{III}	$\lvert^1J^{15}NH\rvert$/Hz	$\lvert^1J^{29}Si^{15}N\rvert$/Hz	$\nu_{1/2}$(corr.)/Hz
H	$SiMe_2H$	$SiMe_2H$ [m]	--	8.74	1.46
H	H	$SiMe_2H$ [n]	68.98	13.68	5.30
Me	$SiMe_3$	$SiMe_3$	--	7.76	0.36
Me	H	$SiMe_3$ [o]	66.58	13.64	2.05
CH_2Cl	H	$SiMe_2(CH_2Cl)$ [p]	67.47	14.39	1.05
Me	Me	$SiMe_3$ [q]	--	14.13	1.35
		[r]	69.69	16.20	2.44
Me	C_6H_5	H [s]	78.73	16.35	0.49
Me	=C=S		--	-- [t]	6.45
Me	=C=N-$SiMe_3$	[u]	--	15.89	1.72
Me	=C=O	[v]	--	14.55	7.84

---

[a] ^{29}Si corrected linewidth is defined as sample linewidth at half-height minus TMS linewidth at half-height.

[b] For coupling constants involving nuclei of the trimethylsilyl group for trimethylsilyl substituted compounds, see table 4-5.

[c] For coupling constants involving nuclei of the methylsilyl group for methylsilylamines, see table 4-9.

[d] For the α,β notation see the text.

[e] $\lvert^1J^{29}SiH\rvert$ = 207.54 Hz, $\lvert^2J^{13}CSiH\rvert$ = 14.30 Hz, $\lvert^3J^{13}CNSiH\rvert$ = 1.59 Hz, and $\lvert^3JHCSiH\rvert$ = 2.44 Hz.

[f] Not obtained, since sample decomposed.

[g] $\lvert^1J^{29}SiH\rvert$ = 187.36 Hz, $\lvert^3J^{13}CNSiH\rvert$ = 1.16 Hz, and $\lvert^2J^{15}NSiH\rvert$ = 10.13 Hz.

[h] $\lvert^1J^{29}Si^{13}C\rvert$ = 96.95 Hz.

[i] $\lvert^2J^{15}NCH\rvert$ = 0.44 Hz; $\lvert^3J^{15}NSiCH\rvert$ = 0.0 Hz.

[j] $\lvert^3J^{15}NSiCH\rvert$ = 0.89 Hz, $\lvert^1J^{29}SiH\rvert$ = 193.67 Hz, $\lvert^2J^{13}CSiH\rvert$ = 10.93 Hz, $\lvert^3J^{13}CNSiH\rvert$ = 1.90 Hz, and $\lvert^3JHCSiH\rvert$ = 3.20 Hz.

[k] The ^{15}N INEPT spectrum was not obtained since the resulting spectrum would be too complex to interpret.

Table 4-13 continued.

[l] $|^{1}J^{15}N^{13}C|$ = 2.61 Hz; $|^{2}J^{15}NC^{13}C|$ = 1.18 Hz.

[m] $|^{1}J^{29}SiH|$ = 193.48 Hz, $|^{3}J^{29}SiNSiH|$ = 4.62 Hz, $|^{2}J^{15}NSiH|$ = 5.31 Hz, $|^{2}J^{13}CSiH|$ = 9.78 Hz, and $|^{3}JHCSiH|$ = 3.34 Hz.

[n] $|^{1}J^{29}SiH|$ = 192.99 Hz, $|^{2}J^{15}NSiH|$ = 5.68 Hz, $|^{3}J^{15}NSiCH|$ = 1.03 Hz, $|^{2}J^{13}CSiH|$ = 10.96 Hz, and $|^{3}JHCSiH|$ = 3.15 Hz.

[o] $|^{3}J^{15}NSiCH|$ = 0.96 Hz.

[p] $|^{2}J^{29}SiNH|$ = 4.03 Hz, $|^{1}J^{29}Si^{13}C\ (CH_2Cl)|$ = 57.22 Hz, and $|^{2}J^{29}SiCH\ (CH_2Cl)|$ = 3.89 Hz.

[q] $|^{3}J^{29}SiNCH|$ = 4.63 Hz; $^{1}J^{13}CH\ (NCH_3)$ = 134.61 Hz.

[r] $|^{3}J^{15}NSiNH|$ = 0.0 Hz, $|^{3}J^{15}NSiCH|$ = 0.76 Hz, and $|^{2}J^{29}SiNH|$ = 0.0 Hz.

[s] $|^{2}J^{29}SiNH|$ = 2.02 Hz.

[t] The S/N of the ^{15}N INEPT and INEPTD spectra was too poor to detect the ^{29}Si satellites.

[u] $|^{3}J^{15}NSiCH|$ = 1.20 Hz.

[v] $|^{3}J^{15}NSiCH|$ = 1.27 Hz.

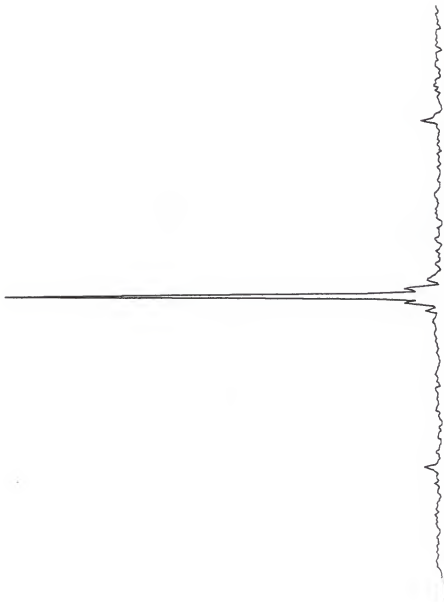

Figure 4-11. ^{15}N INEPTD spectrum of N,N-diethylaminomethyldichlorosilane.

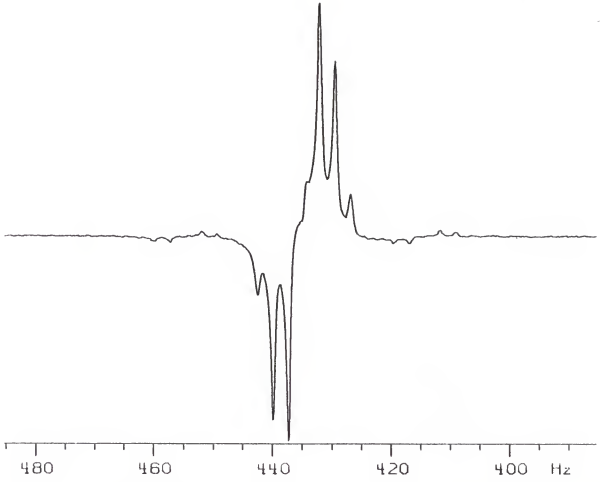

Figure 4-12. ^{15}N INEPT spectrum of N,N-diethylaminotrichlorosilane.

satellites from the one-bond coupling of the ^{29}Si nucleus to the nitrogen of N,N-diethylaminotrichlorosilane in the ^{15}N INEPT spectrum.

The $^{1}J(^{29}Si^{15}N)$ is strongly correlated (99.9% level of significance) with the sum of Huggins' electronegativities (210), $\Sigma\chi_R$, of the R-group atom directly bonded to silicon and nitrogen (see Fig. 4-13). The relationship is:

$$|^{1}J(^{29}Si^{15}N)| = 9.6\ \Sigma\chi_R - 102\ [Hz] \qquad [14]$$
$$(r = 0.90,\ \sigma = 3.3,\ N = 30)$$

This correlation indicates that the Fermi contact term is dominant. This result is somewhat surprising since large deviations were expected because of (d-p)π bonding. In addition, since the shift data seems to indicate varying amounts of (d-p)π bonding in the silylamines, it was expected that there would be a varying amount of non-contact contribution to the spin-spin coupling. A plausible explanation for this observation is that the orbital and dipolar terms vary with the extent of the (d-p)π bonding but are of opposite signs, thereby producing a small non-contact contribution. Clearly these results indicate the need for quantum mechanical calculations of $^{1}J(^{29}Si^{15}N)$ in silylamines.

From Table 4-13, it is apparent that the corrected ^{29}Si linewidth generally increases with increasing $^{1}J(^{29}Si^{15}N)$. This suggests that T_2 scalar coupling relaxation is dominant for ^{29}Si nuclei in silylamines. The equations defining T_2^{sc} are (214):

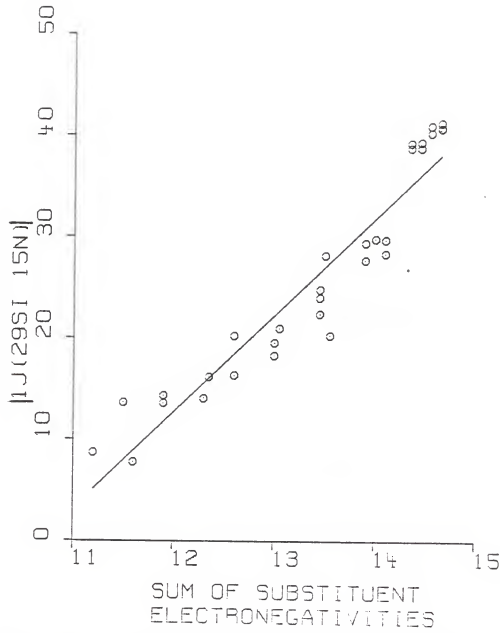

Figure 4-13. Plot of $|^{1}J(^{29}Si^{15}N)|$ in silylamines vs. the sum of substituent electronegativities.

$$1/T_1^{sc} = \frac{8\pi^2 J^2}{3} S(S+1) \frac{\tau_{sc}}{1+(\omega_s-\omega_c)^2\tau_{sc}^2} \quad [15]$$

and

$$1/T_2^{sc} = 1/(2T_1^{sc}) + \frac{4\pi^2 J^2}{3} S(S+1)\tau_{sc} \quad [16]$$

where J is the scalar spin-spin coupling constant, S is the spin of coupling nucleus, τ_{sc} is the relaxation time of the interacting nucleus, and ω_s and ω_c are the Larmor frequencies of the two coupled nuclei. For ^{14}N, S = 1, then,

$$1/T_2^{sc} = \frac{8\pi^2 J^2}{3} \tau_{sc} \left[1 + \frac{1}{1+(^{\omega}14_N - ^{\omega}29_{Si})^2\tau_{sc}^2}\right] \quad [17]$$

and since in a 7.05 T field $^{\omega}14_N$ = 21.7 MHz and $^{\omega}29_{Si}$ = 59.6 MHz and for amines, the T_1 of the ^{14}N are typically about 2 ms then,

$$1/T_2^{sc} = \frac{8\pi^2 J^2}{3} \tau_{sc} \quad [18]$$

The observed linewidth of a sample is given by:

$$\nu_{1/2} = 1/\pi T_2^* \quad [19]$$

$$1/T_2^* = 1/T_2 + 1/\Delta \quad [20]$$

where T_2^* is the effective T_2 and Δ is the magnetic field inhomogeneity. As a mesure of the magnetic field inhomogeneity, the half-height linewidth of TMS can be used. The $^1J(^{29}Si^{15}N)$ is equal to the $^1J(^{29}Si^{14}N)$ times $^{\delta}15_N/^{\delta}14_N$. Therefore, the corrected linewidth, $\nu_{1/2}$(corr) can be related to the $^1J(^{29}Si^{15}N)$ as shown

$$\nu_{1/2}(\text{corr}) \cdot \pi = 1/T_2^{sc} = \frac{8\pi^2 J^2}{3} \tau_{sc} \qquad [21]$$

$$|{}^1J({}^{29}Si{}^{15}N)| = \frac{{}^{15}N}{{}^{14}N} \left(\nu_{1/2}(\text{corr}) \frac{3}{8\tau\pi_{sc}} \right)^{1/2} \qquad [22]$$

Thus, a correlation between $|{}^1J({}^{29}Si{}^{15}N)|$ and the square root of $\nu_{1/2}(\text{corr})$ may be taken as evidence of the dominance of T_2 scalar coupling relaxation.

The ${}^1J({}^{29}Si{}^{15}N)$ in N,N-diethylaminosilanes is correlated (95% level of significance) with the square root of the corrected ${}^{29}Si$ linewidth (see Fig. 4-14). The relationship is

$$|{}^1J({}^{29}Si{}^{15}N)| = 13 \ (\nu_{1/2}(\text{corr})^{1/2} + 3.3 \ [\text{Hz}] \qquad [23]$$

$$(r = 0.67, \sigma = 5.2, N = 9)$$

A similar correlation (95% level of significance) is found for the N,N-dimethylaminosilanes (see Fig. 4-15). The relationship is:

$${}^1J({}^{29}Si{}^{15}N) = 8.5 \ (\nu_{1/2}(\text{corr})^{1/2} + 3.5 \ [\text{Hz}] \qquad [24]$$

$$(r = 0.64, \sigma = 5.2, N = 13)$$

These correlations indicate that T_2 scalar coupling relaxation, T_2^{sc} is dominant for the ${}^{29}Si$ nucleus. The deviations from these relationships and the fact that there are two separate correlations for the N,N-dimethylaminosilanes and the N,N-diethylaminosilanes are due to difference in the ${}^{14}N$ T_1 relaxation time.

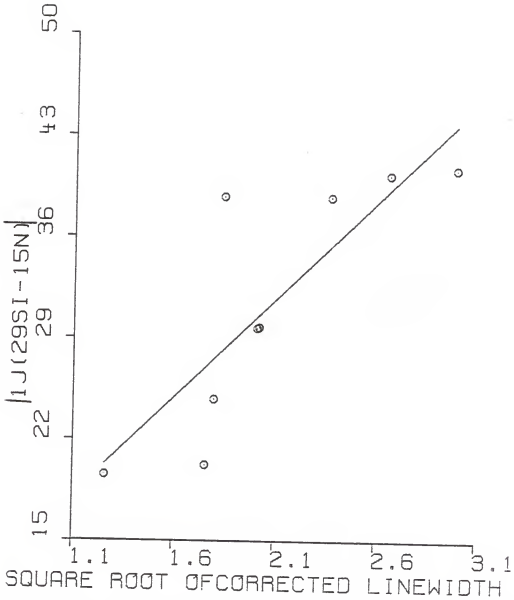

Figure 4-14. Plot of $|^{1}J(^{29}Si^{15}N)|$ in N,N-diethylaminosilanes vs. the square root of the corrected ^{29}Si linewidth (see text).

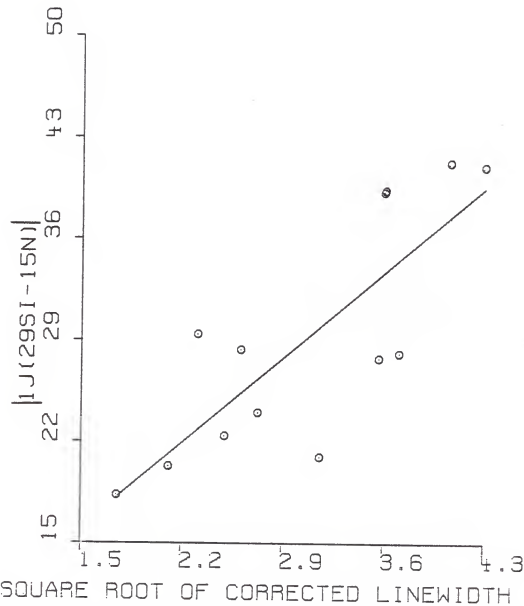

Figure 4-15. Plot of $|\,^{1}J(^{29}Si^{15}N)|$ in N,N-dimethylaminosilanes vs. the square root of the corrected ^{29}Si linewidth (see text).

Other values of spin-spin couplings involving protons coupled to carbon-13 or silicon-29 in silylamines are reported in Table 4-13. The $^{1}J(^{13}CH)$ of the N,N-dimethylamino group increases with increasing electronegative substitution at the silicon. The value of $|^{3}J(^{13}CNCH)|$ within the N,N-dimethylamino group decreases with increasing electronegative substitution at the silicon. These results suggest that the Fermi contact term is dominant. The relationship between the values of other spin-spin couplings and substitution at silicon are less clear indicating that there are variations in bond angles and/or transmission of inductive effects through the bonds. These variations may result from (d-p)π bonding.

CHAPTER V
CONCLUSIONS

For ^{29}Si nuclei in silylamines, it is concluded that scalar coupling relaxation, T_2^{SC} is dominant since there is a correlation between $|^1J(^{29}Si^{15}N)|$ and the square root of the linewidth.

The chemical shift data of trimethylsilanes, methylsilanes, and silylamines are best interpreted in terms of competing (d-p)π and inductive effects. The $^1J(^{29}Si^{13}C)$ and $^1J(^{29}Si^{15}N)$ are strongly dominated by the Fermi contact term. Although the Fermi contact term is not expected to be dominant for compounds in which the chemical shift data clearly indicates (d-p)π bonding, the dominance of the Fermi contact term suggests that the orbital and dipolar terms may be large but opposite in sign. This thereby produces only a small non-contact contribution to spin-spin coupling. Certainly, these results indicate the need for quantum mechanical calculations of $^1J(^{29}Si^{15}N)$ in silylamines and $^1J(^{29}Si^{13}C)$ in methylsilanes containing Si-O or Si-N bonds. These results are consistent with a model of competing (d-p)π and inductive effects. From the data it is concluded that there is significant (d-p)π bonding for Si-N and Si-O bonds, moderate to negligible (d-p)π bonding for Si-C (unsaturated carbon), and negligible (d-p)π bonding for Si-S and Si-Cl bonds.

REFERENCES

1. H. Kwart and K. King, "d-Orbitals in the Chemistry of Silicon, Phosphorus and Sulfur," Springer-Verlag, New York (1977).

2. P.R. Jones, J. Organometal. Chem. 109, 113 (1976).

3. P.R. Jones, J. Organometal. Chem. 83, 213 (1974).

4. F.A. Cotton and G. Wilkinson, "Advanced Inorganic Chemistry," 4th ed., John Wiley and Sons, Inc., New York (1980).

5. V. Schomaker and D.P. Stevenson, J. Am. Chem. Soc. 63, 37 (1941).

6. M. Veith and H. Baernighausen, Acta Cryst. 30B, 1806 (1974).

7. L.V. Vilkov and N.A. Tarasenko, Chem. Comm. 1176 (1969).

8. W. Zeil, J. Haase, and M. Dakkouri, Discuss. Faraday Soc. 47, 149 (1969).

9. I. Shen, J. Mol. Struct. 95, 215 (1982).

10. Y. Shiki, A. Hasegawa, and M. Yasaki, J. Mol. Struct. 78, 185 (1982).

11. C. Glidewell and G.M. Sheldrick, J. Chem. Soc. 3127A (1971).

12. C. Glidewell and D.C. Liles, Acta Cryst. 34B, 124 (1978).

13. C. Glidewell and H.D. Holden, Acta Cyrst. 37B, 754 (1981).

14. A.G. Robiette, G.M. Sheldrick, W.S. Sheldrick, B. Beagley, D.W.J. Cruickshank, J.J. Monaghan, B.J. Aylett, and I.A. Ellis, Chem. Comm. 909 (1968).

15. B. Rozsondai, I. Hargittai, A.V. Golubinskii, L.V. Vilkov, and V.S. Mastyukov, J. Mol. Struct. 28, 339 (1975).

16. C. Kratky, H.G. Schuster, and E. Hengge, J. Organometal. Chem. 247, 253 (1983).

17. E. Vajada, M. Kolonits, and B. Rozsondai, J. Mol. Struct. 95, 197 (1982).

18. C. Glidewell, D.W. H. Rankin, A.G. Robiette, and G.M. Sheldrick, J. Mol. Struct. 6, 231 (1970).

19. W. Airey, C. Glidewell, A.G. Robiette, and G.M. Sheldrick, J. Mol. Struct. 8, 435 (1971), unpublished work therein.

20. W. Airey, C. Glidewell, A.G. Robiette, G.M. Sheldrick, and J.M. Freeman, J. Mol. Struct. 8, 423 (1971).

21 R.L. Hilderbrandt and S.H. Bauer, J. Mol. Struct. 3, 325 (1969).

22. D.R. Jenkins, R. Kewley, and T.M. Snyder, Trans. Faraday Soc. 58, 1284 (1962).

23. D.W.H. Rankin, A.G. Robiette, G.M. Sheldrick, W.S. Sheldrick, B.J. Aylett, I.A. Ellis, and J.J. Monaghan, J. Chem. Soc. A 1224 (1969).

24. G. Glidewell, D.W.H. Rankin, A.G. Robiette, and G.M. Sheldrick, J. Mol. Struct. 4, 215 (1969).

25. L. Parkanyi, G.Y. Argay, P. Hencsei, and J. Nagy, J. Organometal. Chem. 116, 299 (1976).

26. H. Hedberg, J. Am. Chem. Soc. 77, 6491 (1955); B. Beagley and A.R. Conrad, Trans. Faraday Soc. 66, 2740 (1970).

27. C. Glidewell, D.W.H. Rankin, A.G. Robiette, and G.M. Sheldrick, J. Chem. Soc. A 318 (1970).

28. C. Glidewell and A.G. Robiette, Chem. Phys. Lett. 28, 290 (1974).

29. M.J. Barrow, E.A. V Ebsworth, and M.M. Harding, Acta Cryst. 35B, 2093 (1979).

30. H. Bock, P. Mollére, G. Becker, and G. Fritz, J. Organometal Chem. 61, 113 (1973).

31. C. Glidewell, D.W.H. Rankin, A.G. Robiette, G.M. Sheldrick, B. Beagley, and J.M. Freeman, J. Mol. Struct. 5, 417 (1970).

32. W. Airey, C. Glidewell, A.G. Robiette, and G.M. Sheldrick, J. Mol. Struct. 8, 413 (1971).

33. W. Clegg, Acta Cryst. 38B, 1648 (1982).

34. W. Airey, C. Glidewell, D.W.H. Rankin, A.G. Robiette, and G.M. Sheldrick, Trans. Faraday Soc. 66, 551 (1970).

35. A. Almenningen, K. Hedberg, and R. Seip, Acta Chem. Scand. 17, 2264 (1963).

36. A. Almeningen, H.M. Seip, and R. Seip, Acta Chem. Scand. 24, 1697 (1970).

37. C. Glidewell and D.C. Liles, Acta Cryst. 34B, 696 (1978).

38. J.E. Wollrod and V.W. Laurie, J. Chem. Phys. 48, 5058 (1968).

39. R.G. Lett and W.H. Flygare, J. Chem. Phys. 47, 4730 (1967).

40. C. Glidewell, D.W.H. Rankin, A.G. Robiette, G.M. Sheldrick, B.J. Aylett, I.A. Ellis, and J.J. Monaghan, J. Chem. Soc. A 1224 (1969).

41. C. Glidewell and H.D. Holden, Acta Cryst. 37B, 754 (1981).

42. H. Siebert, Z. Anorg. Allg. Chem. 273, 170 (1953).

43. J. Koput and J. Konanski, Spectrochim. Acta 35A, 1107 (1979).

44. H. Bürger, U. Goetze, and W. Sawodny, Spectrochim. Acta 26A, 671, 685 (1970).

45. H. Bürger and W. Sawodny, Spectrochim. Acta 23A, 2827 (1967).

46. F. Höfler, Monatsh. Chem. 107, 705 (1976).

47. A.J.F. Clark and J.E. Drake, Spectrochim. Acta 37A, 391 (1981).

48. Y. Imai and K. Aida, Bull. Chem. Soc. Jpn. 54, 925 (1981).

49. T.J. Veszprémi, J. Nagy, I.A. Barta, and G. Zsombok, J. Organometal. Chem. 185, 323 (1980).

50. K. Ulbricht, J. Jakoubkova, and V. Chvalovsky, Coll. Czech. Comm. 33, 1691 (1968).

51. E.W. Abel, D.A. Armitage, and D.B. Brady, Trans. Faraday Soc. 62, 3459 (1966).

52. V. Fialova, V. Bazant, and V. Chvalovsky, Coll. Czech. Chem. Comm. 38, 3837 (1973).

53. R. West, L.S. Wilson, and D.L. Powell, J. Organometal. Chem. 178, 5 (1979).

54. P.G. Perkins, Chem. Comm. 268 (1967).

55. J. Nagy and P. Hencsei, J. Organometal. Chem. 38, 261 (1972).

56. M. Horn and J.N. Murrell, J. Organometal. Chem. 70, 51 (1974).

57. R.A.N. McLean, Can. J. Chem. 51, 2089 (1973).

58. E. Zeeck, Theor. Chim. Acta 35, 301 (1974).

59. F. Bernardi and A. Ricei, J. Organometal. Chem. 128, 331 (1977).

60. T. Veszprémi, M. El-Hersch, and J. Naggy, J. Organometal. Chem. 184, 147 (1980).

61. J.B. Stothers, "Carbon-13 NMR Spectroscopy," A.T. Blomquist and H. Wasserman (eds.), Academic Press, New York (1972).

62. R. Ditchfield and P.D. Ellis, "Topics in Carbon-13 NMR Spectroscopy," G.C. Levy (ed.), vol. 1, 1-52, John Wiley and Sons, New York (1974).

63. G.C. Levy, R.L. Lichter, and G.L. Nelson, "Carbon-13 Nuclear Magnetic Resonance Spectroscopy," 2nd ed., John Wiley and Sons, New York (1980).

64. F.W. Wehrli and T. Wirthlin, "Interpretation of Carbon-13 NMR Spectra," Heyden, London (1978).

65. M. Witanowski, L. Stefaniak, and G.A. Webb, "Nitrogen NMR Spectroscopy," G.A. Webb (ed.), Annual Reports on NMR Spectroscopy 11B, Academic Press, London (1981).

66. M. Witanowski, L. Stefaniak, and G.A. Webb, "Nitrogen NMR Spectroscopy," G.A. Webb (ed.), Annual Reports on NMR Spectroscopy 7, 118-245, Academic Press, London (1977).

67. M. Witanowski and G.A. Webb, "Nitrogen NMR," Plenum Press, London, (1973).

68. G.J. Martin, M.L. Martin, and J.P. Gouesnard, ^{15}N-NMR Spectroscopy, P. Diehl, E. Fluck, and R. Kosfeld, (eds.), "NMR-Basic Principles and Progress 18," Springer-Verlag, Berlin (1981).

69. W.G. Klemperer, Angew. Chem. Int. Ed. 17, 246 (1978).

70. C. Rodgers and N. Sheppard, "NMR and the Periodic Table," R.K. Harris and B.I. Mann (eds.), 383-400, Academic Press, New York (1978).

71. T. St. Armour and D. Fiat, Bull. Magn. Reson. 1, 118 (1979), and references therein.

72. J.P. Kintziner, "Oxygen NMR Characteristic Parameters and Applications," P. Diehl, E. Fluck, and R. Kosfeld (eds.), NMR-Basic Principles and Progress 17, 1-64, Springer-Verlag, Berlin (1981).

73. H. Marsmann, ^{29}Si-NMR Spectroscopic Results, P. Diehl, E. Fluck, and R. Kosfeld (eds.),"NMR-Basic Principles and Progress 17," 65-235, Springer-Verlag, Berlin (1981).

74. E.A. Williams and J.D. Cargioli, Silicon 29 NMR Spectroscopy, G.A. Webb (ed.),"Annual Reports on NMR Spectroscopy 9," 221-319, Academic Press, London (1979).

75. J. Schraml and J.M. Bellama, ^{29}Si Nuclear Magnetic Resonance, F.C. Nachod, J.J. Zuckerman, and E.W. Randall (eds.),"Determination of Organic Structures by Physical Methods 6," 203-270, Academic Press, New York (1976).

76. A. Saika and C.P. Slichter, J. Chem. Phys. 22, 26 (1954).

77. W.E. Lamb, Jr., Phys. Rev. 60, 817 (1941).

78. C.J. Jameson and H.S. Gutowsky, J. Chem. Phys. 40, 1714 (1964).

79. K.A.K. Ebraheem and G.A. Webb, J. Magn. Reson. 30, 211 (1978).

80. M. Jallali-Heravi and G.A. Webb, J. Magn. Reson. 32, 429 (1978).

81. J. Mason, J. Chem. Soc. A 2196 (1970).

82. J. Mason, J. Chem. Soc. A 1038 (1971).

83. W.M. Litchman, J. Magn. Reson. 12, 182 (1973).

84. K.A.K. Ebraheem, G.A. Webb, and M. Witanowski, Org. Magn. Reson. 8, 317 (1976).

85. M. Witanowski, L. Stefaniak, S. Szymánski, and G.A. Webb, Tetrahedron 32, 2127 (1976).

86. R. Wolff and R. Radeglia, Z. Phys. Chem. Leipzig 258, 145 (1977).

87. G. Engelhardt, R. Radeglia, H. Jancke, E. Lippmaa, and M. Magi, Org. Magn. Reson. 5, 561 (1973).

88. R. Wolff and R. Radeglia, Z. Phys. Chem. Leipzig 257, 181 (1976).

89. R. Wolff and R. Radeglia, Z. Phys. Chem. Leipzig 258, 145 (1977).

90. C.R. Ernst, L. Spiatler, G.R. Buell, and D.L. Wilhite, J. Am. Chem. Soc. 96, 5375 (1974).

91. J.H. Letcher and J.R. Van Wazer, J. Chem. Phys. 44, 815 (1966).

92. J.H. Letcher and J.R. Van Wazer, J. Chem. Phys. 45, 2916, 2926 (1966).

93. P.C. Lauterbur, "Determination of Organic Structure by Physical Methods," F.C. Nachod and W.D. Philips (eds.) 2, 511, Academic Press, New York (1962).

94. B.K. Hunter and L.W. Reeves, Can. J. Chem. 46, 1399 (1968).

95. R.K. Harris and B.J. Kimber, J. Magn. Reson. 17, 174 (1975).

96. R.K. Harris and B. Lemarié, J. Magn. Reson. 23, 371 (1976).

97. P.E. Rakita and L.S. Worsham, Inorg. Nucl. Chem. Letters 13, 547 (1977).

98. G.A. Olah and L.D. Field, Organometallics 1, 1485 (1982).

99. L. Delmule and G.P. Van Der Kelen, J. Mol. Struct. 66, 315 (1980).

100. L.Delmule and G.P. Van Der Kelen, J. Mol. Struct. 66, 309 (1980).

101. E.V. Van Den Berghe and G.P. Van Der Kelen, J. Organometal. Chem. 59, 175 (1973).

102. E.V. Van Den Berghe and G.P. Van Der Kelen, J. Organometal. Chem. 122, 329 (1976).

103. R.K. Harris and B.J. Kimber, Org. Magn. Reson. 7, 460 (1978).

104. J. Pola, Z. Papouskova, and V. Chvalovsky, Coll. Czech. Chem. Comm. 41, 239 (1976).

105. J. Schraml, V. Chvalovsky, M. Mägi, and E. Lippmaa, Coll. Czech. Chem. Comm. 42, 306 (1977).

106. C.G. Pitt, J. Organometal. Chem. 61, 49 (1973).

107. Y.P. Yuriev, A.A. Panasenko, V.S. Khvostenko, L.M. Khalilov, Y.B. Yasman, M.M. Timoshenko, V.V. Chizhov, B.G. Zykov, I.I. Furlei, and S.R. Rafikov, J. Organometal. Chem. 166, 169 (1979).

108. Nguyen-Duc-Chuy, V. Chvalovský, J. Schraml, M. Mägi, and E. Lippmaa, Coll. Czech, Chem. Comm. 40, 875 (1975).

109. R.L. Scholl, G.E. Maciel, and W.K. Musker, J. Am. Chem. Soc. 94, 6376 (1972).

110. J. Schraml, J. Pola, H. Jancke, G. Engelhardt, M. Cerný and V. Chvalovský, Coll. Czech. Chem. Comm. 41, 360 (1976).

111. J. Schraml, V. Chavlovský, M. Mägi, and E. Lippmaa, Coll. Czech. Chem. Comm 46, 377 (1981).

112. H.H. Jaffé, J. Phys. Chem. 58, 185 (1954).

113. J.P. Kintzinger, C. Delseth, and T. Thank-Tâm Nguyen, Tetrahedron 36, 3431 (1980).

114. T. Sugawara, Y. Kawada, M. Katoh, and H. Iwamura, Bull. Chem. Soc. Jpn. 52, 3391 (1979).

115. H. Jancke, G. Engelhardt, M. Mägi, and E. Lippmaa, Z. Chem. 13, 435 (1973).

116. M.L. Filleux-Blanchard and Nguyen Dinh An, Org. Magn. Reson. 12, 12-16 (1979).

117. K.A. Andrianov, V.F. Andronov, V.A. Drozdov, D. Ya. Zhinkin, A.P. Kreshkov, and M. M. Morgunova, Acad. Sc. USSR Proc. Chem. Sec. 202, 58 (1972).

118. H. Nöth, W. Tinhof, and B. Wrackmeyer, Chem. Ber. 107, 518 (1974).

119. K. Barlos, G. Hübler, H. Nöth, P. Wanninger, H. Wiberg, and B. Wrackmeyer, J. Magn. Reson. 31, 363 (1978).

120. N.F. Ramsey, Phys. Rev. 91, 303 (1953).

121. A.C. Blizzard and D.P. Santry, J. Chem. Phys. 55, 950 (1971). Erratum: J. Chem. Phys. 58, 4714 (1973).

122. J.M. Schulman and T.J. Venanzi, J. Am. Chem. Soc. 98, 4701 (1976).

123. Tun Khim and G.A. Webb, Org. Magn. Reson. 11, 487 (1978).

124. J.M. Schulman and T.J. Venanzi, J. Am. Chem. Soc. 98, 6739 (1976).

125. T. Axenrod, M.J. Wieder, Tun Khin, G.A. Webb, H.J.C. Yeh, and S. Bulusii, Org. Magn. Reson. 12, 1 (1979).

126. L. Ernst, E. Lustig, and V. Wray, J. Magn. Reson. 22, 459 (1976).

127. Tun Khin and G.A. Webb, Org. Magn. Reson. 10, 175 (1977).

128. P. Lazzeretti, F. Taddei, and R. Zanasi, J. Am. Chem. Soc. 98, 7989 (1976).

129. J. Kowalewski, "Calculations of Nuclear Spin-Spin Couplings," G.A. Webb (ed.), Annual Reports on NMR Spectroscopy 12, 140, Academic Press, London (1982).

130. M.D. Newton, J.M. Schulman, and M.M. Manus, J. Am. Chem. Soc. 96, 17 (1974).

131. F.J. Weigert and J.D. Roberts, J. Am. Chem. Soc. 94, 6021 (1972).

132. J.M. Schulman, J. Ruggio, and T.J. Venanzi, J. Am. Chem. Soc. 99, 2045 (1977).

133. Tun Khin and G.A. Webb, J. Magn. Reson. 33, 159 (1979).

134. K.D. Summerhays and G.E. Maciel, J. Am. Chem. Soc. 94, 8348 (1972).

135. G.C. Levy, D.M. White, and J.D. Cargioli, J. Magn. Reson. 8, 280 (1972).

136. K. Kovacević and Z.B. Maksić, J. Mol. Struct. 17, 203 (1973).

137. H.Dreeskamp and K. Hildenbrand, Leibigs Ann. Chem. 712 (1975).

138. K.D. Summerhays and D.A. Deprez, J. Organometal. Chem. 118, 19 (1976).

139. M.D. Beer and R. Grinter, J. Magn. Reson. 31, 187 (1978).

140. S. Duangthai and G.A. Webb, Org. Magn. Reson. 20, 225 (1982).

141. E.W. Randall and J.J. Zuckerman, J. Am. Chem. Soc. 90, 3167 (1968).

142. A.J.R. Bourn and E.W. Randall, Mol. Phys. 8, 569 (1974).

143. G. Binsch, J.B. Lambert, B.W. Roberts, and J.D. Roberts, J. Am. Chem. Soc. 86, 5564 (1964).

144. A.H. Cowley and J.R. Schweiger, J. Am. Chem. Soc. 95, 4179 (1973).

145. E.E. Liepińsh, I.I. Birgele, G.I. Zelchan, and E. Lukevits, Zh. Obshch. Khim. 49, 1537 (1979).

146. D.W.W. Anderson, J.E. Bentham, and D.W.H. Rankin, J. Chem. Soc. Dalton 1215 (1973).

147. E.A.V. Ebsworth, J.M. Edward, and D.W.H. Rankin, J. Chem. Soc. Dalton 1673 (1976).

148. D.E.J. Arnold, S. Cradock, E.A.V. Ebsworth, J.D. Murdoch, D.W.H. Rankin, D.C.J. Shea, R.K. Harris, and B.J. Kimber, J. Chem. Soc. Dalton 1349 (1981).

149. A. Komoriya and C.H. Yoder, J. Am. Chem. Soc. 94, 5285 (1972).

150. S. Chan, S. Distefano, F. Fong, H. Goldwhite, P. Gysegen, and E. Mazzola, Inorg. Chem. 12, 51 (1973).

151. A. H. Cowley, M.J.S. Dewar, W.R. Jackson, and W.B. Jennings, J. Am. Chem. Soc. 92, 5206 (1970).

152. M. Raban, G.W.J. Kenney, Jr., and F.B. Jones, Jr., J. Am. Chem. Soc. 91, 6677 (1969).

153. W.R. Jackson and T.G. Kee, Tetrahedron Let. 49, 5051 (1972).

154. U. Wannagat and G. Schreiner, Monatsh. Chem. 96, 1889 (1965).

155. J.E. Drake and N.P.C. Westwood, J. Chem. Soc. A 3617 (1971).

156. H. Breederveld and H.I. Waterman, Research Correspondence 5, 537 (1952).

157. L. Tansjo, Acta Chem. Scand. 13, 35 (1959).

158. R.S. Glass, J. Organometal. Chem. 61, 83 (1973).

159. G.A. Morris and R. Freeman, J. Am. Chem. Soc. 101, 760 (1979).

160. D.M. Doddrell, D.T. Pegg, W. Brooks, and M.R. Bendall, J. Am. Chem. Soc. 103, 727 (1981).

161. O.W. Sørensen, H. Bildsøe, and H.J. Jakobsen, J. Magn. Reson. 45, 325 (1981).

162. H.J. Jakobsen, S. AA. Linde, and S. Sørensen, J. Magn. Reson. 15, 385 (1974).

163. H.J. Jakobsen and W.S. Brey, J. Am. Chem. Soc. 101, 774 (1979).

164. S.AA. Linde, H.J. Jakobsen, and B.J. Kimber, J. Am. Chem. Soc. 97, 3219 (1975).

165. K.G.R. Pachler, J. Magn. Reson. 7, 442 (1972).

166. A.A. Bothner-By and S. Castellano, "LAOCN3" Mellon Institute, 4400 Fifth Avenue, Pittsburgh, Pennsylvania.

167. H.J. Jakobsen, P.J. Kanyha, and W.S. Brey, J. Magn. Reson. 54, 134 (1983).

168. H.J. Jakobsen, O.W. Sørensen, W.S. Brey, and P.J. Kanyha, J. Magn. Reson. 48, 328 (1982).

169. S. Sørensen, R.S. Hansen, and H.J. Jackobsen, J. Magn. Reson. 14, 243 (1974).

170. G.A. Morris, J. Am. Chem. Soc. 102, 428 (1980).

171. R.A. Craig, R.K. Harris, and R.J. Morrow, Org. Magn. Reson. 13, 229 (1980).

172. D.M. Doddrell, D.T. Pegg, and M.R. Bendall, J. Magn. Reson. 48, 323 (1982).

173. R.D. Bertrand, W.B. Moniz, A.N. Garroway, and G.C. Chingas, J. Am. Chem. Soc. 100, 5227 (1978).

174. H.J. Jakobsen, O.W. Sørensen, and H. Bildsøe, J. Magn. Reson. 51, 157 (1983).

175. D.P. Burum and R.R. Ernst, J. Magn. Reson. 39, 163 (1980).

176. O.W. Sørensen and R.R. Ernst, J. Magn. Reson. 51, 477 (1983).

177. T. Bundgaard and H.J. Jakobsen, J. Magn. Reson. 18, 209 (1975).

178. W. Städeli, P. Bigler, and W. Von Philipsborn, Org. Magn. Reson. 16, 170 (1981).

179. E. Nygaard and H. Bildsøe, presented at the Vth European Experimental NMR Conference, Königstein (1981).

180. J.-P. Marchal and D. Canet, J. Am. Chem. Soc. 97, 6581 (1975); M. Llinas, W.J. Horsley, and M.P. Kelin, J. Am. Chem. Soc. 98, 7554 (1976).

181. A.A. Chalmers, K.G.R. Pachler, and P.L. Wessels, J. Magn. Reson. 15, 415 (1974).

182. S.AA. Linde and H.J. Jakobsen, J. Am. Chem. Soc. 98, 1041 (1976).

183. A. Bax, R. Freeman, and S.P. Kempsell, J. Am. Chem. Soc. 102, 4849 (1980).

184. A. Bax, R. Freeman, and S.P. Kempsell, J. Magn. Reson. 41, 349 (1980).

185. A. Bax and R. Freeman, J. Magn. Reson. 41, 507 (1980).

186. P.J. Hore, R.M. Scheek, A. Volbeda, R. Kaptein, and J.H. Van Boom, J. Magn. Reson. 50, 328 (1982).

187. R. Freeman, T.H. Mareci, and G.A. Morris, J. Magn. Reson. 42, 341 (1981).

188. M.R. Bednall, D.T. Pegg, D.M. Doddrell, and J. Field, J. Am. Chem. Soc. 103, 934 (1981).

189. T.C. Farrar and E.D. Becker, "Pulse and Fourier Transform NMR," p. 83, Academic Press, New York (1971).

190. D.T. Burum and R.R. Ernst, J. Magn. Reson. 39, 163 (1980).

191. D.M. Doddrell and D.T. Pegg, J. Am. Chem. Soc. 102, 6388 (1980).

192. F.A.L. Anet, N. Jaffer, and J. Strouse, 21st Experimental NMR Conference, Tallahassee, FL (1980).

193. D.L. Rabenstein, T.T. Nakashima, and D.W. Brown, 22nd Experimental NMR Conference, Asilomar, CA (1981).

194. C. Le Cocz and J.-Y. Lallemand, J. Chem. Soc. Chem. Commun. 150 (1981).

195. D.J. Cookson and B.E. Smith, Org. Magn. Reson. 16, 111 (1981).

196. D.W. Brown, T.T. Nakashima, and D.L. Rabenstein, J. Magn. Reson. 45, 302 (1981).

197. O.W. Sørensen, Thesis, University of Aarhus (1980/81).

198. M.R. Bendall, D.M. Doddrell, and D.T. Pegg, J. Am. Chem. Soc. 103, 4603 (1981).

199. S.L. Patt and J.N. Shoolery, J. Magn. Reson. 46, 535 (1982).

200. F.W. Wehrli and T. Wirthlin, "Interpretation of Carbon-13 NMR Spectra," p. 66, Heyden, London (1976).

201. J.B. Stothers, "Carbon-13 NMR Spectroscopy," p. 436, Academic Press, New York (1972).

202. C.G. Swain and E.C. Lipton, Jr., J. Am. Chem. Soc. 90, 4328 (1968); C. Hansch and A. Leo, "Substituent Constants for Correlation Analysis in Chemistry and Biology," p. 65, Wiley, New York (1979).

203. C. Delseth and J.P. Kintzinger, Helv. Chim. Acta 61, 1327 (1978).

204. P.A. Couperus, A.D.H. Clague, and J.P.C.M. van Donger, Org. Magn. Reson. 8, 426 (1976).

205. M. Bullpitt, W. Kitching, W. Adcock, and D. Doddrell, J. Organometal. Chem. 116, 187 (1976).

206. G.A. Kalabin, V.M. Bzhezovskii, D.F. Kushnarev, and A.G. Proidakov, J. Org. Chem. USSR Engl. Trans. 17, 1009 (1981).

207. H. Eggert and C. Djerassi, J. Am. Chem. Soc. 95, 3710 (1973).

208. I. Yavari and J.D. Roberts, J. Org. Chem. 43, 4689 (1978).

209. M. Feigel, H. Kessler, and A. Walter, Chem. Ber. 111, 2947 (1978).

210. M.L. Huggins, J. Am. Chem. Soc. 75, 4123 (1953).

211. R.O. Duthaler and J.D. Roberts, J. Am. Chem. Soc. 100, 3889 (1978).

212. I. Yavari, J.S. Storal, and J.D. Roberts, Org. Magn. Reson. 12, 340 (1979).

213. I. Yavarai and J.D. Roberts, J. Org. Chem. 43, 4689 (1978).

214. F.W. Wehrli and T. Wirthlin, "Interpretation of Carbon-13 NMR Spectra," p. 138, Heyden, London (1978).

BIOGRAPHICAL SKETCH

Paul John Kanyha was born in Somerville, New Jersey, on December 1, 1956. After attending Immaculata High School in Somerville, he attended Emory University at Atlanta, Georgia, in September 1974 and graduated in June 1978, receiving the degree of Bachelor of Science with a major in chemistry.

In September 1978, he entered the Graduate School of the University of Florida. From September 1978 until the present time, he has worked as a teaching assistant and the departmental NMR spectroscopist.

I certify that I have read this study and that in my opinion it conforms to acceptable standards of scholarly presentation and is fully adequate, in scope and quality, as a dissertation for the degree of Doctor of Philosophy.

Wallace S. Brey, Jr., Chairman
Professor of Chemistry

I certify that I have read this study and that in my opinion it conforms to acceptable standards of scholarly presentation and is fully adequate, in scope and quality, as a dissertation for the degree of Doctor of Philosophy.

William Weltner, Jr.
Professor of Chemistry

I certify that I have read this study and that in my opinion it conforms to acceptable standards of scholarly presentation and is fully adequate, in scope and quality, as a dissertation for the degree of Doctor of Philosophy.

Samuel O. Colgate
Associate Professor of Chemistry

I certify that I have read this study and that in my opinion it conforms to acceptable standards of scholarly presentation and is fully adequate, in scope and quality, as a dissertation for the degree of Doctor of Philosophy.

Richard A. Yost
Associate Professor of Chemistry

I certify that I have read this study and that in my opinion it conforms to acceptable standards of scholarly presentation and is fully adequate, in scope and quality, as a dissertation for the degree of Doctor of Philosophy.

Raymond J. Bergeron

Raymond J. Bergeron
Associate Professor of
Medicinal Chemistry

This dissertation was submitted to the Graduate Faculty of the Department of Chemistry in the College of Liberal Arts and Science and to the Graduate School, and was accepted as partial fulfillment of the requirements for the degree of Doctor of Philosophy.

April 1984

Dean for Graduate Studies
and Research